Assessing the propensity of drug resistant tuberculosis to enter and exit the differentially culturable state

Bomikazi Nonkula (1421421)

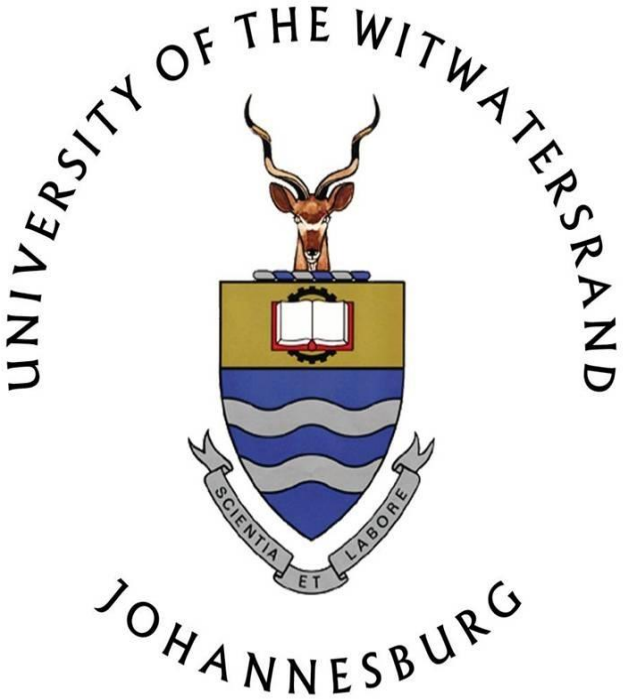

A dissertation submitted to the Faculty of Health Science, University of the Witwatersrand, Johannesburg, in fulfilment of the requirements for the degree of Master of Science in Medicine.

2023

Declaration

I, Bomikazi Nonkula (student number: 1421421) declare that this dissertation is my own work. It is being submitted for the degree of Master of Science in Medicine at the University of the Witwatersrand, Johannesburg. It has not been submitted before for any degree or examination at this or any other University.

08-06-2023

Acknowledgments

First and foremost, I would like to thank the Lord for carrying me through, giving me strength and knowledge to do this research project. Proverbs 3:5-6

I would like to thank my financial sponsors, the National Research Foundation (NRF) and the DST/NRF Centre of Excellence for Biomedical TB Research (CBTBR).

I would also like to thank Professor Bavesh Kana for granting me this opportunity to do this research. Thank you for your guidance, great support and sharing of your exceptional scientific knowledge. I would also like thank my supervisor, Dr Julian Peters, for the guidance and support during the course of this research study.

A big thank to my family, especially my mother- Nothemba Nonkula- , for the abundant love, support and prayers.

Thank you to Moagi, Ofentse, Dale, Itumeleng and Chris who were always willing and enthusiastic to assist in any way they could in my research. To Nontobeko, Palesa, Olivia and Natasha, thank you for becoming my family away from home. Thank you for your companionship and providing a friendly and pleasurable working environment.

List of symbols and abbreviations

µg	Microgram
µL	Microlitre
µm	Micrometer
AIDS	Acquired Immune Deficiency Syndrome
BCG	Bacillus Calmette-Guérin
CBTBR	Centre of Excellence for Biomedical TB Research
CF	Culture Filtrate
CFU	Colony Forming Unit
CTAB	Cetyltrimethylammonium bromide
DCTB	Differentially Culturable Tubercle Bacilli
DNA	Deoxyribonucleic acid
DR	Direct Repeat
ECL	Enhanced Chemiluminescence
EDTA	Ethylenediaminetetraacetic acid
EMB	Ethambutol
gDNA	Genomic DNA
HIV	Human Immunodeficiency Virus
INH	Isoniazid
L	Litre
LAM	Lipoarabinomannan
LTBI	Latent tuberculosis infection
MDR	Multi drug resistant
MGIT	Mycobacterial Growth Indicator tube
ml	Millilitre
MPN	Most Probable Number
Mtb	*Mycobacterium tuberculosis*
MTBC	*Mycobacterium tuberculosis* complex
NHLS	National Health Laboratory Services
OADC	Oliec acid, Albutin, Dextrose, Catalase

PANTA	Polymyxin B, Amphotericin B, Nalidixic acid, Trimethoprim and Azlocillin
PBS	Phosphate Buffer Solution
PCR	Polymerase Chain Reaction
PG	Peptidoglycan
RIF	Rifampicin
Rpf	Resuscitation-Promoting Factor
SDS	Sodium Dodecyl sulphate
SOP	Standard Operating Procedure
TB	Tuberculosis
TE	Tris-EDTA buffer
TNF-α	Tumour Necrosis Factor Alpha
TST	Tuberculin Skin Test
TTP	Time to positivity
UV	Ultra-violet
VNBC	Viable But Not Culturable
VNTR	Viable Number of Tandem Repeats
WHO	World Health Organisation
XDR	Extensively drug-resistant

List of Figures

Figure 1.1: TB incidence rates for 2020

Figure 1.2: Schematic diagram of peptidoglycan (PG)

Figure 1.3: Pathogenic life cycle of *Mycobacterium tuberculosis*

Figure 1.4: Spectrum of tuberculosis infection and transmission

Figure 1.5: Antigen-specific CD4 T cell phenotypic and functional heterogeneity determines preferential depletion during HIV co-infection.

Figure 1.6: *M. tuberculosis* drug targets

Figure 1.7: Tuberculosis strain typing

Figure 1.8: Tuberculosis global strain distribution

Figure 2.1: Strain typing of *M. tuberculosis* using Spoligotyping

Figure 2.2: Purification of frozen stock through antibiotic and antifungal treatment.

Figure 2.3: Purification of TB cultures

Figure 2.4: Schema for producing and counting Differentially culturable Tuberculosis

Figure 2.5: Colony forming unit (CFU) assay

Figure 2.6: Cytological profiling of the *M. tuberculosis* strains

Figure 2.7: RNA isolation

Figure 2.8: Rate of exit from the DCTB state in MGIT cultures

Figure 3.1: Strain type distribution

Figure 3.2: Propensity of clinical strains to adopt the Differentially culturable Tuberculosis state

Figure 3.3: Effect of culture filtate on the resuscitation of DCTB

Figure 3.4: Strain typing

Figure 3.5: Growth kinetics for Beijing strains

Figure 3.6: Growth kinetics for LAM strains

Figure 3.7: Primer optimization

Figure 3.8: The effect of culture filtrate on the recovery of differentially culturable tubercle bacilli starved from an *in vitro* model of starvation of LAM, Beijing and H37Rv strains

Figure 3.9: Quanta of Differentially culturable Tuberculosis in the 5 individual Beijing strains from the carbon starvation model using PBS as a culture medium.

Figure 3.10: Quanta of DCTB in the 5 individual LAM strains from the carbon starvation model using PBS as a culture medium.

Figure 3.11: Assessment of RNA quality for RT-qPCR to assess the expression of regulon genes.

Figure 3.12: Cytological profiling of the *M. tuberculosis* clinical bacteria

Figure 3.13: Mean fluorescence intensity of the starved cells incorporated with the TADA stain

Figure 3.14: *M. tuberculosis* clinical strains cell length

Figure 3.15: Resuscitation of starved Beijing and LAM strains

Figure 3.16: The addition of culture filtrate decreases time to positivity in starved cultures.

List of tables

Table 2.1: List of *M. tuberculosis* strains used in this study

Table 2.2: Primers used for the confirmation of clinical strains

Table 2.3: Reagents used to make the mastermix for the PCR component of Spoligotyping

Table 2.4: Cycling parameters for the PCR reaction

Table 2.5: Reagents used for the PCR mastermix

Table 2.6: Cycling parameters for the PCR reaction

Table 2.7: PCR primers

Table 3.1: Expected band sizes of the resistance conferring genes.

Table 3.2: Mutations of the *katG* and *embB* genes in drug resistant *M. tuberculosis* strains.

Abstract

Tuberculosis (TB), one of the oldest and most contagious infectious diseases, continues to be a global health concern. TB is caused by members of the *Mycobacterium tuberculosis* complex (MTBC) which comprises of several species. These species are further subdivided into strains based on subtle genetic differences. The success of *M. tuberculosis* as a pathogen can be attributed to its ability to survive various stresses by adopting different growth states. Previous studies have shown that sputum from TB infected patients harbours a large proportion of drug-tolerant bacteria that are unable to form colonies on agar plates but can grow in liquid media. This population of organisms, termed differentially culturable tubercle bacilli (DCTB), could be resuscitated to grow by supplementing liquid media with cell free culture filtrates from axenic cultures of wild type *M. tuberculosis* H37Rv or mutant H37Rv lacking all five resuscitation promoting factors (*Rpf*s). Laboratory models that induce this differentially culturable state are critical for studying the physiology and metabolism of these bacteria in order to develop new TB diagnostic tests. In this study, five Beijing and five LAM drug resistant strains of *M. tuberculosis* were selected and used to robustly generate DCTB through an *in vitro* stress model using carbon starvation. The most probable number (MPN) assay and colony forming units were used to determine the amount of DCTB. Furthermore, the phenotype of these cells was studied using microscopy as well as metabolic probes that target the peptidoglycan (PG) component of the bacterial cell wall. Our findings demonstrated that applying the carbon starvation model to clinical *M. tuberculosis* strains (Beijing and LAM) resulted in robust levels of DCTB, as evidenced by limited growth on agar plates and enhanced growth in liquid media supplemented with culture filtrate from LAM and Beijing strains. Comparison of cell length between carbon starved cells to those grown in routine laboratory media suggested that DCTB appeared to be non-replicating and significantly shorter. The metabolic activity of the starved cultures was restored when they were supplemented with H37Rv, LAM and Beijing culture filtrate. Our results also demonstrated that Beijing strains had a higher propensity to produce DCTB compared to LAM strains and that the supplementation with Beijing culture filtrate resuscitated more DCTB. Collectively, our findings allow for the advancement of experimental systems that enable further investigation of DCTB and the properties of the Beijing strain that facilitate better adoption of the differentially culturable state.

Dedication

In loving memory of

Nombalela Priscilla Nonkula

29/09/1948 - 14/07/2020

Table of Contents

Declaration ii

Acknowledgments iii

List of symbols and abbreviations iv

List of Figures vi

List of tables viii

Abstract ix

Dedication x

1. Introduction 1

1.1 Background 1

1.2 Physiology of *M. tuberculosis* 2

1.3 TB Pathogenesis 3

1.4 TB disease presentation 4

1.4.1 Elimination 5

1.4.2 Latent TB infection 5

1.4.3 Incipient TB 5

1.4.4 Subclinical TB 6

1.4.5 Active TB 6

1.5 Co-infection of TB with Human Immunodeficiency virus (HIV) 6

1.6 Diagnosis of *M. tuberculosis* 8

1.7 Treatment of drug sensitive TB 8

1.8 Drug resistance in *M. tuberculosis* 9

1.9 Tuberculosis strain typing 11

1.9.1 Spoligotyping 13

1.9.2 MIRU-VNTR 13

1.9.3 IS*6110* 13

1.9.4 Whole genome sequencing 14

1.10 Tuberculosis strain distribution 14
1.11 Phenotypic growth heterogeneity in *M. tuberculosis* 16
1.11.1 Dormancy 16
1.11.2 Differentially culturable tubercle bacilli (DCTB) 17
1.12 Hypothesis 18
1.13 Aim 18
1.14 Study objectives 19
2. Materials and Methods 20
2.1 Materials used 20
2.2 Selection criteria of bacterial strains 20
2.3 Preparation of media and solutions 20
2.4 Laboratory strains and culturing conditions 20
2.5 DNA extraction: Colony boil 21
2.6 Spoligotyping 22
2.6.1 Polymerase chain reaction (PCR) 22
2.6.2 Hybridization 23
2.6.3 Detecting the binding pattern 24
2.7 Purification and culture of selected strains 24
2.8 Large-scale genomic DNA isolation 26
2.9 Optimization of PCR conditions for resistance determining regions 27
2.10 Growth Kinetics of *M. tuberculosis* clinical strains 29
2.11 *In vitro* stress models 29
2.11.1 Saito *et al*., sequential stress model 29
2.11.2 Most probable number (MPN) assay prior starvation 30
2.11.3 Colony forming units (CFUs) prior starvation 32
2.12 Resuscitation of starved cultures 32
2.12.1 Preparation of specialist DCTB culture media 32

2.12.2 Resuscitation of starved cultures using the MPN assay 32
2.13 Cytological profiling of the *M. tuberculosis* bacteria 33
2.14 RNA extraction 34
2.15 Mycobacteria growth indicator tube (MGIT) assay 35
2.16 Data analysis 36
3. Results 37
3.1 *In silico* analysis of the propensity of drug resistant *M. tuberculosis* strains to adopt the DC state 37
3.1.1 Strain typing of drug resistant *M. tuberculosis* from stored cultures by Spoligotyping 37
3.1.2 Propensity of clinical strains to adopt the DCTB state. 38
3.1.3 Determining the effect of CF on the quanta of DCTB per strain type 39
3.2 Selection and confirmation of clinical strains 41
3.3 Growth kinetics of strains 42
3.4 Detection of mutations in the drug-resistance conferring genes 43
3.4.1 Genomic DNA extraction and PCR primer optimization 43
3.5 PBS based starvation model to generate non-replicating organisms. 46
3.5.1 DCTB resuscitation 46
3.6 Expression of *dos R*egulon genes 49
3.7 Cytological profiling of the *M. tuberculosis* clinical bacteria 50
3.7.1 Metabolic activity of *M. tuberculosis* bacteria 50
3.7.2 Metabolic activity of *M. tuberculosis* bacteria produced under the carbon starvation model 52
3.8 Resuscitation of Starved cells 54
4. Discussion 57
4.1 Concluding remarks 59
5. Limitations and future studies 60
6. Appendix 61

6.1 Appendix A: Materials 61
6.2 Appendix B : Supplementary Figures 65
Appendix- C- Ethics clearance certificate 72
Appendix D- Turn-it in report 73
7. References 75

1. Introduction

1.1 Background

Tuberculosis (TB), caused by the bacterium *Mycobacterium tuberculosis (M. tuberculosis)*, remains a global health concern with 1.5 million deaths and 10 million new infections annually (WHO, 2020). TB is the second leading cause of death globally (WHO, 2020) with high incidence and mortality rates, predominantly in developing countries such as those in South-Asia, Africa and West-Pacific regions as shown in Figure 1.1. Risk factors contributing to the high number of TB cases and deaths include diabetes, smoking, malnutrition, alcohol abuse and coinfection with HIV as well as rising numbers of multi-drug resistance cases (WHO, 2020). TB is predominantly a pulmonary infection, however the gastrointestinal system, musculoskeletal system, lymphoreticular system, skin, liver, and reproductive system are also commonly affected (MacPherson *et al*., 2020). One out of every ten people infected with *M. tuberculosis* develops an active infection at some point during their lives and the risk of such an event is highest in the first year after infection. That said, most individuals do not acquire active tuberculosis for several years (Schaller *et al*., 2019) .

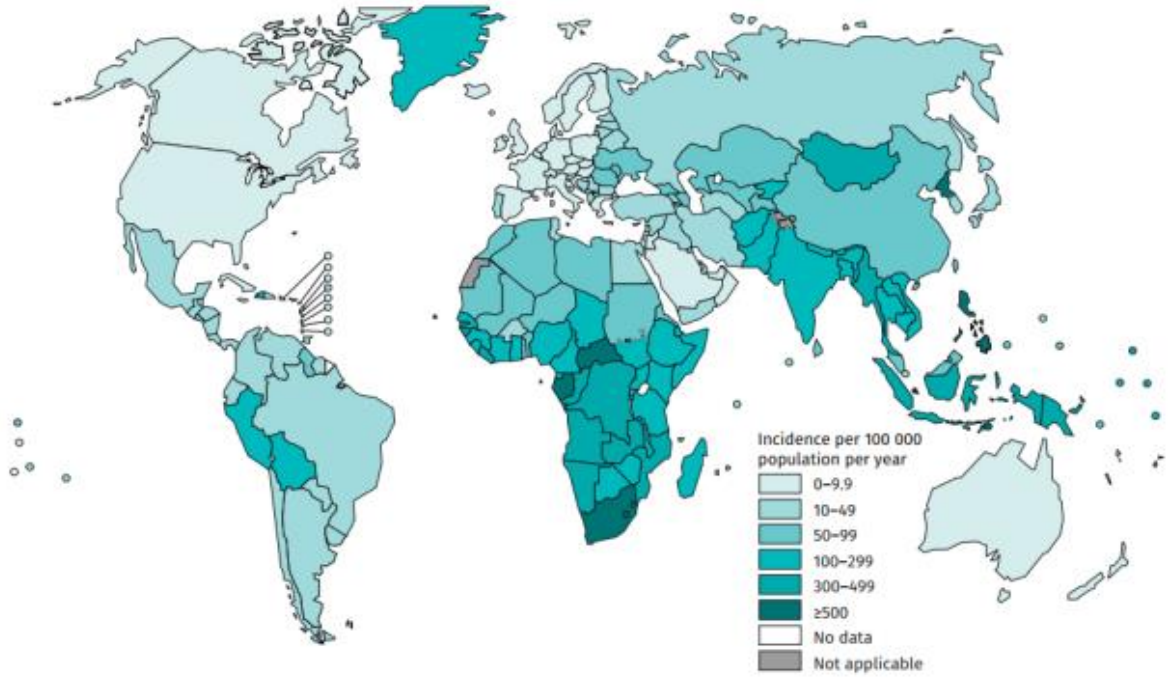

Figure 1.1: TB incidence rates for 2020. Diagram showing the global TB incidence rates with sub-saharan Africa having the highest rates. Map taken from the WHO 2020 report.

1.2 Physiology of *M. tuberculosis*

M. tuberculosis is a well-adapted human pathogen that can promptly remodel its metabolism under stressful conditions during pathogenesis (Gordan *et al*., 2019). This organism is encompassed by a cell wall that has remarkable molecular complexity. The peptidoglycan (PG) layer, arabinogalactan (AG) and the mycolic acid (MA) are the main components of the mycobacterial cell wall (Maitra *et al*., 2019). Peptidoglycan is a rigid polysaccharide polymer that lies between the outer 'mycomembrane component' and the plasma membrane. Several enzymes cleave PG at different positions including lytic transylocyslases; such as resuscitation promoting factors (*Rpf*s), L, D-endopeptidases (RipA and RipB) and amidases (Ami1, Ami3 and Ami4) (Figure 1.2). These enzymes are used for the remodeling of the cells wall through enabling the formation and cleavage of bonds that allow for the breakdown of old cell wall and the insertion of new cell wall material (Healy *et al*., 2020). *Rpf*s are peptidoglycan degrading enzymes that cleave between the *N*-acetylglucosamine (NAG) and *N*-Acetyl muramic acid (NAM) disaccharides of the glycan bone thus allowing separation of daughter cells during cell division (Kana and Mizrahi, 2010). Ami enzymes cleave the peptide stem from the NAM residue on the glycan backbone while RipA cleaves within the peptide stem (Healy *et al*., 2020). These enzymes, among others, are collectively essential for the transition of cells from dormancy to active growth as they enable separation of daughter cells.

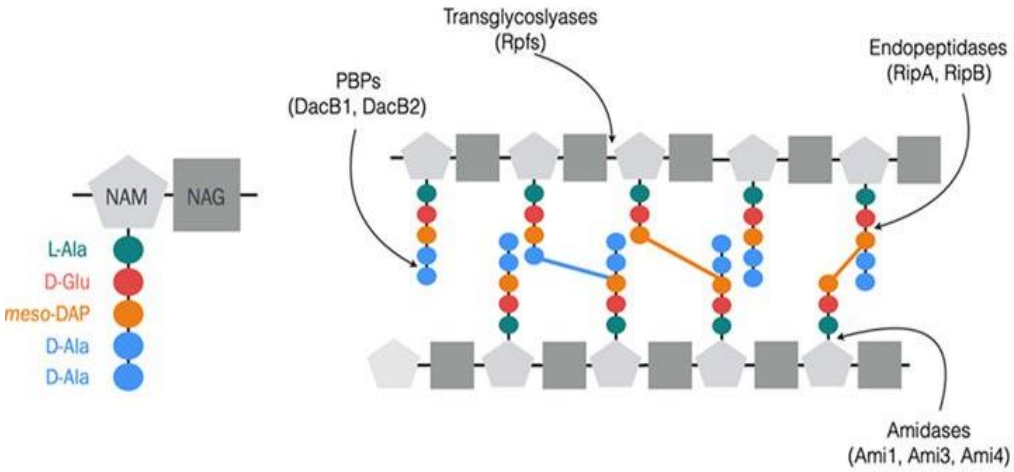

Figure 1.2: Schematic diagram of the peptidoglycan (PG). *N*-Acetyl muramic acid (NAM) (light grey) and *N*-acetylglucosamine (NAG) (dark grey) residues make up the glycan backbone of PG. The pentapeptide stem constitutes of L-alanine (green), D-glutamate (red), *meso*-diaminopimelic acid (mDAP) (orange), and two D-alanine (blue) residues (left panel). Different classes of PG-hydrolyzing enzymes cleave the PG macromolecule at different sites as shown by the arrows. The colored bars between peptide stems represent cross-links between 2 adjacent peptide chains, these can either be 4-3 or 3-3 cross-links depending on which residues in the stem peptide are involved in bond formation. Taken from Healy *et al*., 2020.

1.3 TB Pathogenesis

M. tuberculosis is spread through airborne droplet nuclei (Churchyard *et al*., 2017). It is transmitted when an infected person coughs or sneezes and disperses the droplets, which can be inhaled into the airways of a new host (Baer *et al*., 2015). Upon entry in the potential host, lung alveolar macrophages, which constitute the first-line defense, phagocytose the bacilli leading to the secretion of an array of antimicrobial factors that should ideally result in bacterial control or elimination as shown in Figure 1.3 (Churchyard *et al*., 2017).

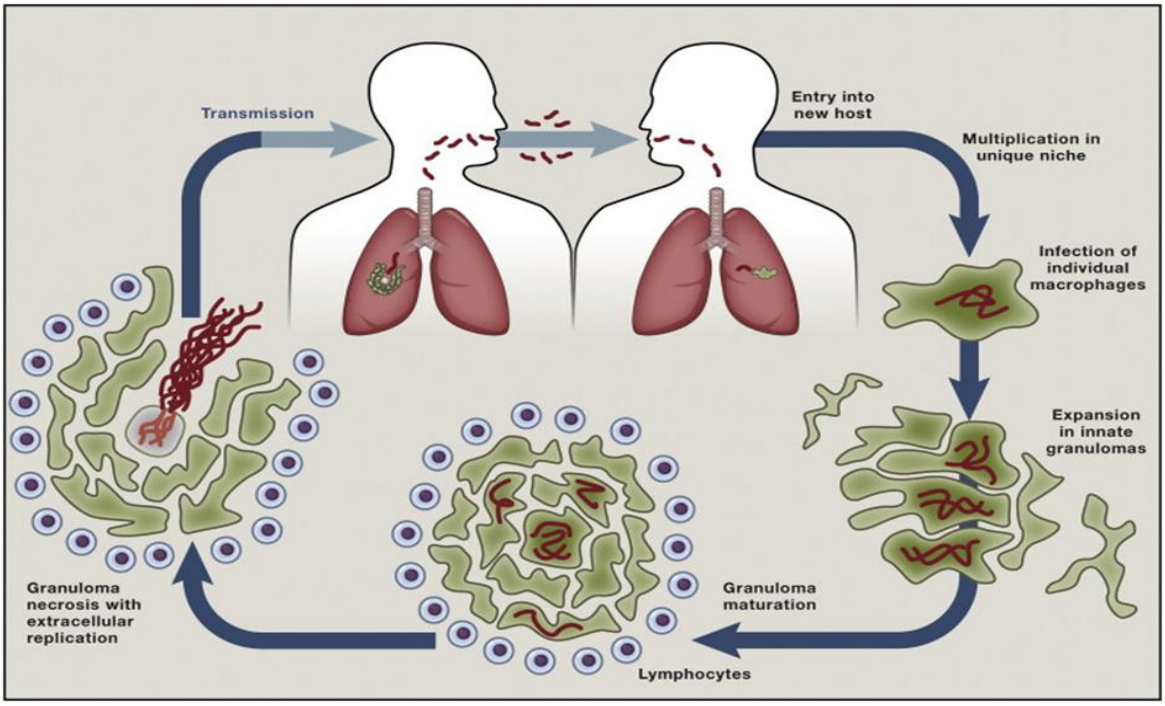

Figure 1.3 Pathogenic Life Cycle of *M. tuberculosis.* *M. tuberculosis* infection begins when fine aerosol particles containing bacteria coughed up by a diseased patient are deposited in the lower lungs of a new host. The bacteria attract macrophages to the lung's surface, where they become infected and transport the bacteria across the lung epithelium to deeper tissues. More macrophages are recruited to the original infected macrophage, resulting in the formation of the granuloma. In its early stages, the granuloma is characterized by infected macrophages and eventually restricts bacterial growth as adaptive immunity develops. However, under certain conditions, infected granuloma macrophages can necrotize, forming a necrotic core that promotes bacterial growth and transmission to the next host. This image was taken from Cambier *et al*., 2014.

Following initial infection, in the presence of an intact immune system, a cascade of immune signaling mechanisms promotes the formation of granulomas, the major function of which is to contain the infection (Hunter, 2018). The alveolar macrophage phagocytoses but does not kill the mycobacterial invaders but does produce chemo attractants. Chemokines released by alveolar macrophages and pneumocytes attract the first wave of inflammatory cells, including neutrophils, monocyte-derived macrophages, NK cells, and -T cells, which promote inflammation and tissue remodeling. However, in some cases, *M. tuberculosis* continues to

divide within the granuloma and escapes containment resulting in necrotizing granulomas. When necrotizing granulomas are exposed to the airways, the organisms are expelled to the air during expectoration (Ehlers and Schaible., 2013). This is known as active TB and occurs in about 5% of infected persons.

In approximately 90% of the cases, the infection is halted at the granuloma stage, resulting in a non-contagious infection that may or may not progress at a later stage, depending on various factors such as host immunity. This is called latent TB infection (LTBI) which is prevalent in approximately one third of the world's population (Dulberger *et al*., 2019). Incipient and subclinical TB are transient reversible disease states that occur along the continuum of TB disease and begin to manifest as the immune system loses its ability to contain the infecting bacteria. These are characterized by the presence or absence of clear symptoms and some level of radiological or microbiological evidence of disease (Drain *et al*., 2018). These TB transmission outcomes are explained in detail below.

1.4 TB disease presentation

In TB infection, there are five major infection outcomes: elimination, latency, incipient TB, subclinical TB, and active disease.

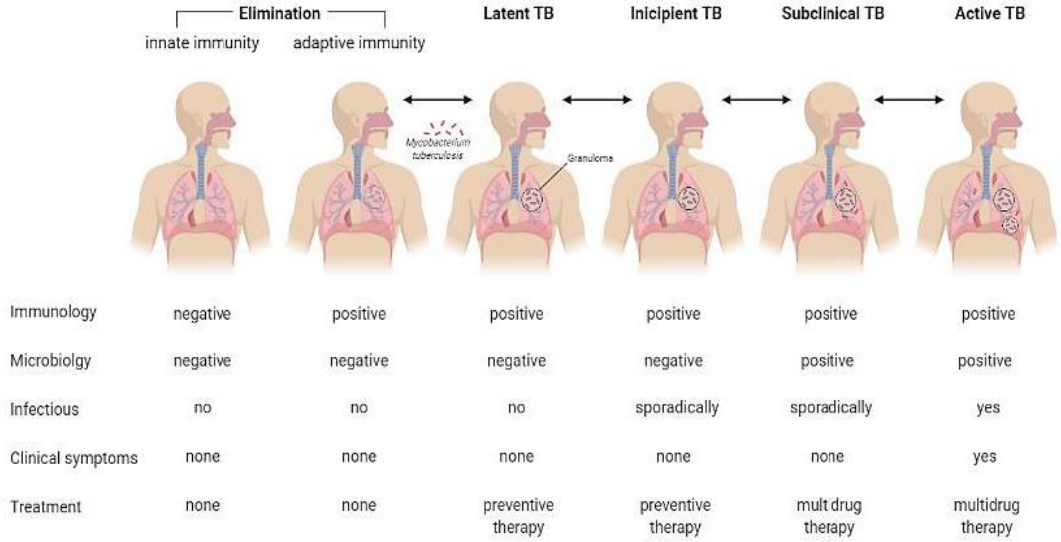

Figure 1.4: Spectrum of Tuberculosis infection and transmission. Diagram showing the dynamic continuum of TB disease and distinguishing properties, ranging from early elimination, latent infection, incipient TB, subclinical TB and active TB disease. Taken from Pai *et al*., 2016.

These outcomes exist as a dynamic spectrum of disease states, with infected individuals presenting in a variety of ways depending on host immunity and bacterial determinants (Pai

et al., 2016; Drain *et al*., 2018). The outcome of the disease is usually determined by the strength of the immune response. Figure 1.4 above summarizes the five outcomes and their distinguishing characteristics.

1.4.1 Elimination

Once an infection has been established, the bacteria can be eradicated by either the host immune system or anti-tuberculosis drugs. Because of the development of an effective cell-mediated immune response, the bacteria can be completely eradicated within two to eight weeks of infection. As a result, the granuloma becomes caseating and necrotic. The majority of bacilli are unable to survive in this necrotic environment and are eradicated (Schluger and Rom, 1998; Frieden *et al*., 2003; Ahmad, 2011). Individuals who have recovered from the infection remain immunologically positive and can be identified using tuberculin skin tests (TST) (Frieden *et al*., 2003; Ahmad, 2011).

1.4.2 Latent TB infection

LTBI is a dynamic state of persistent immunological response to stimulation by *M. tuberculosis* antigens without clinically evident TB disease or radiological symptoms (Kiazyk and Ball, 2017). LTBI affects about one-third of the world's population, with the majority of cases concentrated in 22 high-burden nations. In resource-poor countries with a high TB prevalence, early detection and treatment of active TB remains a key priority (Sharma *et al*., 2012). Testing for LTBI is done using Tuberculin skin tests and Interferon Gamma Release Assays (IGRA). This approach can be problematic in BCG vaccinated countries as the immune response to BCG may still be active and therefore yielding false positive results. As LTBI adds significantly to the pool of active TB, it is critical to diagnose and treat it, particularly in high-risk groups. However, the sheer scale of the LTBI burden in low resource countries makes universal treatment impossible. Furthermore, the lack of economically practical tests that report on progression of LTBI to active TB presents a major constraint to large scale testing of populations for LTBI (Surendra *et al*., 2012, Carranza *et al*., 2020).

1.4.3 Incipient TB

Incipient TB infection is defined as an infection with viable *M. tuberculosis* bacteria that, in the absence of further intervention, is likely to progress to active disease but has not yet induced clinical symptoms, radiographic abnormalities, or microbiologic evidence consistent with active TB disease (Drain *et al*., 2018). The bacteria in this state are thought to be metabolically active, indicating the impending progression to active disease and replication.

Immunological tests can detect incipient TB however, these tests cannot predict the risk of progression to active disease (Rangaka *et al*., 2014). In these cases, radiological detection may be a useful tool for monitoring the progression of the disease to active disease.

1.4.4 Subclinical TB

Subclinical TB is characterized by the lack of obvious clinical TB symptoms but presence of other abnormalities that can be detected using existing radiological or microbiological assays (Drain *et al*., 2018). As the bacilli are metabolically active and induce an immune response, they can be detected using immunological tests similar to active TB, despite differences in sensitivity. It is unclear whether subclinical TB is a disease state that is associated with the capacity to transmit TB. Given the considerable number of people that carry this form of TB, further investigation of this remains an urgent global priority (Dowdy *et al*., 2013).

1.4.5 Active TB

Active TB is predominantly a pulmonary infection that can either result from primary infection or a reactivation of a previous infection that was quiescent in the lungs (Talha *et al*., 2020). Primary TB disease occurs when *M. tuberculosis* enters the human body, followed by immediate failure of the immune system to contain the infection as is described in the schematic of the lifecycle of TB in Figure 1.3. A notable burden of TB can be caused by reactivation of disease in latently infected individuals (Jilani *et al*., 2020). In this case, a previous primary infection that was contained by the immune system for a period of time begins to cause disease due to deterioration of the immune system, accompanied by the loss of containment of *M. tuberculosis* from the sequestering granulomas as shown in Figure 1.4.

1.5 Co-infection of TB with Human Immunodeficiency virus (HIV)

Increased reactivation of latent TB and increased susceptibility to *M. tuberculosis* infection can both be attributed to co-infection with HIV. The vast majority of people infected with *M. tuberculosis* do not develop active TB, this is due to a robust immune response that either eliminates bacteria or contains infection in an asymptomatic state. Individuals who are HIV-TB co-infected are at a disadvantage as both diseases drive each other (Pawlowski *et al*., 2012). Immunosuppression in HIV positive patients is characterized by a loss of CD4 T cells in the blood, lymphoid organs, and mucosa, which is clearly a factor for increased risk of developing active TB (Moir *et al*. 2011). The depletion of CD4 T cells is a factor in the

increased risk of latent TB reactivation, and susceptibility to new *M. tuberculosis* infection (Bruchfeld *et al*., 2015).

Antigen-specific CD4 T cell phenotypic and functional heterogeneity in the immune response determines preferential depletion during HIV co-infection. A study by Ahmed *et al*., 2016, demonstrated that in an HIV-infected host, variable loss of pathogen-specific CD4 T cells determines susceptibility to opportunistic infections that are normally controlled by CD4 T cell responses. For example, cytomegalovirus (CMV)-specific CXCR3+CCR6 Th1 CD4 T cells are mature and terminally differentiated, secreting IFN-γ and the CCR5 ligand MIP-1β, which prevents HIV entry. *M. tuberculosis*-specific CXCR3+CCR6+ Th1/Th17 CD4 T cells, on the other hand, are less mature but polyfunctional, secreting IFN-γ, TNF-α (tumor necrosis factor-alpha), and IL-2, making them highly proliferative but producing little MIP-1β, resulting in greater susceptibility to HIV infection. As a result, reactivation of active TB disease following HIV co-infection may be due to preferential depletion of the CXCR3+CCR6+ subset of CD4 memory T cells in LTBI individuals, which may explain why TB is an early opportunistic disease in TB-endemic areas, whereas CMV emerges only after a dramatic decline in CD4 counts (Bruchfeld *et al*., 2015). A schematic representation of this process is shown in Figure 1.5 below.

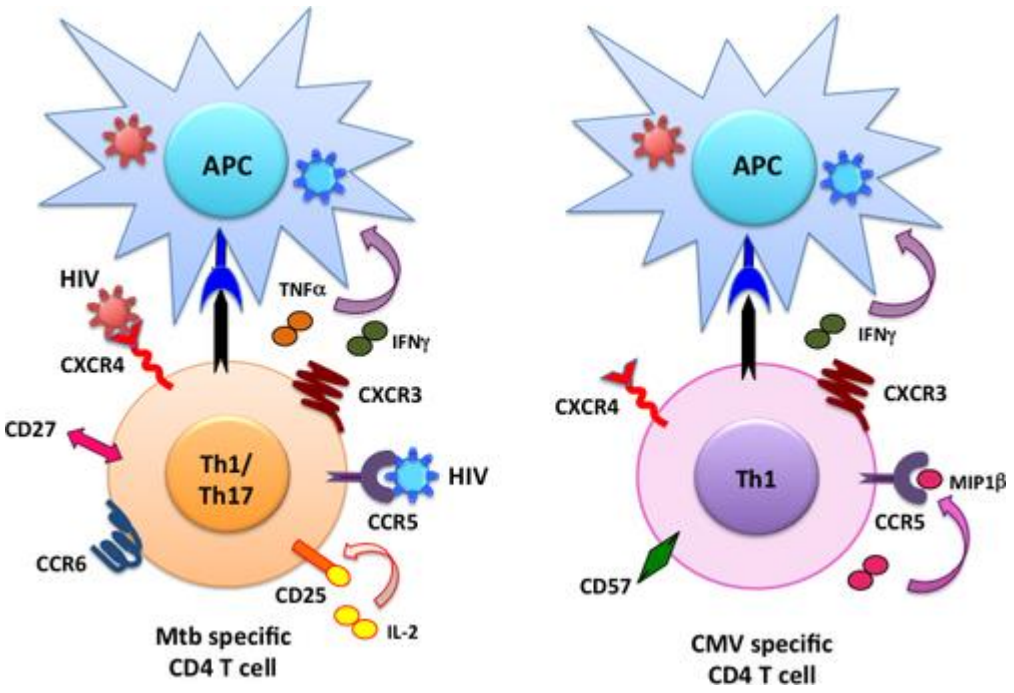

Figure 1.5: Antigen-specific CD4 T cell phenotypic and functional heterogeneity determines preferential depletion during HIV co-infection. CMV-specific CXCR3+CCR6 Th1 CD4 T cells are mature, terminally differentiated and primarily secrete IFN- and the CCR5 ligand MIP1, which blocks HIV entry. *M. tuberculosis*-specific CXCR3+CCR6+ Th1/Th17 CD4 T cells, on the other hand, are less mature but polyfunctional,

secreting IFN-, TNF-, and IL-2, making them highly proliferative but producing little MIP1, making them highly susceptible to HIV infection. Taken from Ahmed *et al*., 2016.

Up-regulation of *M. tuberculosis* entry receptors on macrophages, HIV manipulation of macrophage bactericidal pathways, deregulated chemotaxis, and an altered Th1/Th2 balance are other mechanisms reported to facilitate *M. tuberculosis* infection and disease in HIV infected patients (Pawlowski *et al*., 2012). HIV has also been shown to impair the TNF-mediated macrophage apoptotic response to *M. tuberculosis*, allowing the bacteria to survive (Pawlowski *et al*., 2012).

1.6 Diagnosis of *M. tuberculosis*

Several diagnostic tools are used for the detection of *M. tuberculosis*. Considering that TB is a pulmonary disease, sputum and bronchial washings are the primary sampling materials that are used for diagnosis (Caulfield *et al*., 2016). Active TB is typically diagnosed symptomatically and using a combination of molecular diagnostics and culture-based testing approaches. Symptomatic diagnosis involves a composite of physical symptom assessment such as presence of a cough, weight loss, night sweats with the use of chest radiography to confirm lung anomalies that are associated with *M. tuberculosis* (Caulfield *et al*., 2016). Molecular diagnostics include GeneXpert which detects TB DNA simultaneously with RIF resistance. Other molecular diagnostics include the urine LAM assay which detects the TB lipoarabinomannan (LAM) lipid and the IGRA tests such as the QuantiFERON gold which detect the immune response to TB. Culture based diagnostics are based on the cultivation of *M. tuberculosis* using solid media (LJ slants) or semi-automated liquid assays (BACTEC MGIT) and remains the gold standard for TB diagnosis (Schön *et al*., 2016). Furthermore, culturing is important for the phenotypic confirmation of drug susceptibility. Other supporting tests include direct detection of *M. tuberculosis* by smear microscopy using the Auramine or the Zeihl-Neelsen stain that target the unique *M. tuberculosis* mycolic acid layer. This is a widely used method because of its relatively low cost however, it has very low sensitivity (Sawadogo *et al*., 2012).

1.7 Treatment of drug sensitive TB

About 85% of the *M. tuberculosis* cases are curable with the appropriate treatment (WHO 2020). Drug sensitive TB is treated with a combination of isoniazid (INH) and rifampicin

(RIF), pyrazinamide (PZA), ethambutol (EMB). This combination TB treatment consists of a 4-drug regimen RIF, INH, PZA, and EMB for 2 months followed by 4 months of a combination of 2 drugs (RIF and INH) (Dookie *et al*., 2018). This protracted combinatorial treatment regimen has patient centric and health system related challenges, which contribute to the development of drug resistance (Schön *et al*., 2016). Patient-centric challenges include side effects from the drugs, HIV-co-infection and the associated drug-drug interactions. Health system related challenges include poor drug supplies, weak health systems and delayed diagnosis (Marais., 2015). In some cases, first line treatment does not successfully clear *M. tuberculosis* infection and disease.

In the South African health care system, culture positivity at 5 months of treatment is indicative of treatment failure. At this point, the culture is then tested for drug resistance as it is likely that failure of treatment is due to drug resistance. However, it should be noted that drug resistance can also be identified at the point of initial diagnosis before treatment commences. In this case, if the patient did not have TB before, primary resistance is diagnosed. If the patient had a prior episode of TB, it is possible that resistance developed within the patient. This is known as acquired resistance, which occurs due to intra-patient evolution (Smith *et al*., 2012). Regardless of the method of acquisition of drug resistance, the approach to treatment is not standard across patients as it is determined by the drug resistance profile and individual levels of tolerance to second and third -line drugs (Smith *et al*., 2012).

1.8 Drug resistance in *M. tuberculosis*

The rapid and widespread emergence of drug resistant TB poses a threat to TB treatment programs and ultimate eradication of this disease (Kurz *et al*.,2016). The primary mechanism through which drug resistance emerges in *M. tuberculosis* is through acquisition of mutations in genes that code for drug targets or drug-activating enzymes (Dookie *et al*., 2018, Kurz *et al*., 2016). *M. tuberculosis* strains resistant to INH and RIF , defined as multi-drug resistant TB (MDR-TB), accounted for ~480 000 incident cases and ~ 250 000 deaths in 2015 (WHO, 2016). Additionally, 106 countries to date have reported extensively resistant drug resistant tuberculosis (XDR-TB) strains, which are MDR strains that display resistance to both the fluoroquinolones and second line injectable drugs (WHO, 2016).

Mutations in the *katG* and *inhA* genes, which encode catalase peroxidase (a bifunctional hemoprotein that has been shown to activate INH) and NADH-dependent enoyl-ACP 5

reductase InhA (an enzyme that provides precursors of mycolic acids) respectively are associated with INH resistance (Zumla *et al*., 2013). As INH and ETH both target *InhA*, cross-resistance to these antibiotics due to *inhA* gene mutations is common (Brossier *et al*., 2011). EthA, a NADPH-specific FAD-containing monooxygenase encoded by the *ethA* gene, activates ETH (Brossier *et al*., 2011). As a result, mutations in the genes *ethA* or *ethR* (encoding the EthA regulator) result in ETH resistance (Brossier *et al*., 2011). PZA resistance is caused by mutations in the *pncA* gene, which codes for nicotinamidase or pyrazinamidase (an enzyme required for activation of PZA to its active form, pyrazinoic acid). Mutations in the *embB* gene, which codes for an arabinosyl transferase (an enzyme required for arabinogalactan synthesis), are linked to EMB resistance (Wade and Zhang, 2004). RIF resistance is determined by mutations in the RNA polymerase beta-subunit (Zumla *et al*., 2013) (Figure 1.6). These mutations have been associated with decreased fitness and transmissibility of resistant strains (Melnyk *et al*., 2014). Other mechanisms of TB drug resistance include compensatory mutations, efflux mediated resistance and deficient DNA repair mechanisms (Schön *et al*., 2016). Drug resistance has consistently posed a growing threat to global efforts to control TB, thus driving the need to develop new anti-TB drugs. To preserve the clinical utility of current drugs, TB is not treated with a single drug, rather combination TB regimens are recommended to prevent further emergence of drug resistant *M. tuberculosis* strains (Pai *et al*., 2016).

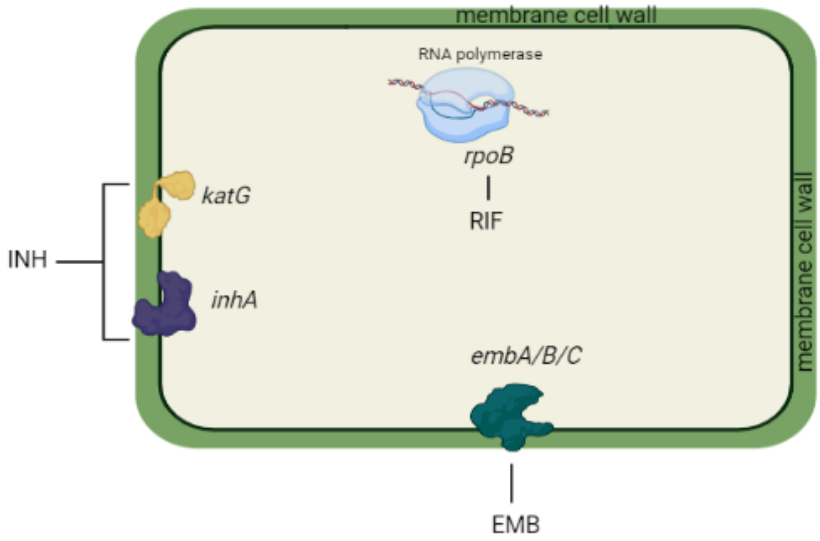

Figure 1.6: *M. tuberculosis* drug targets. Illustration showing a select set of *M. tuberculosis* drug targets. For RIF, mutations in the rifampicin resistance determining region in the *rpoB* gene confer resistance. For INH,

mutations in the *katG* and *inhA* genes confer resistance. Mutations in the *embA/B/C* genes confers ethambutol resistance. RIF- rifampicin, INH- isoniazid and EMB-ethambutol.

The GeneXpert *M. tuberculosis*/RIF assay is the mainstay molecular diagnostic assay used for the detection of drug resistance (Schön *et al*., 2016). In addition to GeneXpert, the Hain line probe assay is also used for the detection of specific mutations in drug resistant *M. tuberculosis*. However, unlike GeneXpert which primarily detects rifampicin resistance, the line probe assay simultaneously detects resistance to INH, RIF, fluoroquinolones and second-line injectables (Dookie *et al*., 2018).

Second-line drugs are used for persons who are resistant to the first-line drugs. These include injectable drugs which are the aminoglycosides kanamycin and amikacin and the cyclic peptide capreomycin (Dookie *et al*., 2018). Second-line drugs also include Fluoroquinolones which are potent bacterial antibiotics such as moxifloxacin and gatifloxacin whose mode of action is primarily the inhibition of DNA replication (Rendon *et al*., 2016). Other second-line drugs include the para-aminosaliyclic acid and ethionamide which inhibit folate synthesis and mycolic acid synthesis respectively, thus halting bacterial cell wall turnover (Streicher *et al*., 2011., Kurz *et al*., 2016). Mutations within the *katG, embB, pncA, rpoB, gyrA, rhyA* genes contribute to the resistance to second-line drugs (Streicher *et al*., 2011) resulting in XDR or totally drug resistant strains (TDR).

1.9 Tuberculosis strain typing

The genome of *M. tuberculosis* is highly conserved but despite this, subtle differences exist that enable differentiation of different strains. TB strain typing is useful in epidemiological studies to determine TB transmission patterns for example the Beijing and LAM strains are responsible for multiple outbreaks of Drug resistant-TB (Streicher *et al*., 2012). TB strain typing methods include spacer oligonucleotide typing (Spoligotyping), mycobacterium interspersed repetitive units-variable numbers of tandem repeat (MIRU-VNTR) and IS*6110* (Figure 1.7).

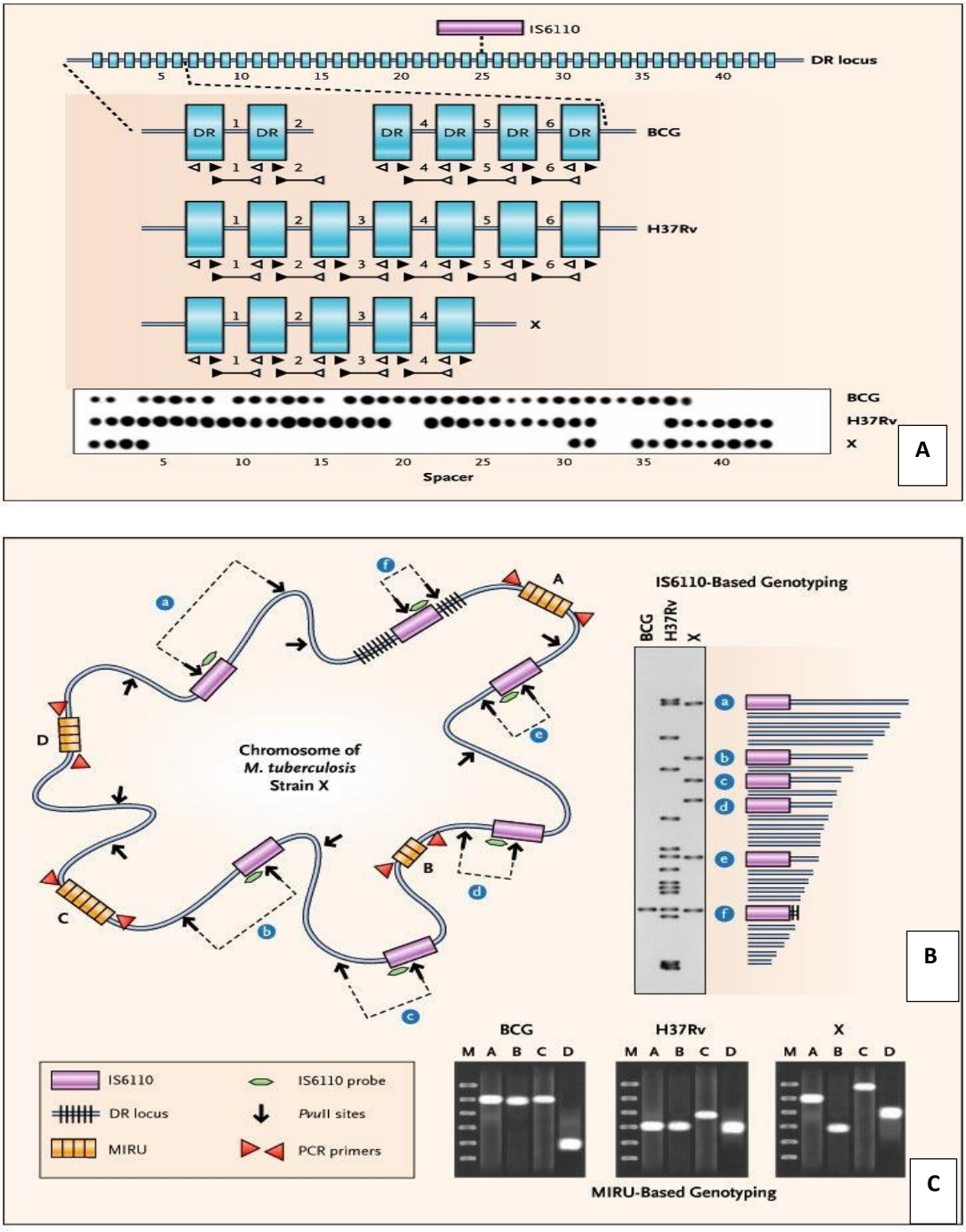

Figure 1.7: Tuberculosis strain typing. TB strain typing methods include IS6110 RFLP, Mycobacterium interspersed repetitive units-variable numbers of tandem repeat (MIRU-VNTR) and Spacer oligonucleotide typing (Spoligotyping). **(A)** Graphical representations of spoligotype patterns of certain strains, the dark spots represent the presence of a certain spacer whereas no spot represents the absence of that spacer. Each spacer has a unique pattern of spots. (**B**) The results of IS6110-based genotyping showing the sizes of each hybridizing fragment based on the distance from this site to the next *Pvu*II site. Examples of the IS6110 banding pattern of BCG, H37Rv, and strain X are reflected by the banding pattern on the gel. (**C**) The results of MIRU-based genotyping showing the bands of specific sizes for the PCR amplicons of 4 MIRU loci (A, B, C, and D) in BCG, H37Rv and strain X. (Taken from:

https://www.cdc.gov/tb/programs/genotyping/chap3/3_cdclab_2description.htm , Barnes and Cave, 2003)

1.9.1 Spoligotyping

Spoligotyping is a polymerase chain reaction-based typing system for the differentiation of mycobacterial strains (Xia *et al*., 2016). This technique exploits the genetic diversity in the CRISPR locus, which is also known as the direct repeat (DR) locus in the *M. tuberculosis* genome (Gori *et al*., 2005). It is one of the most common PCR-based molecular typing methods. The DR region is made up of multiple copies of a conserved 36-bp sequence (the DRs) separated by a variety of unique spacer sequences. PCR is used to amplify the entire DR locus using primers that are complementary to the DR sequence. With 43 spacer oligonucleotides, the PCR products are hybridized to a membrane. A set of 43 unique spacer sequences whose presence or absence is unique per strain are used to classify *M. tuberculosis* strains as shown in Figure 1.7A (Xia *et al*., 2016). The spoligotyping pattern is characteristic of a particular evolutionary lineage of strains and can be used for epidemiological tracking.

1.9.2 MIRU-VNTR

Almost all higher eukaryote genomes contain thousands of copies of tandemly repeated sequences. Because their repeat numbers are highly variable in many loci, they are referred to as "variable number tandem repeat" (VNTR) loci. Different research groups discovered small repetitive DNA sequences with distinct characteristics in *M. tuberculosis* and other mycobacterial genomes (Ei *et al*., 2016). Supply *et al*. identified a novel minisatellite-like structure in the *M. tuberculosis* genome made up of 40- to 100-bp repetitive sequences "mycobacterial interspersed repetitive units"(MIRU) in 1997 (Supply *et al*., 1997). These are found in 41 different places throughout the *M. tuberculosis* H37Rv genome, in intergenic regions. Among the 41 sites, 12 have polymorphisms in the copy number of unrelated *M. tuberculosis* isolates. MIRU-VNTR is used to type loci in the *M. tuberculosis* genome that show polymorphism in the number of tandem repeats (Rasoahanitralisoa *et al*., 2017). MIRU strain typing categorizes the number and size of repeats in 12 independent loci, which are unique per strain using polymerase-chain-reaction (PCR) amplification and gel electrophoresis as shown in Figure 1.7 C (Xia *et al*.,2016).

1.9.3 IS6110

Insertion sequence *6610* (IS*6110*) is a mobile element that is 1,355 bp long and belongs to the IS3 family. The IS6110 sequence is found only in the *M. tuberculosis* complex in multiple copies (Ei *et al*., 2016). IS6110 copy number ranges from 0 to 25, depending on the frequency of transposition, which is largely determined by the nature of the genomic region where transposition occurs (Ei *et al*., 2016) . IS6110 polymorphism is caused by differences

in copy number and location within the genome (Jagielski *et al*., 2014). These features allow IS6110 to be useful as a specific molecular marker for genotyping *M. tuberculosis* strains. The IS6110-based Restriction fragment length polymorphism (RFLP) typing uses agarose gel electrophoresis to determine the size of genome fragments obtained from *Pvu*II restriction digestion of the IS6110 element, which is randomly scattered throughout the genome in a strain specific manner (Ei *et al*., 2016). The resultant banding pattern is specific to the number and position of the IS6110 element in that particular genome and it is unique per strain as shown in Figure 1.7 B.

1.9.4 Whole genome sequencing

While these other typing techniques specifically target polymorphic genetic targets, they interrogate less than 1% of the genome and thus have an intrinsically limited discriminatory power (Ei *et al*., 2016). As a result, they are unable to detect and resolve recent transmission chains optimally. This limitation may be overcome by using next generation whole genome sequencing (WGS) for genome-based epidemiology. WGS provides comprehensive genetic information, including all potential genomic targets, as well as valuable information about drug resistance, virulence determinants, and genome evolution (Merker *et al*., 2017). WGS has the potential to become the ultimate tool for diagnostics and pathogen typing, and to dramatically increase the impact of molecular diagnostics on clinical microbiology, as ongoing technological developments reduce costs.

1.10 Tuberculosis strain distribution

The *M. tuberculosis* complex has evolved into six lineages based on their geographical location, East Asian, Euro-American, West African 1 and 2, Indo-Oceanic, and East African-Indian are among them (Peters *et al*., 2020). The six lineages of *M.tuberculosis* complex are defined by changes in large sequence polymorphisms (LSPs) and single nucleotide polymorphisms (SNPs) in addition to geographical location (Chihota *et al*., 2018) . Several *M. tuberculosis* strain types have evolved from the six lineage strains and are widely disseminated in South Africa, these include Beijing, LAM, CAS, S-family, X, and T1 strains. The founder effect, in which particular *M. tuberculosis* strains were first introduced into the country were as a result of colonization and maritime trade, followed by spread throughout the country by individual movement (Hanekom *et al*., 2011). In South Africa, four strain

types dominate the TB epidemic: LAM, Beijing, T-strains, and X-strains (Chihota *et al*., 2018) as shown in Figure 1.8.

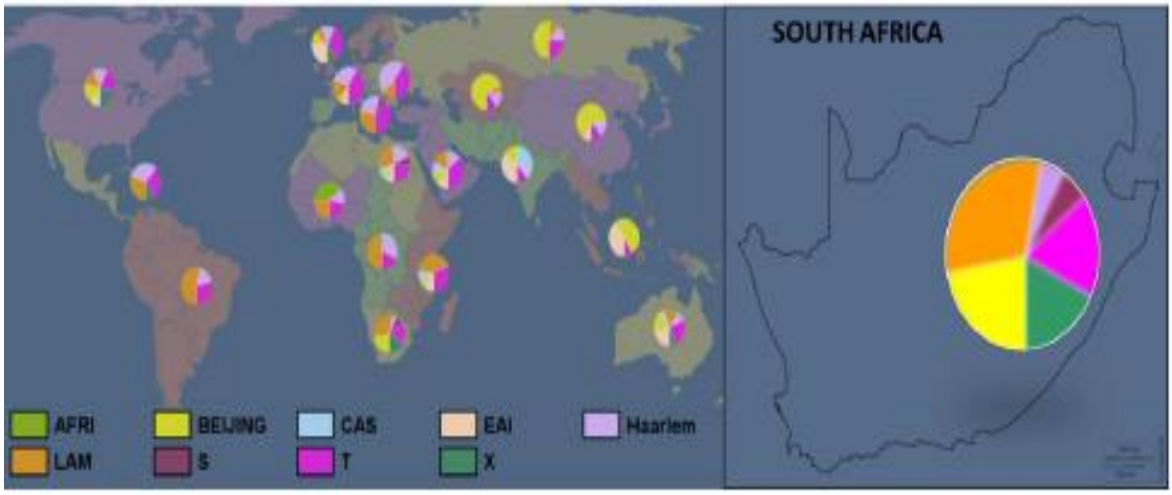

Figure 1.8: TB global strain distribution. Each pie chart segment reflects the relative proportion of *M. tuberculosis* isolates belonging to respective major lineages for each country. On the right is a map of South Africa showing that the LAM, X, Beijing and T strains are the dominate strain type infecting the population (Taken from: online SITVIT database: www.pasteur-guadeloupe.fr:8081/SITVIT_ONLINE).

The Beijing and LAM strains have been the focus of much research aimed at elucidating the mechanisms behind their greater penetration in human populations. Due to its increased virulence and transmission properties compared to other clinical strains, the Beijing strain, first identified in 1995, has evolved into a successful strain (Liu *et al*., 2017). The strain has expanded globally since its origins in East Asia, and it was transferred to South Africa via trade routes (Chihota *et al*., 2018). The HIV epidemic is thought to be the primary driver for the rise in Beijing lineage prevalence in South Africa (Viegas *et al*., 2013). The sub-lineage strain LAM is assumed to have arrived in Southern Africa via Portuguese expeditions and trade (Chihota *et al*., 2018). A LAM derivative: F15/LAM4/KZN strain has been linked to MDR-TB and was the source of South Africa's first case of XDR-TB (Gandhi *et al*., 2014). The Beijing and LAM associated phenotype includes characteristics such as alternative host modulation, distinct pathological features and drug resistance (Kumar *et al*., 2017; Liu *et al*., 2017).

Recent studies have reported that the frequency of mutations causing drug resistance varies according to the lineage to which the *M. tuberculosis* strain belongs (Rad *et al*., 2003). The Beijing group of strains is strongly associated with increased mutation rates *in vitro* and higher proportions of drug resistance in comparison to other strains in the clinical setting (Parwati *et al*., 2010). Research suggests that Beijing strains have alterations in putative mutator genes, resulting in altered DNA repair mechanisms which eventually result

in elevated mutagenesis and drug resistance (Rad *et al*., 2003, Dookie *et al*., 2018, Melnyk *et al*., 2014). LAM strains have also been linked to drug resistant outbreaks especially in Southern Africa (Gandhi *et al*., 2016, Said *et al*., 2021) . Based on this, these two strain types have been chosen for further analysis in this study.

1.11 Phenotypic growth heterogeneity in *M. tuberculosis*

1.11.1 Dormancy

During TB infection, the mycobacterial cell wall provides significant resistance to antimicrobial stresses posed by the immune system. *M. tuberculosis* is also capable of adapting to environmental changes such as hypoxia, nitrogen and nutrient limitation by entering a dormant state (defined as a reversible state of metabolic shiftdown in which bacteria persist without cell division) (Kana and Mizrahi, 2010). Because mycobacteria do not form spores, the transition to this dormant state is accomplished through a transcriptional response that allows the bacteria to remain viable but not culturable (Kana and Mizrahi, 2010). To resume growth, dormant bacteria require an exogenous supply of growth factors, including resuscitation promoting factors (*Rpf*s) (Kana *et al*., 2008). No definitive link has been established between resuscitation of dormant bacteria and progression to active disease in individuals with LTBI. That said, dormant bacteria may represent a subpopulation of bacteria that resist immunological stresses and anti-TB drugs.

The success of *M. tuberculosis* as a pathogen has been attributed to its ability to shift between active growth and dormancy. Dormant cells are non-replicating cells that are characterized by low metabolic activity and phenotypic drug tolerance (Ayrapetyan *et al*., 2015). Dormant cells can resuscitate and subsequently regain growth when the environment becomes permissive (Buerger *et al*., 2012). Persister cells are slow or non-growing subpopulations present within a growing culture and can be induced by stressful environments which include exposure to antibiotics, stressful pH, oxidative stress, DNA damage and starvation (Ayrapetyan *et al*., 2015). It is unclear what triggers the establishment of these states however, studies suggest that these populations spontaneously exist within bacterial populations naturally so as to preserve a proportion of the population when adverse environmental conditions prevail (Ayrapetyan *et al*., 2015). The difference between viable but non-culturable (VBNC) cells and persister cells is that persisters regain growth on

nutrient medium shortly after the removal of stress, whereas VBNC cells are unable to do so unless the growth is supplemented with special growth factors (Ayrapetyan *et al*., 2015).

Despite their inability to grow in normally permissive media, VBNC cells are not considered dead due to a variety of differences. Dead cells have a damaged membrane that makes it impossible for chromosomal DNA to be retained, whereas VBNC cells have an intact membrane that contains undamaged genetic information (Heidelberg *et al*., 1997; Cook and Bolster, 2007). Plasmids, if present, are also retained in VBNC cells (Oliver, 2010). Unlike dead cells, which are metabolically inactive, VBNC cells can maintain metabolic activity and respire. Furthermore, dead cells do not express genes, whereas VBNC cells maintain transcription and thus mRNA production (Lle *et al*., 2000). VBNC cells, as opposed to dead cells that no longer use nutrients, were found to have continued uptake and incorporation of amino acids into proteins (Li *et al*., 2014).

Although VBNC cells share many general characteristics with viable cells, they differ significantly physiologically and molecularly from viable, culturable cells. Cellular morphology, cell wall/membrane composition, metabolism, gene expression, physical and chemical resistances, adhesion properties, and virulence potential are all examples of differences (Li *et al*., 2014). In terms of cellular morphology, VBNC cells commonly exhibit a reduction in cell size and thus an increase in the surface area to volume ratio, most likely as a strategy to reduce energy requirements (Li *et al*., 2014). It is important to note that bacteria that enter the VBNC state can revert to culturable status, implying that this state is reversible. A variety of stimuli, such as an increase in temperature, an increase in nutrient concentration, and the presence of host cells, can cause resuscitation (Li *et al*., 2014, Aryapetyan *et al*., 2015).

1.11.2 Differentially culturable tubercle bacilli (DCTB)

Previous studies have shown that the sputum from TB infected patients harbors a large proportion of drug-tolerant bacteria, referred to as differentially culturable tubercle bacilli (DCTB) (Chengalroyen *et al*., 2016). This distinct population of bacteria is unable to form colonies on agar plates but can be resuscitated in liquid media. Different DCTB populations have been identified in sputum, some of which are resuscitation promoting factor (*Rpf*)-dependent, while others can resuscitate independently of *Rpf*s (Chengalroyen *et al*., 2016). In these experiments, culture filtrate (CF) with and without *Rpf*s was used for stimulation of DCTB. *Rpf*s, first discovered in *Micrococcus luteus*, are lytic transglycosylases needed for

cell wall remodelling and synthesis (Vollmer *et al*., 2008). *Rpf*s are a group of peptidoglycan degrading enzymes that are secreted by mycobacteria and enhance bacterial culturability (Dusthackeer *et al*., 2019). These proteins are secreted by actively growing bacteria into the growth media and are capable of activating the growth of DCTB (Chengalroyen *et al*., 2016).

The quantum of DCTB is expected to decrease at a slower rate than metabolically active TB during anti-TB treatment, and there is evidence that DCTB subpopulations can be identified in sputum samples even late in treatment (Beltran *et al*., 2020). When genetically susceptible bacteria are not killed by inhibitory concentrations of the drug, temporary, reversible drug tolerance occurs and is the primary reason for longer TB treatment durations (Júnior *et al*., 2020). Since the dynamics of the DCTB subpopulation during infection and treatment may underpin the difficulty in improving TB treatment, accurate quantification of the DCTB could predict individual patient outcomes as well as assess the efficacy of new drug candidates (Rosser *et al*., 2017). Furthermore, the presence of live bacilli in sputum samples later in standard anti-TB treatment may be useful in detecting patients at risk of failure or relapse, particularly on shorter regimens. A previous unpublished study on sputum from drug susceptible TB patients (Padarath, MSc dissertation) demonstrated that some strains have a greater propensity than others to enter the DCTB state. This study showed that Beijing strains produced more DCTB compared to LAM when cultured under carbon starvation conditions (Padarath, MSc dissertation).

1.12 Hypothesis

In *M. tuberculosis*, chromosomal mutations result in drug resistance. These mutations can affect several aspects of metabolism in drug resistant bacilli, often referred to as a fitness cost, which may be differentially impacted in clinical isolates. Examples of these effects include changes in the ability to grow in laboratory media. We therefore hypothesized that different clinical isolates of *M. tuberculosis* differ in their ability to enter and exit the differentially culturable (DC) state.

1.13 Aim

The main aim of this study is to determine drug resistance strain types and associate these with their propensity to adopt the DC state using an *in-vitro* carbon starvation model by incubating the cells in PBS. Furthermore, we aim to assess the ability of different DR strains to exit the DC state using Culture filtrate (CF) from cognate *M. tuberculosis* strains.

1.14 Study objectives

1. Molecular typing of drug resistant *M. tuberculosis* strains by Spoligotpying.
2. Assessment of propensity of different DR strains to adopt the DCTB state according to strain typing outcome from objective 1 and previously obtained DCTB results (results from a DCTB assay available in the lab)
3. Selection and purification of 5 LAM and 5 Beijing strains from the strains characterised in objective 1 and 2 through antibiotic and antifungal treatment.
4. Application of the carbon starvation model to generate DCTB.
5. MPN assays to assess quanta of DCTB from the carbon starvation model using PBS as a culture medium in objective 4.
6. Supplementation of MGIT assays with culture filtrates to assess the rate of exit of the DCTB generated in objective 4.
7. Staining of DCTB cells with various dyes for microscopy to assess changes in cell morphology.
8. RNA extraction to determine the expression of the *dosR* gene on the Beijing and LAM strains.
9. Sequencing of the resistance conferring genes on *M. tuberculosis* clinical strains.

2. Materials and Methods

2.1 Materials used

A detailed list of materials used in this study can be found in Appendix A.

2.2 Selection Criteria of bacterial strains

The samples used in this study were obtained from frozen bacterial cultures. These cultures were generated by culturing sputum in DCTB assays in laboratory media and the resulting bacteria was frozen. The samples were collected from a previous study where the main purpose was to compare treatment success of a WGS-derived individualized drug resistant TB regimen to a standard regimen based on South African National Tuberculosis guidelines (termed the InDEX study - BFC584/16 at CAPRISA). DCTB assays were performed in the study and in this dissertation, the quanta of DCTB according to lineage was investigated. No DCTB assays were conducted directly on sputum in this MSc study.

2.3 Preparation of media and solutions

The laboratory strain H37Rv and frozen clinical strains Beijing and LAM were grown in sterile Middlebrook 7H9 liquid media. To prepare this, 4.7 g of the 7H9 powder was added into 900 ml of filtered water and supplemented with 0.2 % glycerol, Middlebrook oleic acid-albumin-dextrose-catalase (OADC) supplement and 0.05% Tween80. The cultures were also grown in solid BBL Middlebrook 7H11 prepared by adding 20.5 g of 7H11 powder with 900 ml of filtered water supplemented with OADC. To prevent contamination, the antibiotic mixture Polymyxin B, Amphotericin B, Nalidixic acid, Trimethoprim and Azlocillin (PANTA) was added into 7H9 and 7H11 media. In 48 ml of 7H9, 2 ml of PANTA was added to make up a preparation containing 1X PANTA. For solid media, 32 ml PANTA was added to 7H11 to make up 1X PANTA preparation. To prepare the PBS that was used for carbon starvation, 8 g of NaCl, 0.2 g of KCl, 1.44 g of Na_2HPO_4 , 0.24 g of KH_2PO_4 and 2 ml of tyloxapol were dissolved in 1000 ml of filtered water.

2.4 Laboratory strains and culturing conditions

For this study, 5 frozen stocks of LAM and 5 Beijing strains were selected from the InDEX study. In addition, culture filtrate from a wild type H37Rv, LAM and Beijing strains were utilized in this study. These strains and their culture conditions are described in table 2.1 below.

Table 2.1: List of *M.tuberculosis* strains used in this study.

Strain	Description	Culture conditions
H37Rv	Johannesburg laboratory strain (ACCT:25618) was used as a control strain for this study.	37°C, without shaking in Middlebrook 7H9 media supplemented as described in section 2.3.
Beijing	Clinical strain. Five Beijing strains (Beijing 1, Beijing 2, Beijing 3, Beijing 4 and Beijing 5) were isolated from TB infected patients in the InDEX study	
LAM	Clinical strain. Five LAM strains (LAM 1, LAM 2, LAM 3, LAM 4 and LAM 5) were isolated from MPN assays that were stored	

2.5 DNA extraction: Colony boil

To extract crude DNA for spoligotyping, the colony boil method was used. A *M. tuberculosis* colony from a solid media plate was picked using a sterile inoculation loop and re-suspended in 100 µl dH2O in an O-ring screw cap tube. The suspension was then incubated at 95 °C for 5 minutes in a heating block and 100 µl chloroform was added after cooling the suspension and vortexing for a few seconds. This was then centrifuged at 13 000 rpm for 5 minutes and 80 µl of the aqueous phase containing the gDNA was removed and aliquoted into a sterile 1.5 ml O- ring screw cap tube. The gDNA was then used for PCR analysis.

2.6 Spoligotyping

2.6.1 Polymerase chain reaction (PCR)

To determine the strain type, the spoligotyping method was used as described in Figure 2.1. DNA was obtained using the colony boil method, as described in section 2.7, from cryopreserved decontaminated sputum.

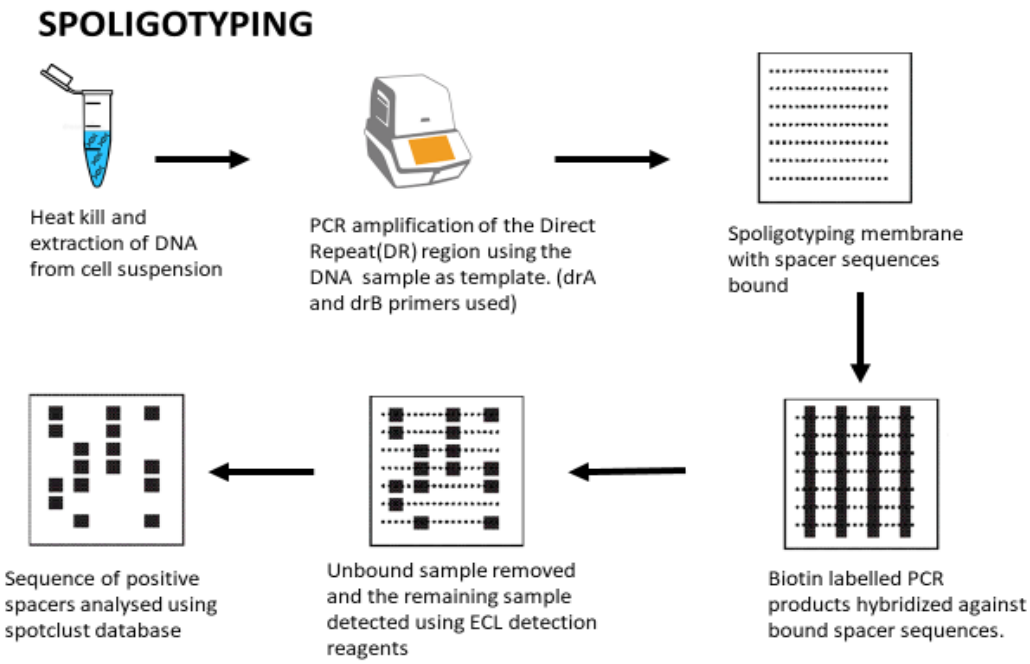

Figure 2.1: Strain typing of *M. tuberculosis* using spoligotyping. A flow diagram showing the steps carried during the spoligotyping procedure. DNA is extracted from *M. tuberculosis* and the Direct Repeat region amplified using PCR. The amplified DNA products are hybridised to a spoligotyping membrane, which contains bound oligo spacer sequences. The bound products are detected using enhanced chemiluminescence (ECL).

For further confirmation of strain types, spoligotyping was carried out again using DNA obtained from cryopreserved cultures of bacteria derived from sputum that was taken through the specialist DCTB culture assays. Pure DNA from *M. bovis* BCG and *M. tuberculosis* H37Rv (Mapmygenome, India) and a no template control (distilled water) were added as controls. Amplification of the direct repeat loci was carried out by PCR using streptavidin bound DrA and DrB primers described in table 2.2 (Mapmygenome, India). The mastermix was prepared according to table 2.3 below.

Table 2.2: Primers used for the confirmation of clinical strains

Primer	Primer oligonucleotide sequence (5'-3')	Annealing (Tm) of the primer	Storage temperature
DrA	GGTTTTGGGTCTGACGAC	55°C	4°C
DrB	CCGAGAGGGACGGAAAC	55°C	-20°C

Table 2.3: Reagents used to make the mastermix for PCR component of spoligotyping.

	1x reaction (µl)
Kapa ready mastermix (Add concentration for all exept H20)(Sigma)	12.5
dH_2O	6.5
DrA Primer (Mapmygenome)	2
DrB Primer (Mapmygenome)	2
DNA	2
Total volume	25

The PCR reaction was briefly spun down for 30 seconds to ensure that all components were mixed and that there were no air bubbles. The PCR tubes were placed into a thermocycler machine (BioRad) and cycling parameters were programmed according to the table 2.4 below.

Table 2.4: Cycling parameters for the PCR reaction

	Temperature (°C)	Duration
Initial denaturation	95	3 min
Denaturation	94	1 min
Annealing	55	1min
Extension	72	30 sec
Final Extension	72	10 min
Hold	4	∞

2.6.2 Hybridization

Following the PCR amplification, amplicons were denatured in 150 µl of 2× SSPE/0.1 SDS at 99 ºC for 10 minutes in a thermocycler and immediately placed on ice to prevent the re-

annealing of the denatured DNA. The denatured PCR amplicons were added to a membrane containing probes for the 43 direct repeat spacer sequences that are present in the *M. tuberculosis* genome in a mini-blotter cassette system to allow for hybridization. Hybridization was carried out at 60 ºC for an hour and the membrane was washed twice using 2X SSPE/0.5% SDS for 5 minutes each to remove any unbound DNA. Contents of each solution are given in the appendix.

2.6.3 Detecting the binding pattern

To determine the binding pattern, the membrane was incubated for an hour in a 0.025% Streptavidin-HRP (Thermofischer) solution at 42 ºC. The membrane was then washed twice with 2x SSPE/0.5% SDS at 42ºC for 5 minutes and twice with 2X SSPE at room temperature for 5 minutes to remove any unbound Strep-HRP. The Enhanced chemiluminescence (ECL) detection reagents (Amersham) were added directly to the membrane to detect the binding pattern using a chemiluminiscent reaction that detects streptavidin-HRP. The blot was then exposed to an X-ray film for 30 minutes and the blot was developed using X-ray developing and fixing solutions (Africa Xray Industrial). The resultant spots on the X-ray film were then entered into the Spotclust database to determine strain type. The strain types were then determined using Spotclust, a freely available online database for spoligotyping: https://tbinsight.cs.rpi.edu/run_spotclust.html. Contents of each solution are given in the appendix.

2.7 Purification and culture of selected strains

Based on the spoligotyping results, 5 LAM (LAM 1, LAM 2, LAM 3, LAM 4 and LAM 5) and 5 Beijing (Beijing 1, Beijing 2, Beijing 3, Beijing 4 and Beijing 5) strains were selected and re-cultured in Middlebrook 7H9 liquid and 7H11 solid agar as described in section 2.4 above. Purification of *M. tuberculosis* from stored sputum cultures was carried out by careful selection of TB growth over other oral organisms by cultivation in media with PANTA as described in Figure 2.4. A volume of 5 ml of 7H9-PANTA was added into a culture flask and approximately 1 ml of each decontaminated sputum sample was added into the appropriate flask. A volume of 100 µl of the cell suspension in the culture flask was plated int 7H11-PANTA plates prepared as described in section 2.3 above. The 7H11 plates and culture flasks containing the cell suspension were then incubated at 37°C and monitored weekly for growth as depicted in Figure 2.2 below.

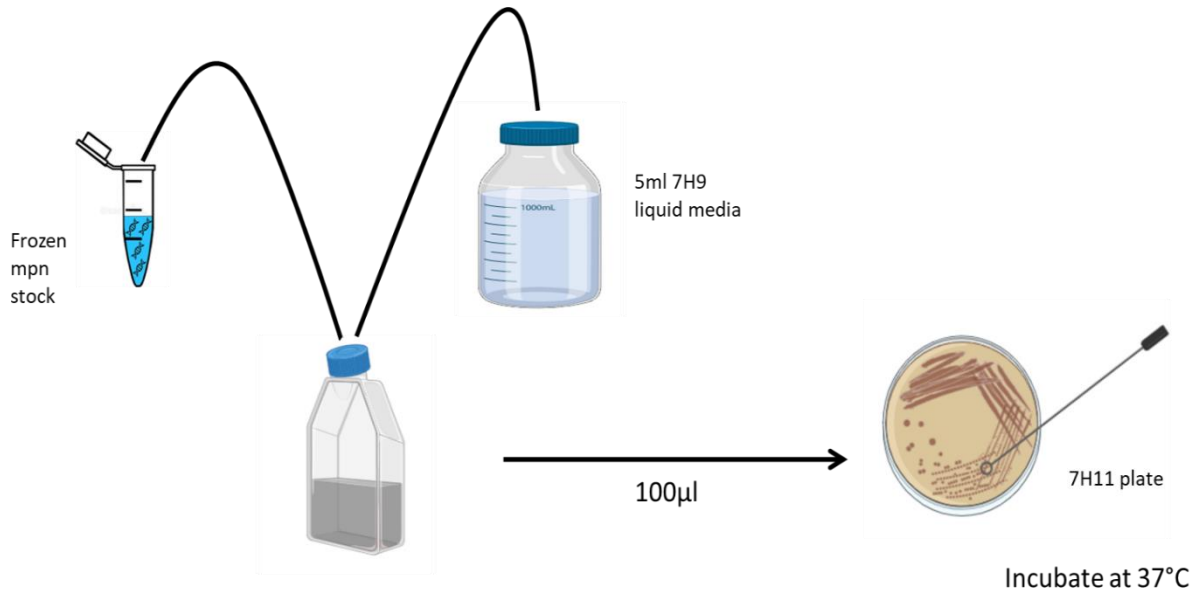

Figure 2.2: Purification of frozen stock through antibiotic and antifungal treatment. Decontaminated sputum or stored cultures from MPN wells were added into 7H9-PANTA. 100 µl of this cell suspension was used to spread onto 7H11-PANTA to select *M. tuberculosis* colonies.

To obtain single colonies from cultures, 10-fold serial dilutions of the cultures were carried out in screw cap Eppendorf tubes and plated on 7H11 plates supplemented with PANTA as depicted in Figure 2.3.

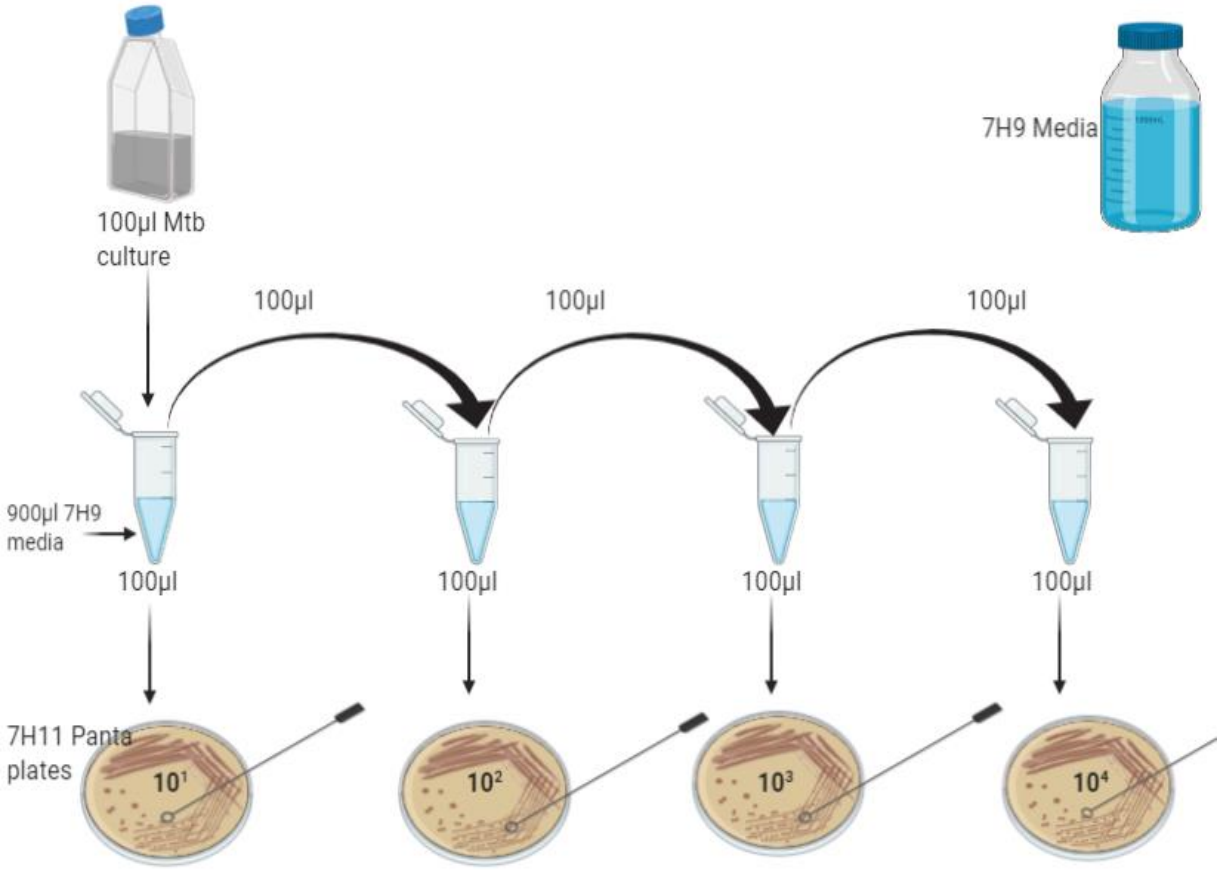

Figure 2.3: Purification of TB cultures. Shown is the preparation of 10-fold serial dilutions of the cultured cell suspension following incubation. To dilute the cultures, 900µl of 7H9 liquid media was added into 1.5ml Eppendorf tubes. A volume of 100 µl of the culture was then added into the first Eppendorf tube (10^1). This was vortexed for 5 seconds and 100 µl of this was added into the next Eppendorf tube and vortexed as before to create the 10^2 dilution. This was repeated up to the 4^{th} dilution. The serial dilutions were then plated into the appropriately labelled 7H11 plates with PANTA and incubated at 37°C and growth was assessed weekly.

2.8 Large-scale genomic DNA isolation

The Cetyltrimethylammonium Bromide/ Sodium Chloride (CTAB/NaCl) method was used for large-scale genomic DNA isolation from *M. tuberculosis*. This method was used to extract pure DNA for sequencing. Briefly, *M. tuberculosis* strains were grown in Middlebrook 7H9 media to an OD_{600nm} of 2.5. A volume of 10 – 25 ml of each culture was transferred to a 50 ml Falcon tube and pelleted by centrifugation at 4500 rpm for 10 minutes. The supernatant was discarded and the pellet re-suspended in 500 µl of 1x Tris-HCL EDTA (TE) buffer (10mM Tris-HCL, 10mM EDTA, pH 8). The suspension was transferred into a 1.5 ml O-ring screw-cap tube and heat killed at 75 °C for 30 minutes in a heating block. The tubes were removed from the heating block and placed in a rack and allowed to cool. A volume of 50 µl of lysozyme (10mg/ml) was added to the cells and mixed by gently inverting

the tube 2-3 times. The tubes were incubated at 37 °C for 1 hour. A volume of 70 µl of 10% SDS and 6 µl of 10 mg/ml Proteinase K was added to each tube and incubated at 65 °C for 1 - 2 hours in a heating block. After the 2 hours, 100 µl of pre-warmed (65°C) NaCl (5 M) was added and mixed by inverting a few times. A volume of 80 µl of pre-warmed CTAB/NaCl (10% CTAB + 4.1% NaCl) was added to each tube and this was mixed a few times and incubated in the heating block at 65 °C for 15 minutes. Thereafter, 900 µl of chloroform:isoamyl alcohol (24:1 v/v) was added and thoroughly mixed by inversion up to 20 times until a milky white homogenous solution was formed. This was centrifuged at 13 000 rpm for 10 minutes to separate the phases. The upper aqueous phase was carefully removed using a pipette into a new O-ring Eppendorf tube taking care not to disrupt the interface. To precipitate the DNA, a volume of 450 µl of isopropanol was added to each tube and this was mixed by inverting a few times. The tubes were then incubated at -20 °C for 30 minutes and centrifuged at 13 000 rpm for 20 minutes to pellet the DNA. The supernatant was discarded and the pellet was washed with 1 ml of 70 % Ethanol followed by centrifugation at 13 000 rpm for 10 minutes. The ethanol was discarded and the pellet dried in a SpeedVac (Eppendorf) at 60 °C for 10 minutes. The dried pellet was then re-suspended in 100 µl TE and allowed to dissolve at 65 °C for 10 minutes. This gDNA was used for PCR . Contents of each solution is given in the appendix.

2.9 Optimization of PCR conditions for resistance determining regions

To amplify resistance-conferring genes (*katG* and *embB)* of isoniazid and ethambutol, PCR was performed. The primers (described in table 2.8) were optimized using gradient PCR at different temperatures. To perform the PCR, a mastermix was made using the reagents in table 2.5. The cycling conditions for the PCR are shown in table 2.6 and 2.7. The PCR products were then run on a 4% agarose gel for 1 hour at 90V. Marker V was used as the molecular marker.

Table 2.5: Reagents used for the PCR mastermix

PCR component	**Volume (µl)**
5x Q5 Reaction buffer	4
5x Q5 High GC enhancer	4
1.25 mM dNTPs	3.2
10 mM Forward primer	1
10 mM Reverse primer	1
2U/µl Q5 High fidelity DNA polymerase	0.2
Template DNA	1
Nuclease-free water	5.6

Table 2.6: Cycling parameters for the PCR reaction

	Temperature	Time
Initial denaturing	98 °C	30 sec
Denaturing	98 °C	10 sec
Annealing	*****	*****
Extension	72 °C	*
Final extension	72 °C	2 min
Hold	12 °C	∞

*****different for each primer, refer to table 2.8.

Table 2.7: PCR primers. Primers used to amplify

Gene	**Primer type**	**Primer sequence (5'-3')**	**Annealing temperature (°C)**	**Extension time**	**Fragment size (base pairs)**
katG	Forward	GAAACAGCGGCGTGATCGT	66 °C	6 sec	210
	Reverse	GTTGTCCCATTTCGTCGGGG			
embB	Forward	CCGACCACGCTGAAACTG	66 °C	11 sec	368
	Reverse	GTAATACCAGCCGAAGGGATCCT			

DNA sequencing of the PCR products was done by the DNA sequencing facility at the University of Stellenbosch.

2.10 Growth Kinetics of *M. tuberculosis* clinical strains

The growth rates of the clinical strains were assessed by conducting growth curve experiments in triplicate and compared to wild type *M. tuberculosis* H37Rv. Briefly, the bacterial strains were grown to an OD_{600nm} of 0.6 at 37 °C in 9 ml of Middlebrook 7H9 broth. Thereafter, the pre-culture of each strain was diluted to an OD_{600nm} of 0.05 in 20 ml of Middlebrook 7H9 broth. The cultures were incubated at 37 °C and the growth rate was assessed by generating a scatter plot from data obtained by recording the OD_{600nm} of each culture after every 48 hours. GraphPad Prism 8 software (student's t-test)was used for statistical analysis.

2.11 *In vitro* stress models

2.11.1 Saito *et al*., sequential stress model

A Phosphate buffered saline (PBS) based carbon starvation model was used to create DCTB according to Saito *et al*., 2017. Briefly, *M. tuberculosis* strains that were purified from decontaminated sputum in section 2.9 above were grown in triplicate in 20 ml of Middlebrook 7H9 complete media to an OD_{600nm} between 0.4 and 0.8. The cultures were then split equally into 2 Falcon tubes. The cell suspensions were centrifuged at 4 000 x g for 8 minutes and the pellet was resuspended in PBS-Tx(Tyloxapol) and 7H9 respectively. This wash step was repeated twice to ensure the removal of previous media. Following the second wash and resuspension, a single-cell suspension was created by centrifugation at 200 × g for 8 min at 0 de-acceleration. The supernatant of this single-cell suspension was then carefully aspirated from the surface of the liquid front using a serological pipette ensuring that the pellet was left untouched and leaving behind approximately 3–5 ml volume in the falcon tube. The OD_{600nm} of both the PBS and 7H9 single-cell suspensions was then assessed and the PBS single cell suspension was diluted using PBS-Tx to an OD_{600nm} of 0.1 and incubated at 37 °C, 20% O_2, and 5% CO_2, without shaking for 1 week. The 7H9 single cell suspension was used for pre-starvation MPN and CFU assays (described below), to obtain the initial number of organisms prior to starvation. After 1 week's incubation, 1 ml of the starved culture was used for MPN and CF assays to obtain the number of culturable organisms after starvation.

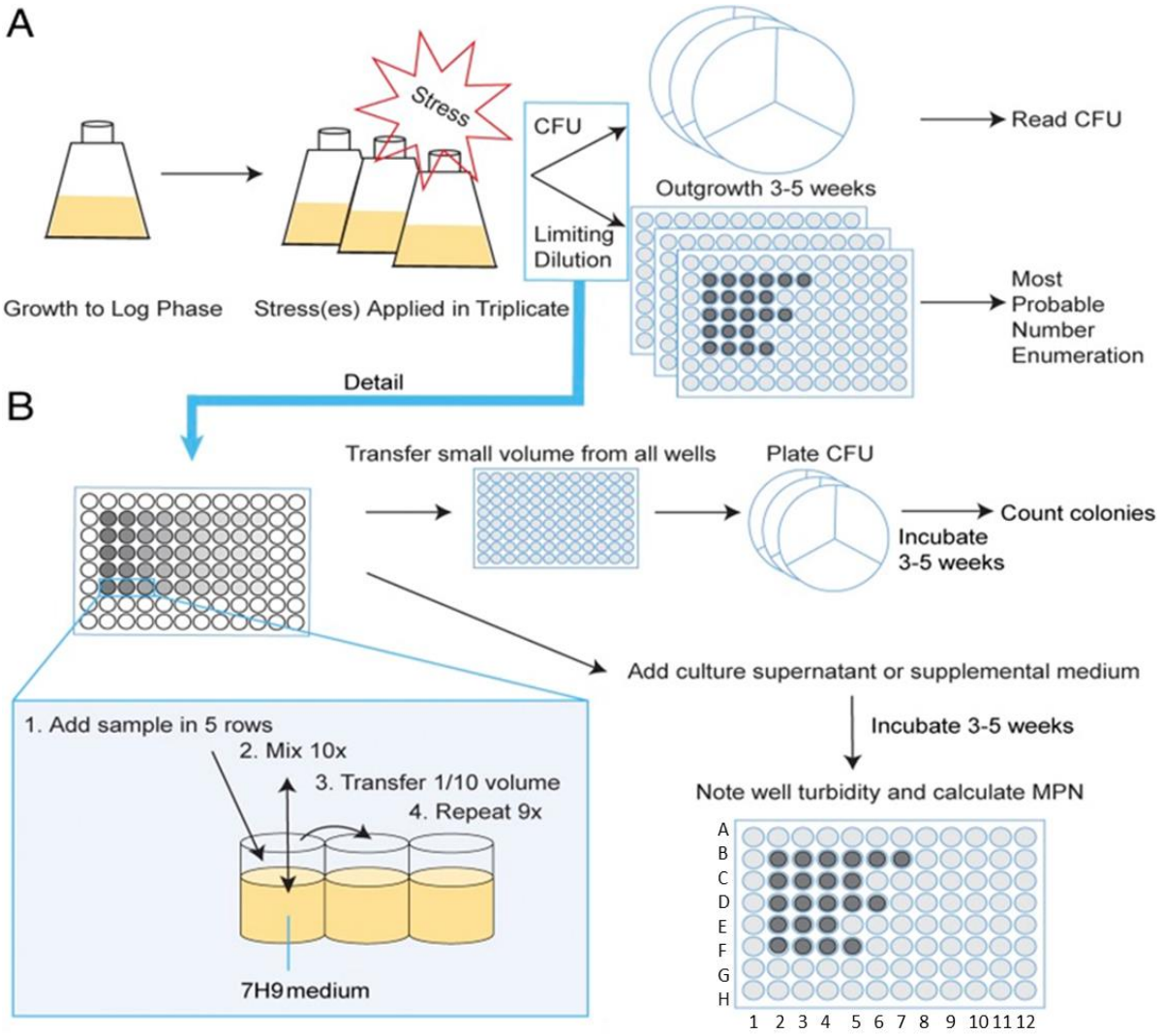

Figure 2.4: Schema for producing and counting DCTB. (A) General schema. *M. tuberculosis* was grown to log phase, subjected to stresses, and diluted serially in a rich medium in pentaplicate to the point that no growth is observed at the higher dilutions. Samples from the same dilution series were spread on agar plates made from nutrient-rich medium to count CFUs. When there is no further outgrowth in the dilution series, the pattern of growth of *M. tuberculosis* in the dilution series was recorded and used to determine the MPN. Differentially culturable *M. tuberculosis* = MPN – CFUs. (B) Detailed schema. After vortexing, samples were added to five replicate rows of a 96-well plate filled with 7H9 complete medium. Each well was mixed 10 times before transferring 1/10 of the volume to the next column, using filtered pipet tips and changing tips at each step. This procedure was repeated for a total of nine dilutions. The CFUs were determined directly from aliquots of the dilution plates, not from the original suspension. Turbidity of dilution wells was recorded beginning at 3 wk and again as necessary until 2 weeks have passed with no turbidity appearing at a higher dilution than at the previous reading (Taken from Saito *et al*., 2017).

2.11.2 Most probable number (MPN) assay prior starvation

To determine the initial number of culturable and unculturable organisms in the single cell suspensions prepared in section 2.11.1 above prior to starvation, MPN and CFU assays were carried out. For MPN assays, 15 µl of the single cell suspensions of *M. tuberculosis* cultures were resuspended in 135µl of Middlebrook 7H9 media in the column 2 (B2 to G2, Figure 2.4). A 10-fold serial dilution was then carried out across the 96 well microtiter plates up to

column 11 (B11 to G11, Figure 2.5) in triplicate. The quanta of organisms in the MPN assay was then calculated using the freely available MPN calculator tool.

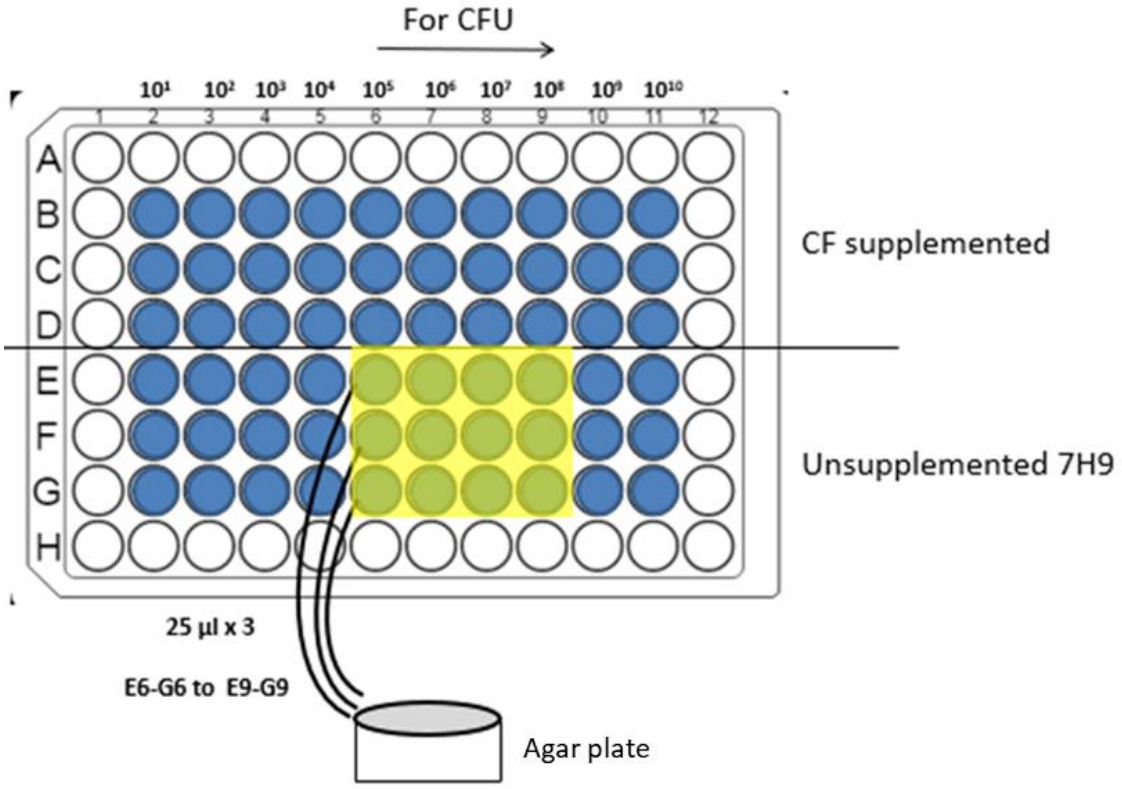

Figure 2.5: Colony forming Unit (CFU) assay. From the MPN assay 96 well plate, 20µl was obtained from each well of the triplicate dilution and pooled into a separate well in a new 96 well plate. From the pooled wells, 25 µl was plated in duplicate in Middlebrook quarter plates and incubated at 37°C for 3 weeks.

The equation for calculation of number of organisms is depicted below:

$$\sum_{i=1}^{k}\left(\frac{x_i d_i w_i}{1-\exp(-d_i w_i \hat{\mu})} - n_i d_i w_i\right) = 0$$

Where k represents number of dilutions, x_i represents the number of positive tubes at dilution i, d_i represents relative dilution per tube, n_i represents the number of tubes, w_i represents the volume (or weight) of the inoculum at dilution level i. (https://www.wiwiss.fu-berlin.de/fachbereich/vwl/iso/ehemalige/professoren/wilrich/InDEX.html).

2.11.3 Colony forming units (CFUs) prior starvation

For CFU analysis, serial dilutions were taken directly from the MPN plate in section 2.11.2 above. A volume of 20 µl was obtained from each well of the triplicate dilution and pooled into one as shown in Figure 2.5. This was carried out from dilutions 10^{-5} – 10^{-8} (rows B6 - B9 to G6 – G9). From the pooled wells, 25 µl was plated in duplicate into a Middlebrook 7H11 quarter plates. The plates were then incubated at 37 °C, 20% O_2, and 5% CO_2 for 3 weeks. The colonies were counted and the CFU calculation was then done.

$$\text{CFU} = \frac{colonies\ x\ dilution\ factor}{volume\ (ml)}$$

To calculate the quantum of DCTB, the following formula was used:

DCTB = Log (MPN/CFU)

2.12 Resuscitation of starved cultures

2.12.1 Preparation of specialist DCTB culture media

To enable the emergence of DCTB, *M. tuberculosis* was cultivated in specialist cultures containing culture filtrates with secreted growth as previously described in Chengalroyen *et al*. Briefly, CF was obtained from wild-type *M. tuberculosis* Cultures of H37Rv were grown to an Optical Density600nm = 0.6-0.9 and the cells were harvested by centrifugation. The supernatant was filtered using a 0.2 µm filter (Amicon) to remove any residual cells. The CF preparations were then diluted 1:1 with fresh Middlebrook 7H9 media.

2.12.2 Resuscitation of starved cultures using the MPN assay

After 7 days of starvation in PBS at 37 ºC, the cell suspensions were removed from the incubator. To resuscitate DCTB, specialist media containing wild type *M. tuberculosis*, LAM and Beijing culture filtrate as a source of growth factors were prepared as described in section 2.6.1 above. A 96 well format was used. A volume of 130 µl of the freshly prepared specialist culture media was added into each well of the 96 well plate. The PBS starved cultures were vortexed to obtain a homogenous cell suspension. A volume of 20 µl of this cell suspension was added to 130 µl of Middlebrook 7H9 media with or without culture filtrate in wells B2 to G2 as depicted in Figure 2.5 above. A 10-fold serial dilution was then carried out across the 96 well microtiter plates in triplicate up to column 11.

Colony forming units (CFU) were plated in 7H11 quarter plates as described in section 2.11.3 from the un-supplemented 7H9 MPN plate dilutions. The MPN and CFU plates were incubated at 37 ºC for 4 weeks. The quanta of organisms in the MPN and CFU assay was then calculated as previously described.

2.13 Cytological profiling of the *M. tuberculosis* bacteria

For cytological profiling of the DR *M. tuberculosis* bacteria, microscopy was performed as depicted in Figure 2.6. TAMRA D-alanine (TADA) (Sigma-Aldrich)was used to stain the cells, TADA is a fluorescence stain that is incorporated into the cell wall of the cells. *M. tuberculosis* cultured in 7H9 was grown to an OD_{600nm} of 0.6 and the culture was then transferred to a falcon tube and centrifuged for 5 minutes in a bench-top centrifuge at 4000 rpm, thereafter, the supernatant was discarded and the pellet resuspend in 7H9. After the pellet was resuspended in 7H9, 500 µl of each strain was added into 1.5 ml Eppendorf tubes and 2.5 µl of the TADA stain was added into each tube. This was incubated for 30 minutes to allow TADA dye to be incorporated into the cells. The stained cells were then washed three times with PBS to remove residual stain and cells were resuspended in 300 µl of 2.5% glutaraldehyde for 24 hours prior to viewing. After 24 hours the cells were pelleted by centrifugation in a mini bench-top centrifuge(Eppendorf) at 13 000 rpm for 5 minutes. The glutaraldehyde was discarded and cells were resuspended in 100 µl 1X PBS. Thereafter, 10µl of the sample was placed on a glass slide, with a pad made of 2% agarose and covered with a coverslip. The cells were then viewed under a Fluorescence microscope (Nikon). This process is summarized in Figure 2.6.

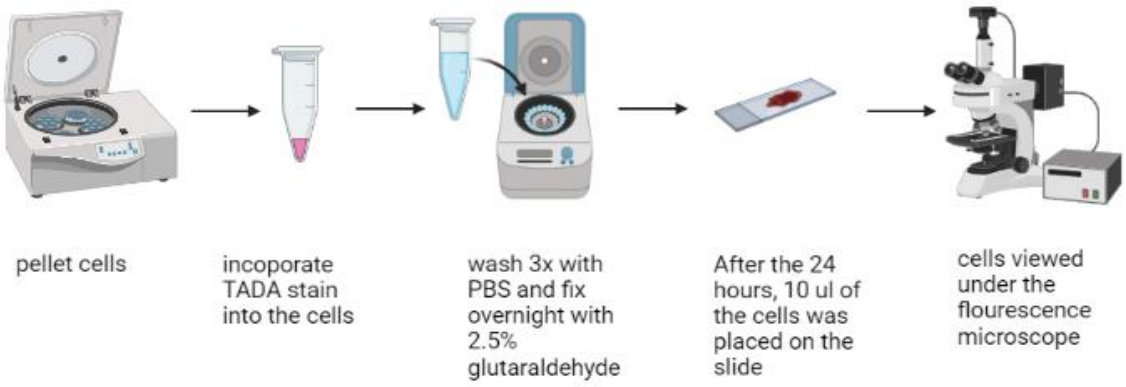

Figure 2.6: Cytological profiling of the *M. tuberculosis* clinical strains. Schematic illustration of TADA staining viewed under a fluorescence microscope.

2.14 RNA extraction

To investigate the expression of the *dosR* gene on the two strains (Beijing and LAM), RNA was extracted from cultured cells using the Nucleospin® RNA extraction kit as shown in Figure 2.7.

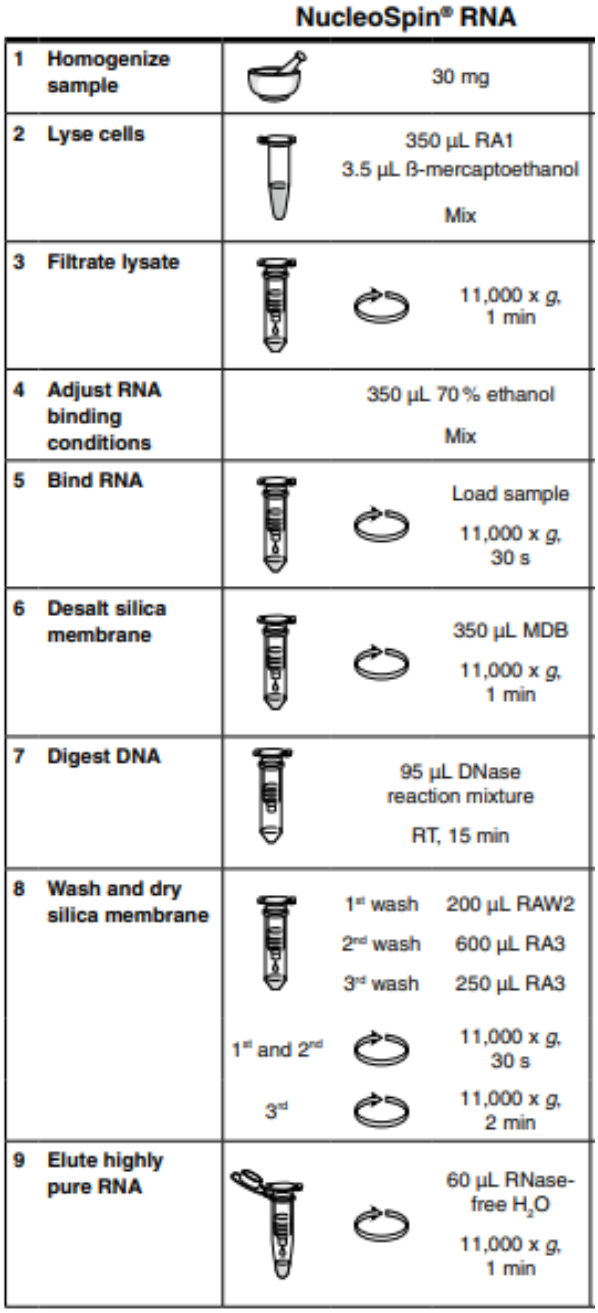

Figure 2.7: RNA isolation. Schematic diagram showing RNA purification from cultured cells. Taken from Nucleospin® RNA extraction kit.

Briefly, 10-15 ml of the sample was spun down using the benchtop centrifuge, thereafter the cells were lysed using 350 µl of the Buffer RA1 and 3.5 µl β-mercaptoethanol (provided in

the kit). The solution was then vortexed using nucleospin filter for 1 minute at 11 000 x g. To adjust the RNA binding conditions, 350µl of 70% ethanol was added into the homogenized lysate and spun down on a Nucleospin RNA column for 30 seconds at 11 000 x g to bind the RNA on the membrane. To desalt the silica membrane, 350 µL of the membrane desalting buffer (MDB) was added on to the column and centrifuged at 11 000 x g for 1 minute. The DNA was then digested using 95 µL of the DNase reaction mixture which was added directly onto the center of the silica membrane of the column. Thereafter, the silica membrane was washed and dryed using the provided buffers (RAW2 – which inactivates rDNase and RA3). After the 3 wash steps , the RNA was eluted in 60 µL of RNase-free water and centrifuged at 11 000 x g for 1 minute and there were stored at – 80 °C. These samples were then run on a 1% agarose gel and the purity and concentration taken on the nanodrop (Thermofisher Scientific, United States).

2.15 Mycobacteria growth indicator tube (MGIT) assay

MGIT assays supplemented with CFs were used to assess the rate of exit of different strains from the PBS-induced DCTB state described in section 2.11.1 above. Briefly, the MGIT tubes were prepared by adding PANTA and OADC according to the manufacturer's instructions (Rusche Gerdes., 2006). PANTA was resuspended in the OADC supplement and 800 µl of this was added into each MGIT tube. For CF un-supplemented experiments, 500 µl of the starved cultures or control cultures were added into each MGIT tube. For the experiments that were supplemented with CF, 3.5 ml of the MGIT media was removed and replaced with 3.5 ml of cell free CF obtained from log phase axenically grown *M. tuberculosis* prepared as described in section 2.6.1. A volume of 300 µl of starved cultures was then added to each tube as shown in Figure 2.8 and incubated at 37°C in the BD BACTEC™ MGIT™ 960 instrument and checked weekly for a period of 6 weeks or until the instrument signalled positive. If negative after 6 weeks, the result was recorded as negative and the tubes were removed from the machine.

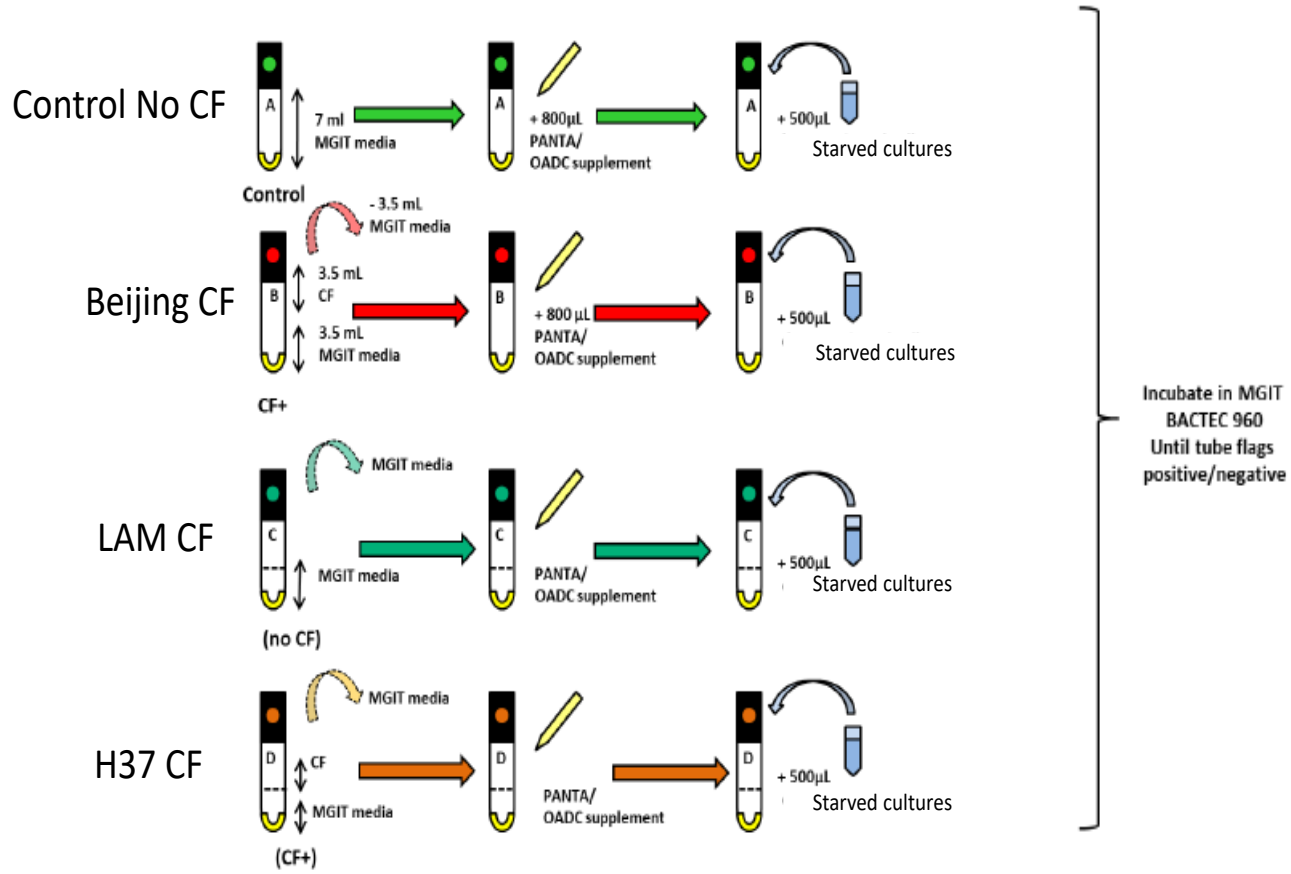

Figure 2.8: Rate of exit from the DCTB state in MGIT cultures. Illustration showing the MGIT assays supplemented with culture filtrates.

2.16 Data analysis

A detailed list of bioinformatics and software for statistical analysis used can be found in Appendix B. To determine significance a student's t-test , chi-squared test and ANOVA analysis were used.

3. Results

3.1 *In silico* analysis of the propensity of drug resistant *M. tuberculosis* strains to adopt the DC state

3.1.1 Strain typing of drug resistant *M. tuberculosis* from stored cultures by Spoligotyping

The first objective of this study was to identify the strain type in stored cultures that are known to harbor drug resistant *M. tuberculosis*. In prior work, DCTB assays were conducted on sputum specimens that habour these specimens, herein we first set out to determine strain types in these specimens with the outlook of assessing any correlation between the quantum of DCTB and strain type. A total of 80 potential drug resistant *M. tuberculosis* cultures were genotyped using the spoligotyping technique. Out of the 80 genotyped samples, 44 samples were assigned a strain type while the remaining 36 samples could not be determined either due to contamination of the cultures or insufficient DNA. Of the successfully genotyped samples, 4 dominant strains emerged, namely: the Beijing, LAM, S and T strains (Figure 3.1). Other strains included CAS, *M. africanum* and Manu, which contributed 8% of the total strain identity in combination as shown in Figure 3.1. Beijing strains were identified in approximately a third of the samples in which strain typing was possible.

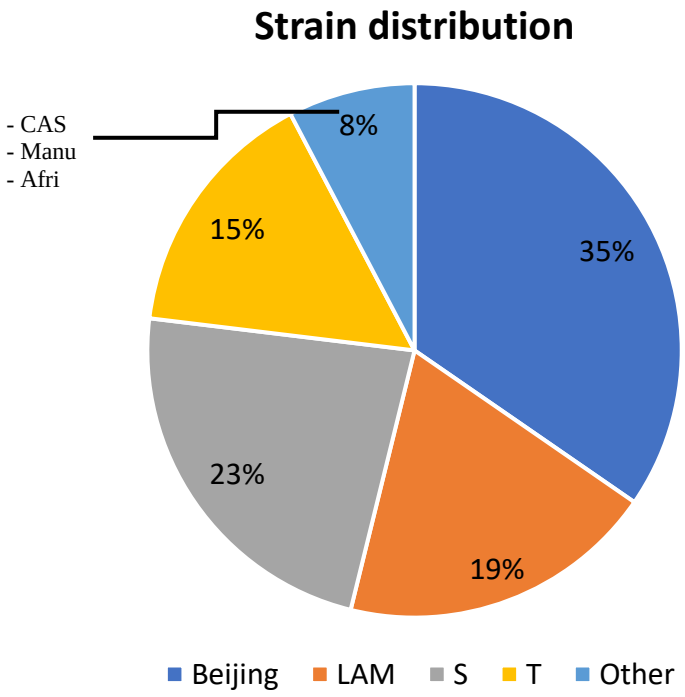

Figure 3.1 : Strain type distribution. Pie chart showing the dominant strains from the genotyped InDEX samples using the spoligotyping technique (n=44).

3.1.2 Propensity of clinical strains to adopt the DCTB state.

Following the determination of strain distribution among DR samples, we set out to determine the propensity of different DR strains to adopt the DCTB state. The DCTB status was obtained from another study (unpublished, conducted by Dr. B.Gordhan, CBTBR) using DCTB assays, directly on sputum as described previously in literature (Chengalroyen *et al*., 2016). Strain types that were observed in less than 10 samples were excluded and 4 strains (Beijing, LAM, S and T) were used for further analysis. Within the four dominant strain types, samples were split into two categories: (1) samples with and (2) samples without DCTB. Those specimens with DCTB had a resuscitation index (calculated using the equation [log (MPN/CFU]) that was greater than one while those without DCTB had a log DCTB value less than one. For each strain type, the ratio of DCTB to no DCTB was calculated, and the results demonstrated that Beijing strains had the highest likelihood to harbor DCTB populations (75%), while T-strains had the lowest (22,2%) likelihood to harbor DCTB (Figure 3.2). To determine if there was a significant difference in the propensity to adopt the DCTB state, a chi square test was used to compare the proportions of DCTB between strains. This test indicated that there is a significant difference in the propensity to adopt the DCTB state between Beijing, LAM, S and T strains, as shown by the asterisks in Figure 3.2.

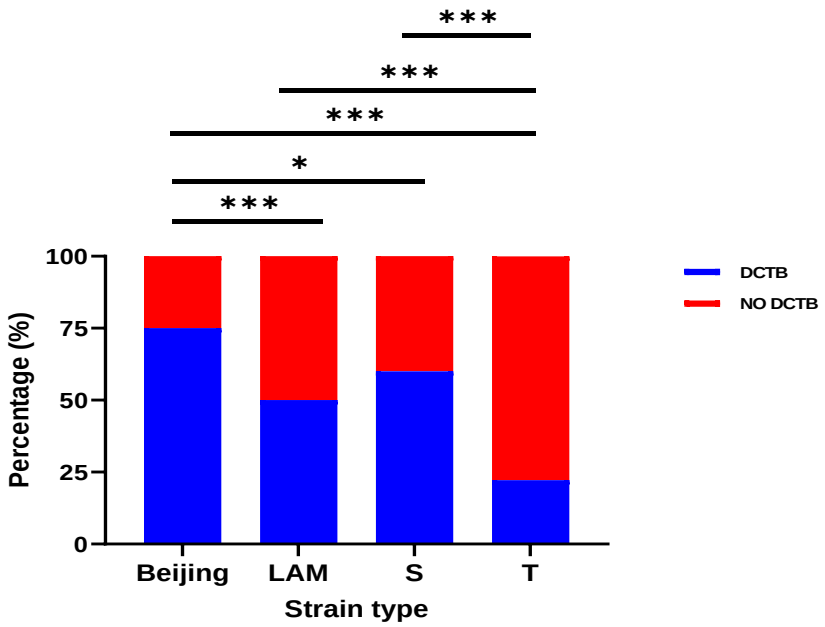

Figure 3.2: Propensity of clinical strains to adopt the DCTB state. Stacked bar graph showing the percentage of strains with and without DCTB (p < 0,05*, p<0.01**, p<0.001***, p<0.0001****).

3.1.3 Determining the effect of CF on the quanta of DCTB per strain type

We next sought to determine if the different strain types of drug resistant *M. tuberculosis* had a bearing on the quanta of DCTB obtained using culture filtrate supplementation in comparison to DCTB obtained in un-supplemented 7H9 Middlebrook media as described in section 2.1.3. Culture filtrate dependent DCTB assessment was split into 2 groups: (1) the first group probed *RPF* dependent DCTB obtained from the CF of wild type H37Rv (Johannesburg) with all 5 *RPF* genes intact and (2) the second group probed *RPF* independent DCTB obtained from a mutant of the Johannesburg strain of *M. tuberculosis* lacking all 5 *Rpf* genes (shown as BG-CF in Figure 3.3). Overall, the results demonstrated that DCTB emerges in most *M. tuberculosis* clinical strains in the presence of CF compared to CF un-supplemented media (Figure 3.3). The results demonstrated that the Beijing, S and T strains resuscitated more DCTB when supplemented with culture filtrate when compared to un-supplemented media, whereas the LAM strain produced the same amount of DCTB when supplemented or un-supplemented with CF. There was a statistical difference between the supplemented and un-supplemented cultures in the Beijing, S and T strains whereas there was no significant difference in the LAM strains. This suggests that Beijing strains harbour CF dependent DCTB while LAM strains are able to resuscitate DCTB with or without CF.

To determine the effect of *Rpf*s on the amount of DCTB resuscitated, the percentage of DCTB supplemented with wild-type H37Rv (with *Rpf*s) and BG (without *Rpf*s) was calculated and the results demonstrated that there is no difference in the amount of DCTB resuscitated in Beijng and LAM strains, and that S and T showed an increase in the Wild-type H37Rv with *Rpf*s.

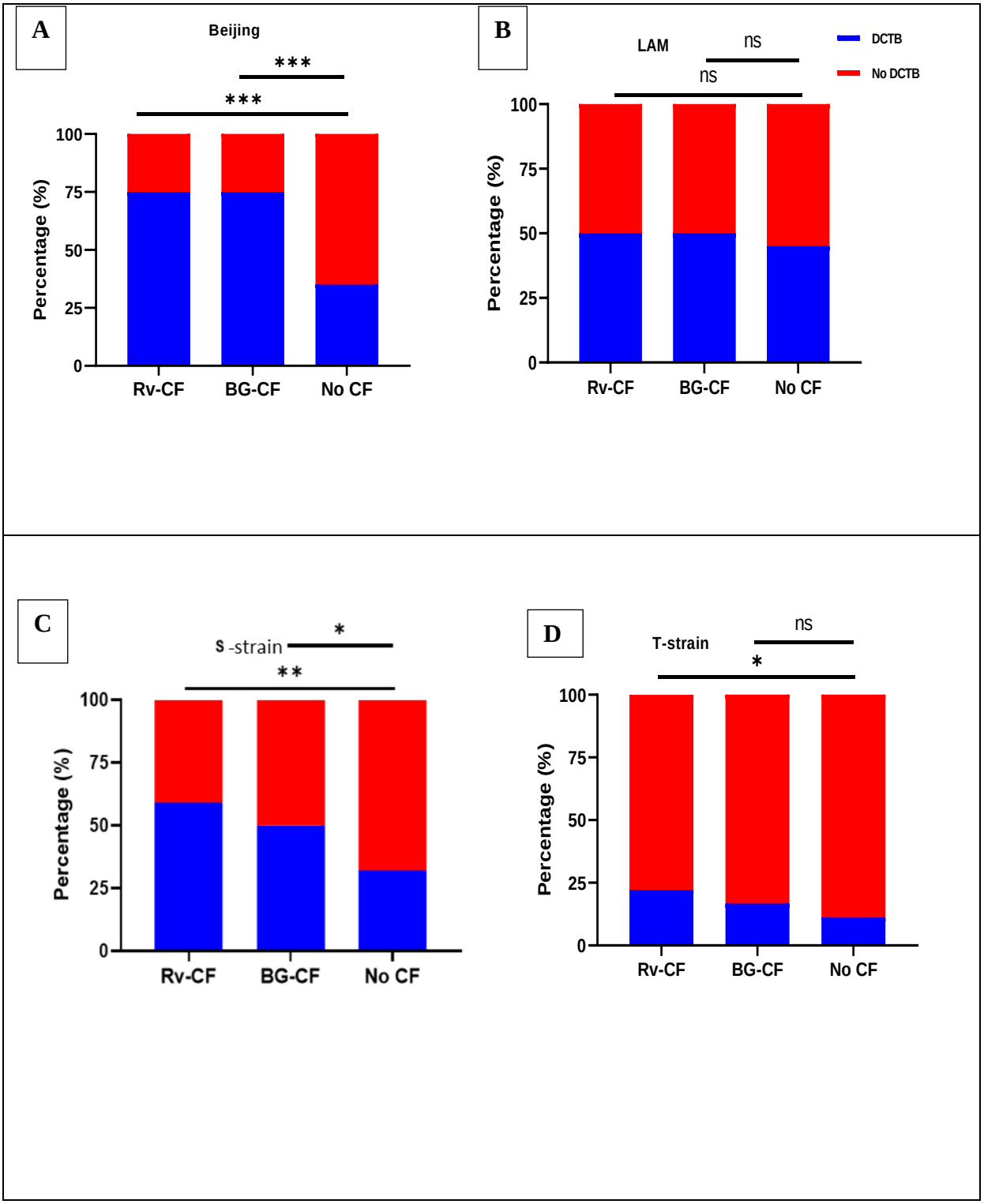

Figure 3.3: Effect of CF on the resuscitation of DCTB. Stacked bar graphs showing the percentage resuscitation in the different strains when supplemented with Culture filtrate (CF) and un-supplemented. **Rv-CF** -Quanta of DCTB emerging in media supplemented with H37Rv CF**, BG-CF** -Quanta of DCTB emerging in media supplemented with H37Rv lacking *Rpf*s**, No CF** - Quanta of DCTB emerging in un-supplemented media. **A-** Beijing**, B-** LAM, **C-** S and **D-** T strain. (p < 0,05*, p<0.01**, p<0.001***, p<0.0001****, ns- not statistically significant).

3.2 Selection and confirmation of clinical strains

Previous data from the InDEX study as described in section 3.1 indicated that Beijing strains had the highest likelihood to adopt the DCTB state when compared to other clinical strains. In addition, our findings suggested that Beijing strains were better adapted to resuscitate from the DCTB state using CF supplementation when compared to LAM and other clinical strains. Furthermore, a previous study conducted in a drug sensitive cohort, also demonstrated that the Beijing strains were better adopted to resuscitate from the DCTB state when supplemented with CF compared to the LAM strains (Padarath, MSc Dissertation). Based on these observations, we decided to set up an *in vitro* carbon starvation model to assess the robustness of these findings in drug resistant strains. For comparison, we opted to use LAM strains which form DCTB but do not require CF. LAM strains also form significantly lower DCTB as compared to the Beijing strain as shown in figure 3.3. Using the spoligotyping results obtained in section 3.1.1 above, five Beijing clinical strains and five LAM clinical strains were selected and cultured according to the protocol described in section 2.4. To confirm the strain type of the selected isolates, single colonies from each clinical strain were picked from agar plates and DNA was extracted using the colony boil method as described in section 2.5. Strain type was confirmed using the spoligotyping method as described in section 2.6. The Beijing and LAM spoligotypes (Figure 3.4 A and B) showed the same pattern as those initially spoligotyped in section 3.1. These were then used for subsequent analysis.

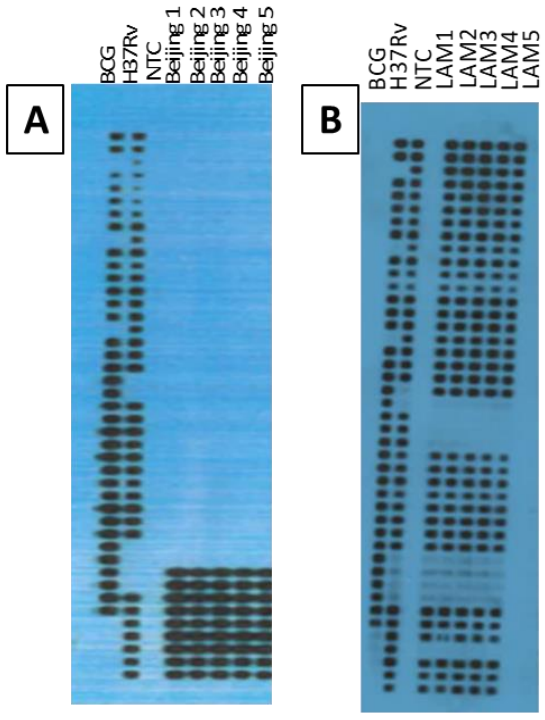

Figure 3.4: Strain typing. Shown are spoligotypes of the 5 Beijing **(A)** and 5 LAM **(B)** samples and the controls (BCG, H37Rv and the NTC [no template control]). Each spot represents the presence of spacers 35-43 which are the only spacers present in Beijing strains.

3.3 Growth kinetics of strains

The growth rates of the clinical strains (Beijing and LAM) in comparison to wild-type H37Rv were assessed by conducting growth curves of each strain in triplicate as described in section 2.10. As indicated in Figure 3.5, Beijing strains showed identical or slightly higher growth rates than those of the laboratory strain H37Rv, whilst the LAM strains showed a reduced growth compared to H37Rv. The results also indicated that Beijing strains had a higher growth rate compared to the LAM strains and this difference was statistically significant (Figure 3.6). These differences in growth rates between the LAM and Beijing strains could be attributed to the numerous other differences observed in the literature between these strains (Hanekom *et al.*, 2011; Kong *et al.*, 2007; G. Kumar *et al.*, 2017; Parwati *et al.*, 2010). Several studies have previously assessed the intracellular growth of Beijing clinical strains in macrophages and found that Beijing genotypes grow significantly faster than non-Beijing genotype strains and have thus been linked to hypervirulence (Hanekom *et al.*, 2011).

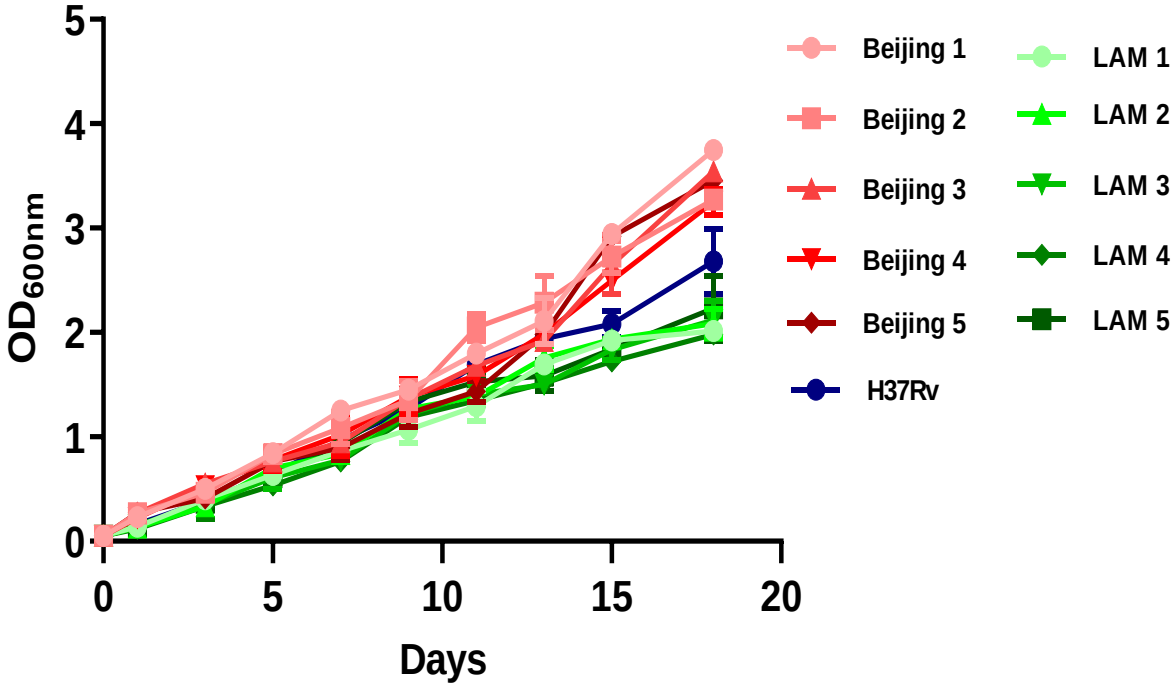

Figure 3.5: Growth kinetics for the Beijing and LAM strains. Growth curves of 5 Beijing and LAM strains and the control (H37Rv) done in a period of 18 days.

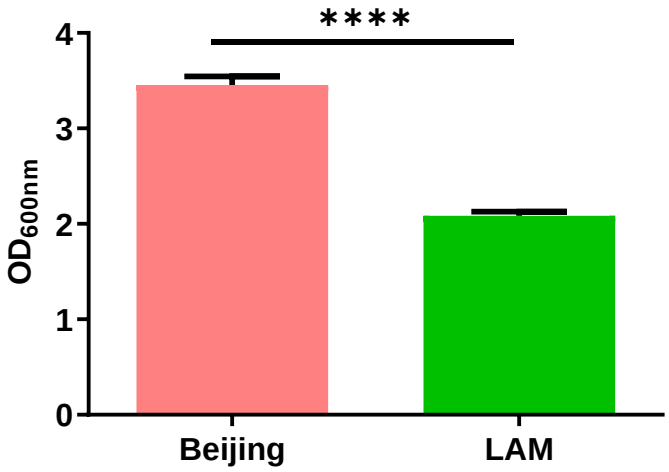

Figure 3.6: Growth kinetics for Beijing and LAM strains. OD_{600nm} of the LAM and Beijing strains on day 18. ($p<0.0001$****).

3.4 Detection of mutations in the drug-resistance conferring genes

3.4.1 Genomic DNA extraction and PCR primer optimization

For the detection of mutations in drug resistance conferring genes, DNA was isolated from *M. tuberculosis* cultures using CTAB/NaCl as outlined in section 2.8. All extractions were performed in triplicate and the extracted DNA was viewed using SYBR stained agarose gels (GeneSnap) (Appendix B). The $A_{260/280}$ ratios for extracted DNA as determined by the nanodrop (ND-1000) were within the accepted range (1.8 – 2.0) indicating that DNA integrity and purity was acceptable for sequencing (appendix B table 3.2). Thereafter, DNA samples were used for gradient PCR in order to optimize primers for the amplification of DR genes (*katG* and *embB*) as outlined in section 2.9. The gels for gradient PCR optimization can be found in Appendix B Figure 7 and 8. Resistance-conferring genes (*katG* and *embB*) were used to report antibiotic resistance in the selected strains. Figure 3.7 and table 3.5 below show the successful amplification of *katG* and *embB* post primer optimization for the selected strains. These PCR products were then sent for sequencing at the Stellenbosch sequencing facility (Central Analytical Facilities (CAF) genomics centre).

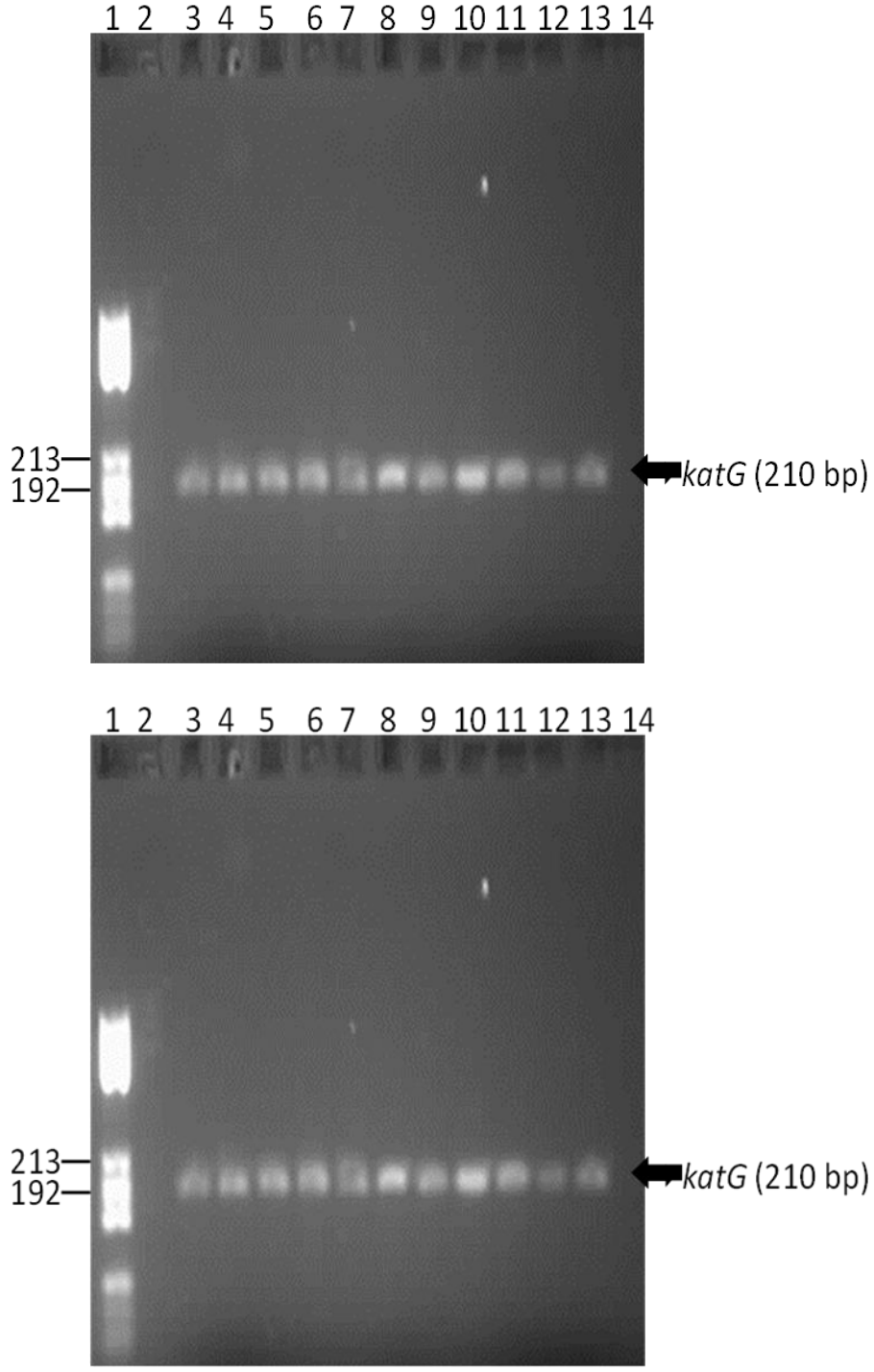

Figure 3.7: Primer optimization. Gel electrophoresis for the optimised primers of the resistance-conferring genes (**(A)** *katG* and **(B)** *embB*) through gradient PCR. Marker V was used as a molecular weight marker and the bands from 3-12 represent LAM 1-5 and Beijing 1-5 respectively, with the last well having a negative control. The expected band sizes of resistance conferring genes are indicated on table 3.5 below.

Table 3.5: Expected band sizes of the resistance conferring genes

Resistance conferring genes	**Size (bp)**
KatG	210
EmbB	368

3.4.2 Sequencing of resistance-conferring genes

The PCR products from section 3.6.1 were sent for capillary sequencing at the DNA Sequencing Unit, Stellenbosch University. The Jalview 2.11.2.0 , BioEdit 7.2 and FinchTV 1.2 softwares were used to edit and align the sequences to the reference sequences for the determination of *katG* and *embB* mutations. The mutations in the *embB* gene associated with EMB resistance include changes in codons 306, 406 and 497, with the 306 mutation being the most common. For INH resistance, *katG* mutations that are indicative of INH resistance include changes in codons 315 and 463 (Isakova *et al*., 2018, Xu *et al*., 2015). In this study $katG_{315}$ and $embB_{306}$ mutations were used for the determination of drug resistance in the selected Beijing and LAM strains. Table 3.6 shows that 7 (4 Beijing and 3 LAM) of the 10 samples have the $katG_{315}$ mutation, indicating isoniazid resistance in these samples, whereas none of the samples had mutations on the $embB_{306}$ gene. With respect to other INH mutations, we anticipate that those strains without a *katG* mutation harbored mutations in *inhA/inhA* promoter, however this was not probed further due to time constraints. All the samples were shown to be RIF resistant through the GeneXpert test in the InDEX study.

Table 3.6: Mutations of the *katG* and *embB* genes in drug resistant *M. tuberculosis* strains

	Nucleotide replacement	
Sample	$katG_{315}$	$embB_{306}$
Beijing 1	AGC→ACC	-
Beijing 2	-	-
Beijing 3	AGC→ACC	-
Beijing 4	AGC→GCG	-
Beijing 5	AGC→TTG	-
LAM 1	-	-
LAM 2	AGC→CTA	-
LAM 3	AGC→ACC	-
LAM 4	-	-
LAM 5	AGC→TGG	-

3.5 PBS based starvation model to generate non-replicating organisms.

Growth of bacteria under carbon starvation conditions has previously been shown to induce a non-replicating "dormant" state in mycobacteria, which has been defined as the differentially detected tubercle bacilli (DDTB) by Saito *et al* (2017), akin to the DCTB described in this work. It has further been shown that when *M. tuberculosis* is cultured in phosphate-buffered saline (PBS), a solution lacking a carbon source, bacteria gradually shut down various metabolic pathways whilst still retaining viability. These bacteria have been demonstrated to be recoverable in nutrient rich media. In this study, the carbon stress model was used to generate DCTB in the 10 selected samples as described in section 2.3.1. DCTB was calculated as previously described in section 2.11. The results indicated that the PBS based starvation model induces DCTB in the LAM and Beijing strains as the log DCTB value was greater than 1 (Figure 3.8).

3.5.1 DCTB resuscitation

The viability and quanta of starved *M. tuberculosis* was assessed using two resuscitation conditions: (1) CF-dependent (supplemented with Beijing, LAM or H37Rv CF) and (2) CF-independent (growth in 7H9 media without CF supplementation). The results in Figure 3.8 depict the ability of culture filtrate to resuscitate DCTB. The data demonstrate that there is a significant difference between the Beijing(B)-CF and H37Rv(Rv), LAM(L)-CF and un-supplemented 7H9 liquid media (Figure 3.8). The results also demonstrated that there is no difference between the amount of DCTB after starvation supplemented with LAM, H37Rv CF or not supplemented (grown in 7H9. Beijing CF possibly contains unique growth factors with added resuscitation capabilities that warrant further investigation.

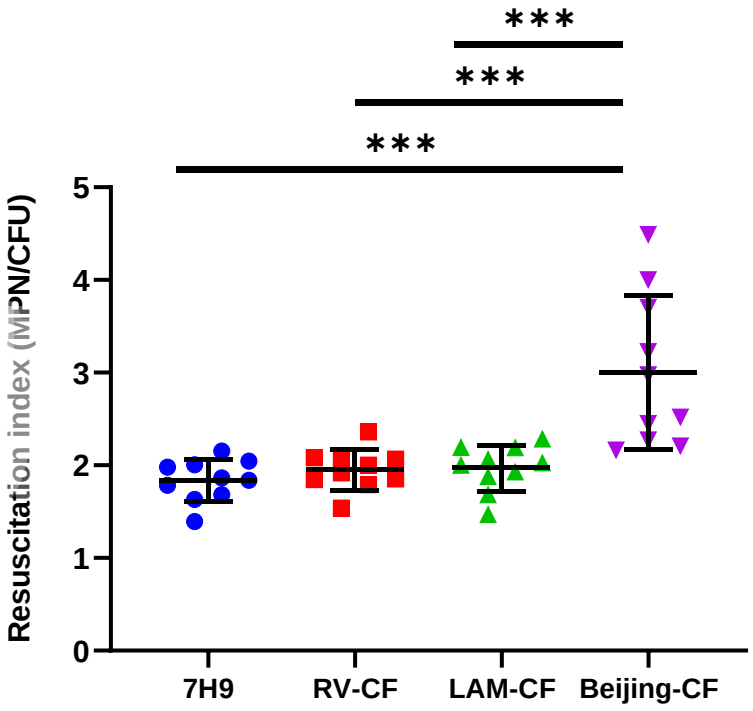

Figure 3.8: The effect of culture filtrate on the recovery of differentially culturable tubercle bacilli obtained from an *in vitro* model of starvation of the LAM, Beijing and H37Rv strains. Scatter plots illustrating resuscitated DCTB from supplemented and un-supplemented (DCTB) cultures of LAM and Beijing strains. **7H9-** supplemented with media, **RV-CF -** supplemented with H37Rv**, L-CF-** supplemented with LAM-CF**, B-CF** – supplemented with Beijing CF. Error bars represent medians and interquartile ranges. Significant differences are depicted in bold. (*p-value ≤0.05, **p-value≤0.01, ***p-value≤0.001 and ****p-value≤0.0001)

DCTB resuscitation was further investigated in Beijing and LAM strains independently and the results demonstrated that the growth of the samples is different within each group of strains as shown in Figure 3.9. This figure is shown to depict the variation in DCTB when strains are batched by the culture condition used. With the exception of Beijing-CF, there appeared a 0.5 log difference between strains. The Beijing-CF gave greater variation when applied to Beijing strains where there was a difference of up to 1.5 log between Beijing isolates.

The different samples within each strain were then grouped together and the assessment of which growth condition resulted in the resuscitation of the largest quantity of DCTB was conducted. The results demonstrated that there was a significant difference between the samples not supplemented (grown in media), H37Rv-CF or LAM-CF and those supplemented with Beijing CF within each strain (Figure 3.10). More DCTB was resuscitated using Beijing CF as compared to LAM or H37Rv CF or media alone (Figure 3.10).

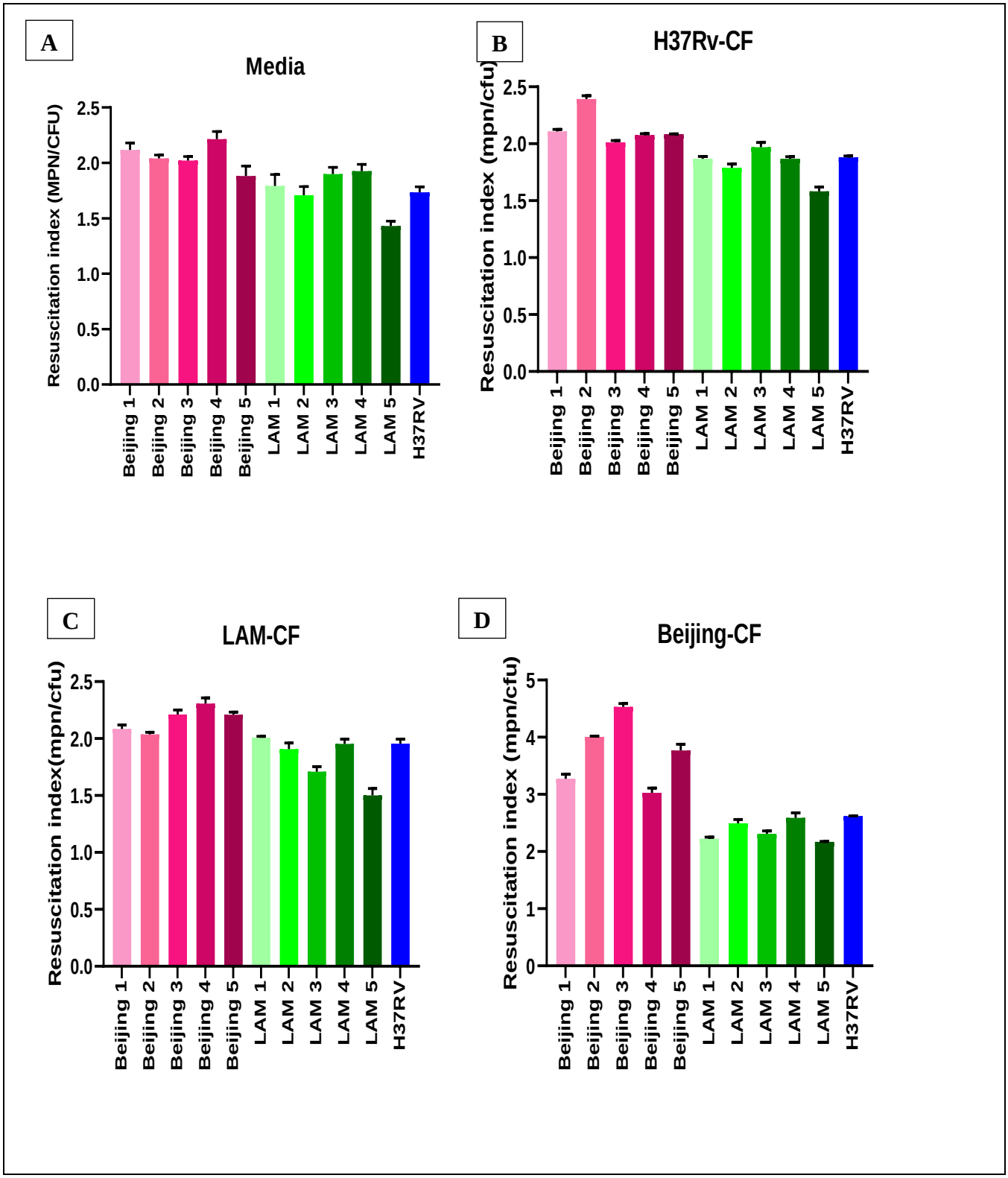

Figure 3.9: Quanta of DCTB in the 5 individual Beijing and LAM strains from the carbon starvation model using PBS as a culture medium. Bar graph showing the amount of DCTB when the different LAM and Beijing clinical samples are supplemented (H37Rv, LAM and Beijing CF) and un-supplemented. **7H9-** supplemented with media, **RV-CF** - supplemented with H37Rv**, L-CF-** supplemented with LAM-CF**, B-CF** – supplemented with Beijing CF.

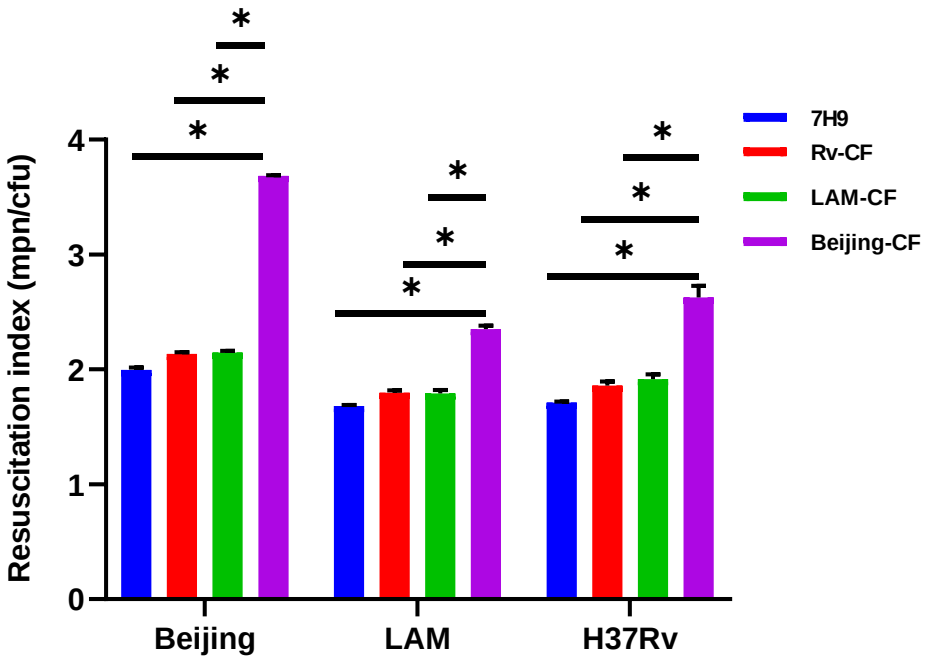

Figure 3.10: Quanta of DCTB in the Beijing, LAM and H37Rv strains from the carbon starvation model using PBS as a culture medium. 7H9- supplemented with media, **RV-CF -** supplemented with H37Rv**, L-CF-** supplemented with LAM-CF**, B-CF** – supplemented with Beijing CF. *p value≤0.05.

3.6 Expression of *dos R*egulon genes

In this study, as well as a previous study (Padarath, Masters thesis 2019 unpublished), Beijing strains displayed a higher propensity to form DCTB as well as to resuscitate from DCTB state. Furthermore, Beijing CF displayed a higher resuscitation capability. Literature has demonstrated that the *dosR* regulon is essential for intracellular adaptation and that Beijing strains have a unique regulation of the *dosR* regulon compared to other *M. tuberculosis* strains (Domenech *et al*.,2017). Based on this, we wanted to determine the expression of *dosR* in the selected strains. To determine the expression of *dosR* regulon genes, RNA was extracted as described in section 2.14. The results demonstrated successful RNA extraction as seen by the 16s and 23s rRNA bands (Figure 3.11 & appendix table 3) that are characteristic of bacterial RNA. The $A_{260/230}$ ratio for most of the samples was within the acceptable range of 2.0-2.2, therefore the RNA extracted was pure. The extracted RNA was then going to be used for the assessment of the expression of the regulon gene (*dosR*) through qPCR, but due to time constraints could not be completed.

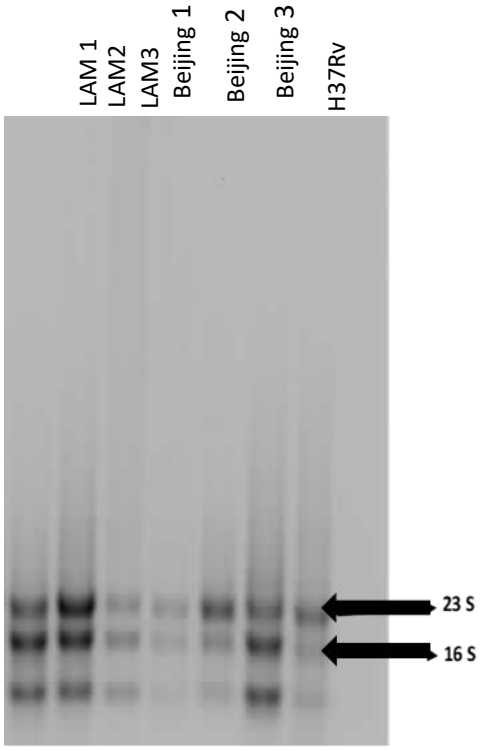

Figure 3.11: Assessment of RNA quality for RT-qPCR to assess the expression of regulon genes (*dosR*). Agarose gel electrophoresis of total RNA extraction from *M. tuberculosis* clinical strains (LAM and Beijing). The 23S and 16S bands indicate large and small subunit of the rRNA.

3.7 Cytological profiling of the *M. tuberculosis* clinical bacteria

3.7.1 Metabolic activity of *M. tuberculosis* bacteria

To determine the cytological profiling of the *M. tuberculosis* clinical bacteria, starved cells were stained with a fluorescent dye and visualized using a fluorescent microscope. The cells were labelled using the TADA dye which labels new PG. Log phase cultures of *M. tuberculosis* (H37Rv) were used as a control to assess the cell length, shape and metabolic activity. The DCTB produced by the carbon starvation model after 1 week were labeled according to the protocol described in section 2.6.1.The results demonstrated that the un-starved log-phase cultures of the clinical strains (Beijing and LAM) and H37Rv incorporated the dye and hence were successfully labelled, whereas the starved cells did not incorporate the dye hence they remained unlabelled (Figure 3.12). This suggests that the starved cells have a decreased metabolic activity compared to the un-starved cells.

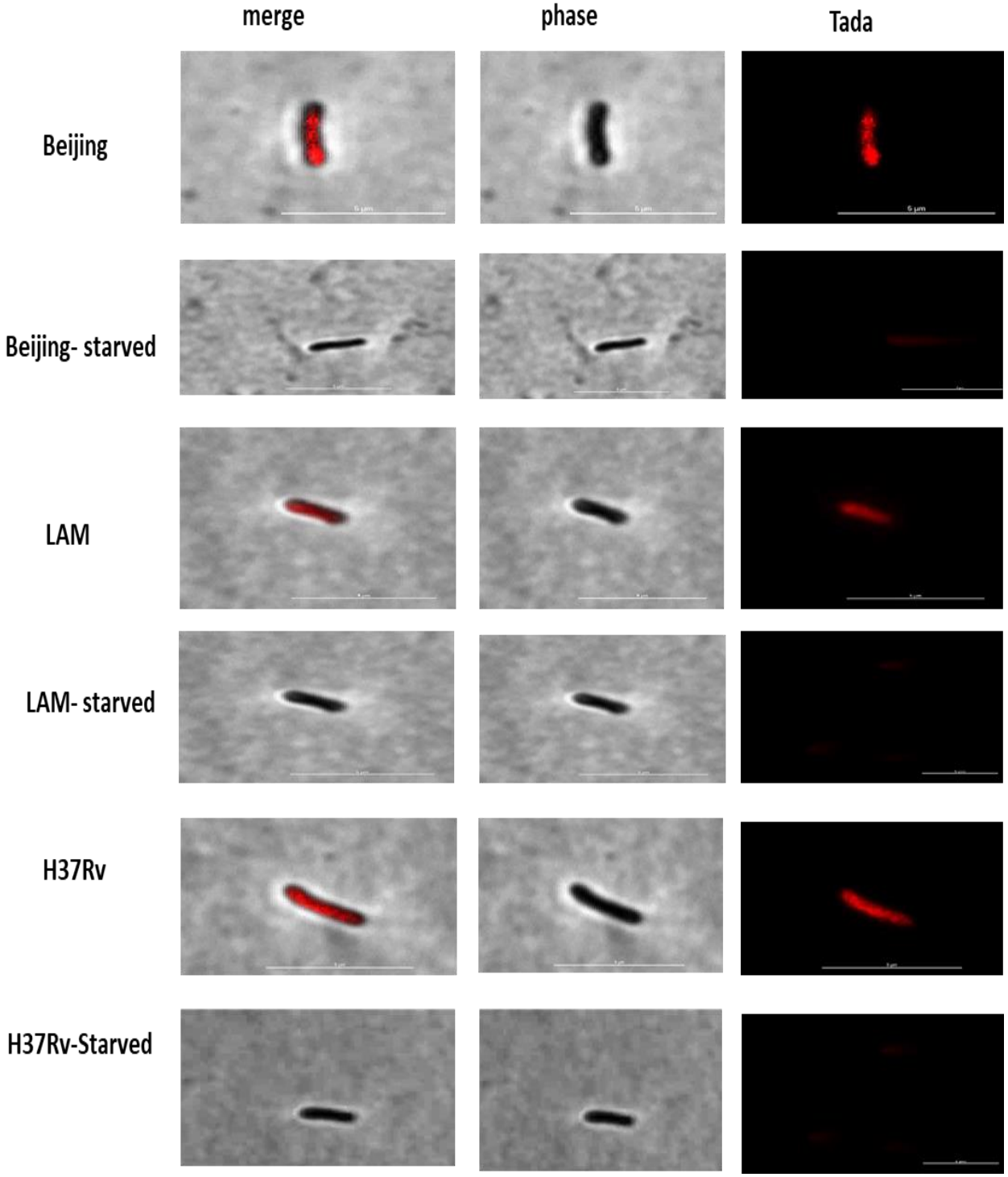

Figure 3.12: Cytological profiling of the *M.tuberculosis* clinical bacteria. Figure showing images of the cells captured on the microscope in the different strains. The cells were labelled with the TADA dye. scale - 5µm.

3.7.2 Metabolic activity of *M. tuberculosis* bacteria produced under the carbon starvation model

The cell length of the starved and un-starved cells was investigated and the results in Figure 3.14 demonstrated that there was a significant difference between the starved and un-starved cells. The un-starved cells appeared longer compared to the starved cells. This also indicated that the metabolic activity of the starved cells is decreased, the starved cells are not replicating hence the shorter cell length. The metabolic activity of bacteria cultured in carbon-depleted media appeared to be reduced.

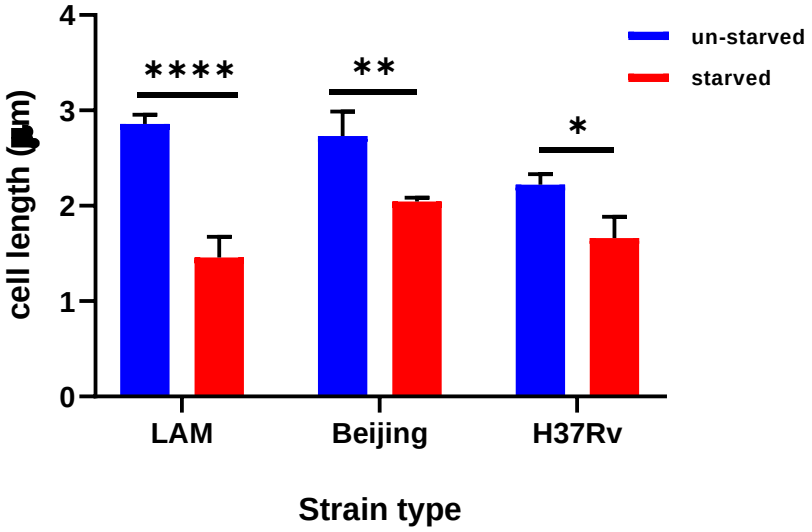

Figure 3.14: *M. tuberculosis* clinical strains cell length. Bar graph showing the cell length (µm) of the clinical strains (Beijing and LAM) and H37Rv when grown in 7H9 (unstarved) and PBS (starved), 50 cells per strain were used. (*p-value ≤0.05, **p-value≤0.01, ***p-value≤0.001 and ****p-value≤0.0001).

To determine the effect of the addition of CF on the metabolic activity of the starved cells. The cells were resuscitated using the Beijing, LAM and H37Rv- CF and were labeled according to the protocol described in section 2.13. ImageJ was used to quantify the signal intensity of the cells. There was a significant difference in the mean fluorescence intensity when comparing cells grown in normal media, and those supplemented with H37Rv-CF and LAM-CF to Beijing-CF in both LAM and Beijing strains. No significant difference was found on the mean fluorescence intensity between cells grown in media, H37Rv-CF and LAM-CF. The results demonstrated that Beijing and LAM starved strains had an increased metabolic activity when supplemented with Beijing CF (Figure 3.13). The rapid uptake of the dye in the presence of CF confirmed that the increased growth yield provided by CF was

associated with replication restart as actively replicating cells incorporate the dye into their cell walls.

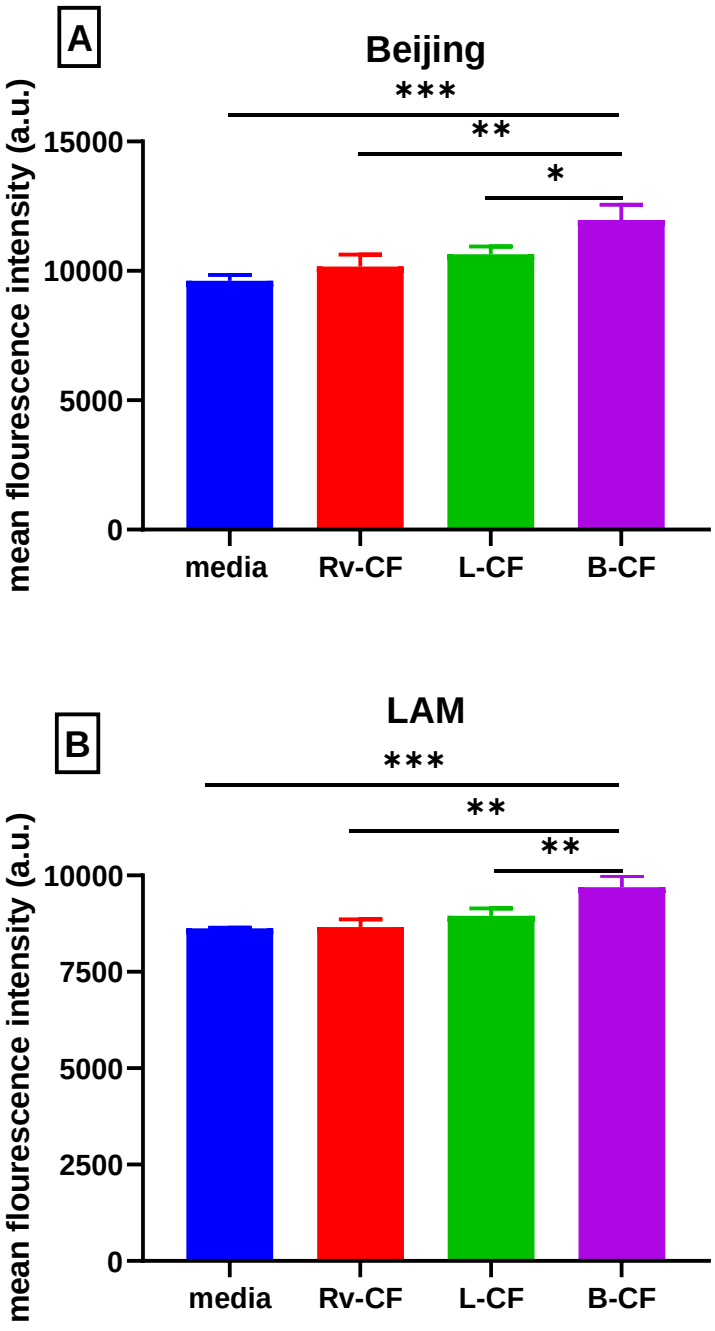

Figure 3.13: Mean fluorescence intensity of the starved cells incorporated with the TADA stain. Bar graphs showing the mean fluorescence intensity in TADA stained starved Beijing (A) and LAM (B) strains. **7H9-** supplemented with media, **RV-CF -** supplemented with H37Rv**, L-CF-** supplemented with LAM-CF**, B-CF** – supplemented with Beijing CF. (*p-value ≤0.05, **p-value≤0.01, ***p-value≤0.001 and ****p-value≤0.0001)

3.8 Resuscitation of Starved cells

Previous results from section 3.4 indicated that the amount of DCTB detected when supplemented with Beijing-CF was higher than that grown in media or supplemented with LAM-CF and H37Rv-CF. As a result, we further investigated the effect of adding H37Rv-CF, Beijing-CF and LAM-CF to MGIT tubes on time to positivity (TTP), when these tubes were inoculated with H37Rv, Beijing and LAM DCTB. To test this, Beijing-CF, LAM-CF, and H37Rv-CF were purified using the protocol described in section 2.5.2. Starved H37Rv, Beijing, and LAM strains (produced according to the protocol described in materials and methods section 2.5.1) were added to the MGIT tubes and incubated in MGIT BACTEC 960 until a positive result was obtained.

The results showed that addition of culture filtrates (H37Rv, LAM and Beijing) decreased the time to positivity of the starved cultures compared to when un-supplemented (grown in media). Analyzing each strain separately revealed that Beijing-CF decreased TTP in the starved Beijing and LAM strains (Figure 3.15 A and B) more than H37Rv-CF and LAM-CF. Statistical analysis was performed on the means of the LAM, Beijing and H37Rv strains using a one-way ANOVA adjusted for multiple comparisons. The test revealed that there was a greater significant difference in TTP when LAM, H37Rv and Beijing strains were cultured with Beijing-CF compared to media, LAM and H37Rv-CF. These findings indicated that addition of Beijing-CF to starved cultures improves DCTB detection (Figure 3.16).

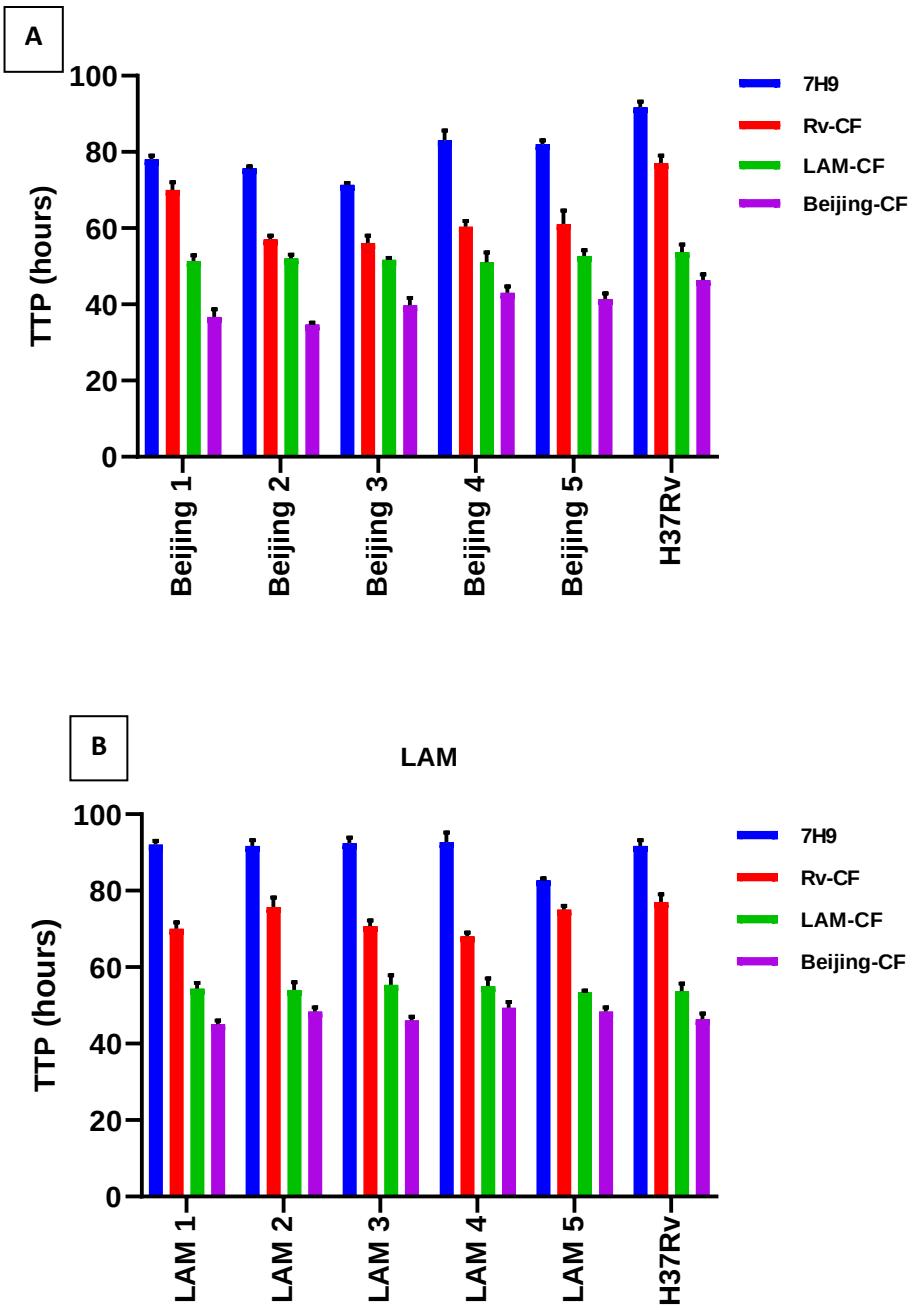

Figure 3.15: Resuscitation of starved Beijing and LAM strains. Bar graphs with error bars showing the time to positivity (TTP) of the starved cultures in the Beijing **(A)** and LAM **(B).**

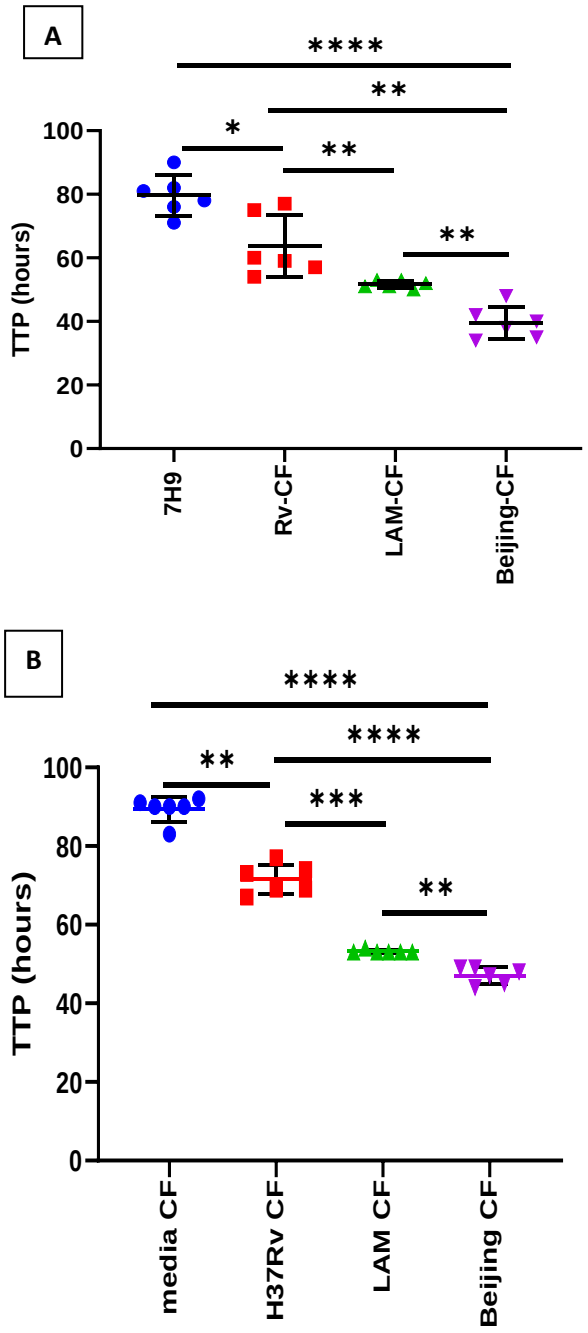

Figure 3.16: The addition of Culture filtrate decreases TTP in starved cultures. Grouped analysis comparing the effect of media, H37Rv-CF, LAM-CF and Beijing- CF on the TTP in starved Beijing **(A)** and LAM **(B** strains. Statistical analysis was performed using a one-way ANOVA adjusted for multiple comparisons (*p-value ≤0.05, **p-value≤0.01 and ****p-value≤0.0001).

4. Discussion

M. tuberculosis is widely regarded as one of the most successful human pathogens and its success can be attributed in a large part to its ability to evade various stresses. The adoption of various forms of non-culturable states, in which the bacterium is more tolerant of stresses that would normally be detrimental to its survival, is a key mechanism used in this evasion. When permissive conditions resume, the bacteria exit from these less culturable states and resume active replication (Kell and Young, 2000; Jones and Lennon, 2010; Lennon and Jones, 2011). Sputum from TB patients contains drug-tolerant, DCTB, which cannot grow on solid media but can be recovered in liquid media supplemented with resuscitation-promoting factors, a group of bacterial growth stimulatory enzymes secreted by *M. tuberculosis* (Chengalroyen *et al*., 2016). These data point to the presence of complex phenotypic heterogeneity in bacteria during colonization of the human host. Rapid detection of the TB infection is critical for preventing further transmission. The ability to detect and quantify DCTB in patients with active TB or latent TB infection is critical for assessing the risk of disease reactivation and monitoring treatment responses. In this study, we used a laboratory model of DCTB to study the ability of drug resistant *M. tuberculosis* strains to adopt the DC state.

The following conditions must be replicated in order to model the conditions within the granuloma: hypoxia, nutrient deprivation, limited carbon sources, and a high concentration of nitric oxide (Alnimr, 2015; Betts *et al*., 2002; Bhatt & Salgame, 2007; Glickman & Jacobs, 2001; Honeyborne *et al*., 2016). There are several *in vitro* models that describe the induction of the differentially culturable state in the literature. Most of these models have been shown to induce a non-replicating state in morphologically and metabolically distinct mycobacteria (Betts *et al*., 2002; Ojha *et al*., 2008; Saito *et al*., 2017; Salina *et al*., 2014). *M. tuberculosis* isolated from infected patients' granulomas has a different morphology in comparison to bacteria grown *in vitro*, and it has been observed that nutrient-starved bacteria have a similar morphology to mycobacteria found in sputum (Keane *et al*., 2000; Lipworth *et al*., 2016). In this study, a nutrient-limiting *in vitro* model for the induction of differentially culturable bacteria in *M. tuberculosis* was tested, using a carbon starvation method described in Saito *et al*., (2017). During carbon starvation, the bacteria are induced into (1) the differentially culturable state, (2) reduced metabolic function, and (3) morphological change. Prior to the performance of carbon starvation, the bacteria were first genotyped via spoligotyping.

Strain typing of drug-resistant *M. tuberculosis* from patient sputum samples in the InDEX study by spoligotyping revealed that the most dominant strains were Beijing, LAM, S and T. The Beijing strains were identified in approximately a third of the cohort in the participants whose strain typing was possible. The strain distribution found in this study mirrors the expected strain distribution in South Africa according to Chihota *et al.*, 2018, however the most dominant strain according to their study was found to be LAM instead of Beijing as observed in the current study. The global emergence of Beijing genotype strains, as well as their association with multidrug resistance, substantiates their high potential for drug resistance (Gupta *et al*., 2020). The higher rate of mutations at the *rpoB*531, *katG*315, and *embB*306 codons among Beijing strains adds to the evidence that drug resistance may contribute to the global dominance of Beijing strains (Gupta *et al*., 2020).

After the determination of strain distribution in the InDEX study, the propensity of clinical strains to adopt the DCTB state was determined. The results demonstrated that Beijing had a higher propensity to adopt the DCTB state compared to the other strains. Similar observations were reported in a previous study on drug sensitive *M. tuberculosis* (Paradath, Masters dissertation). According to our knowledge, the effects of CF from various clinical strains on DCTB resuscitation have not been studied before. Therefore, the effect of the CF on the resuscitation of DCTB was assessed and results demonstrated that the addition of Beijing CF to the starved cultures increased the propensity for resuscitation from the DC state compared to LAM and H37Rv- CF. This suggests that Beijing CF possibly contains unique growth factors with added resuscitation capabilities that should be investigated.

To investigate the effects of carbon starvation on cell morphology and metabolic activity, the cytological profiling of LAM and Beijing strains was performed with the aid of Flourescent D-amino acid (FDAA) staining. During PG subunit synthesis, the terminal D-alanine amino acid is the last molecule to be incorporated into the PG side chain (Kuru et al., 2015). The FDAAs mimic terminal PG D-alanine residues, allowing for incorporation into the PG layer of the cell wall. This enables the monitoring of *de novo* PG synthesis, which consequently indicates metabolic activity (Kuru *et al*., 2015). The labelling of LAM and Beijing cells with FDAA dye TAMRA 5-(and-6)-carboxytetramethylrhodamine, succinimidyl ester (TADA) demonstrated that carbon starvation reduces metabolic activity due to poor dye uptake, lack of *de novo* PG synthesis and reduced cell length observed in carbon starved cells. Wu *et al* demonstrated that the removal of carbon sources resulted in the emergence of a small resting cell (SMRC) morphotype (Wu *et al*., 2016). The morphological change is thought to occur as

a survival mechanism, that is, to reduce permeability and enter a more protective state, which likely contributes to increased survival in a hostile environment (Wu *et al*., 2016). The reduced metabolic activity of Beijing and LAM strains under carbon-depleted conditions is consistent with the non-replicative DCTB state. To observe the effects of DCTB resuscitation on metabolic activity, the starved cultures were then supplemented with H37Rv, LAM and Beijing CF and observed microscopically after TADA staining. It was observed that CF supplementation was able to restore metabolic activity. These findings provided further evidence that the transition of starved clinical isolates from a non-replicative state requires growth factors from CF.

Given the beneficial effect of CF in DCTB assays, we next assessed the effect of CF on the resuscitation of DCTB in diagnostic media . The gold standard for TB diagnosis is bacterial culturing using the MGIT system, which detects *M. tuberculosis* growth by measuring oxygen consumption in a tube. This test takes 2-6 weeks to complete depending on the number of bacteria present. This lengthy period is problematic, and efforts to shorten the detection of TB disease using this system are expected to be beneficial, particularly in specimens with low bacterial loads. In this study, the addition of CFs (H37Rv, LAM and Beijing) decreased TTP of the starved cultures. Moreover, the addition of Beijing CF decreased the TTP in both the strains (LAM and Beijing). McIvor and colleagues also demonstrated in a study that the addition of CF form laboratory *M. tuberculosis* strain (H37Rv) decreased time to positivity in HIV patients with a low bacterial load (Gordhan *et al*., 2021). These observations highlight the potential use of CF, particularly Beijing-CF to reduce detection time in the MGIT system during TB diagnosis.

In this study as well as in a previous study (Paradath, masters dissertation), Beijing strains displayed a higher propensity to form DCTB as well as to resuscitate from the DCTB state. Furthermore, Beijing CF displayed a higher resuscitation capability. Domenech *et al*., (2017) has demonstrated that the *dosR* regulon is essential for intracellular adaptation and that Beijing strains especially have a unique regulation of the *dosR* regulon. Based on this, we wanted to determine the expression of *dosR* in the selected Beijing and LAM strains through qPCR. However, due to time constraints, this could not be taken to completion.

4.1 Concluding remarks

This study demonstrated that there is a significant relationship between drug resistant clinical strains and the propensity to produce DCTB. Experimental and bioinformatics analysis

demonstrated that drug resistant Beijing strains have a higher propensity to produce DCTB than LAM strains, but the mechanisms behind this are not known. The study also demonstrated that Beijing CF resuscitated more DCTB compared to LAM and H37Rv-CF. This unique behaviour of the Beijing strains creates the opportunity for further studies to determine the factors that contribute to the success of Beijing-CF in DCTB resuscitation.

5. Limitations and future studies

In this study, spoligotyping was used to classify the clinical strains in this study, however this technique is known in literature to have low discriminatory power. Furthermore, some strains may be undetected due to overpowering by dominant strains (Ei *et al*., 2016). As a result, whole genome sequencing of all ten clinical isolates in the future could provide detailed insights into the differences in DCTB production observed between the Beijing and LAM isolates. Furthermore, whole genome sequencing would simultaneously reveal any changes in the genome between strains and within different isolates of the same strains. This would have been beneficial as it would have simultaneously identified all drug resistance loci and also indicated potential avenues of the observed phenotypic differences. Furthermore, the use of other *in vitro* models for DCTB such as the Biofilm and Ion deficiency model simultaneously would have provided a more diversified understanding of the behaviour of the strains in stress conditions and possibly different types of dormancy with different requirements for exit from dormancy.

To study the factors that contribute to the success of Beijing-CF in DCTB resuscitation, proteomic studies and Liquid-chromatography mass-spectrometry (LC-MS) can be used to study the CF.

6. Appendix

6.1 Appendix A: Materials

Table 1-DNA extraction reagents

Reagent	Components	Description
TE buffer	10 mM Tris-HCl (pH 8), 10 mM EDTA	Dissolved in 500 ml of distilled water and autoclaved
CTAB/NaCl	4.1% NaCl, 10% N-cetl-N,N,N-trimetyl ammonium bromide	Dissolved in 300 ml of distilled water and filter sterilised

Table 2: Spoligotyping reagents

Components		Description
Stock solutions		
10X SSPE	13.7 g sodium di-hydrogen phosphate, 105.19 g sodium chloride. 3.36 g EDTA	All components were dissolved in 900 ml of dH2O, and the pH of the solution was adjusted to 7.4 with NaOH. Distilled water was added to a total volume of 1 L
10% SDS	50g sodium dodecyl sulphate	Dissolved in 500 ml of distilled water
0.5M Ethylenediaminetetraacetic acid (EDTA)	93 g EDTA	Dissolved in 500 ml of distilled water
Working solutions		

2x SSPE/0.1%SDS	200 ml of SSPE, 10ml of 10% SDS	All reagents and distilled water were added to a total volume of 1 L
2x SSPE/0.5%SDS	200 ml of SSPE, 20ml of 10% SDS	All reagents and distilled water were added to a total volume of 1 L
1% SDS	20 ml of 10% SDS	Added to distilled water to a volume of 200 ml
20 mM EDTA	20 ml of 0.5M EDTA	Added to distilled water to a volume of 500 ml

Table 3: Microscopy reagents

Reagent	**Components**	**Description**
2.5% Glutaraldehyde	25% Glutaraldehyde (SIGMA-G5882)	Diluted to 2.5% in PBS
PBS	8 g of NaCl, 0.2 g of KCl, 1.44 g of Na2HPO4, 0.24 g of KH2PO4	All components were dissolved in 800 ml of dH2O, and the pH of the solution was adjusted to 7.2 with HCL. Distilled water was added to a total volume of 1 L, and the solution was autoclaved

Table 4: Software used in this study

Program	**Description**
Graphpad prism statistical tool (version 8)	GraphPad Prism 8 is a data management and analysis application. This software was used to create graphs and Figures for the

	data in this study. It was also used in statistical analysis to compare statistically significant differences between data groups. (http://www.graphpad.com/scientificsoftware/prism/)
Image J (Fiji)	Fiji software is a free and open source image processing application. This software was used to analyze microscope images captured with a Nikon fluorescence microscope. (http://imagej.net/Fiji)
SPOTCLUST TB	Spotclust is an open access online website that is used for Tuberculosis evolution and epidemiology mathematical models for genotyping and epidemiological data on infectious diseases. The website was used for the spoligotyping of clinical isolates http://tbinsight.cs.rpi.edu/run_spotclust.html
Most probable number (MPN) calculator (version 2)	The MPN calculator is a free and open source tool for calculating the population density of viable microorganisms in a test sample. The MPN calculator was used in this study to calculate the total number of bacteria recovered from the MPN assay. (available at http://www.wiwiss.fuberlin.de/fachbereich/vwl/iso/ehemalige/wilrich/InDEX.html
JalView	Jalview is a free program for editing, visualizing, and analyzing multiple sequence alignments. (https://www.jalview.org/)

BioEdit	BioEdit is a free biological sequence alignment editor with an intuitive multiple document interface and convenient features designed to make sequence alignment and manipulation on desktop computers relatively simple.
FinchTV	FinchTV is a software program that allows you to view Deoxyribonucleic acid (DNA) sequence traces. This is a chromatogram viewer that can show an entire trace in scalable multi-pane views.

6.2 Appendix B : Supplementary Figures

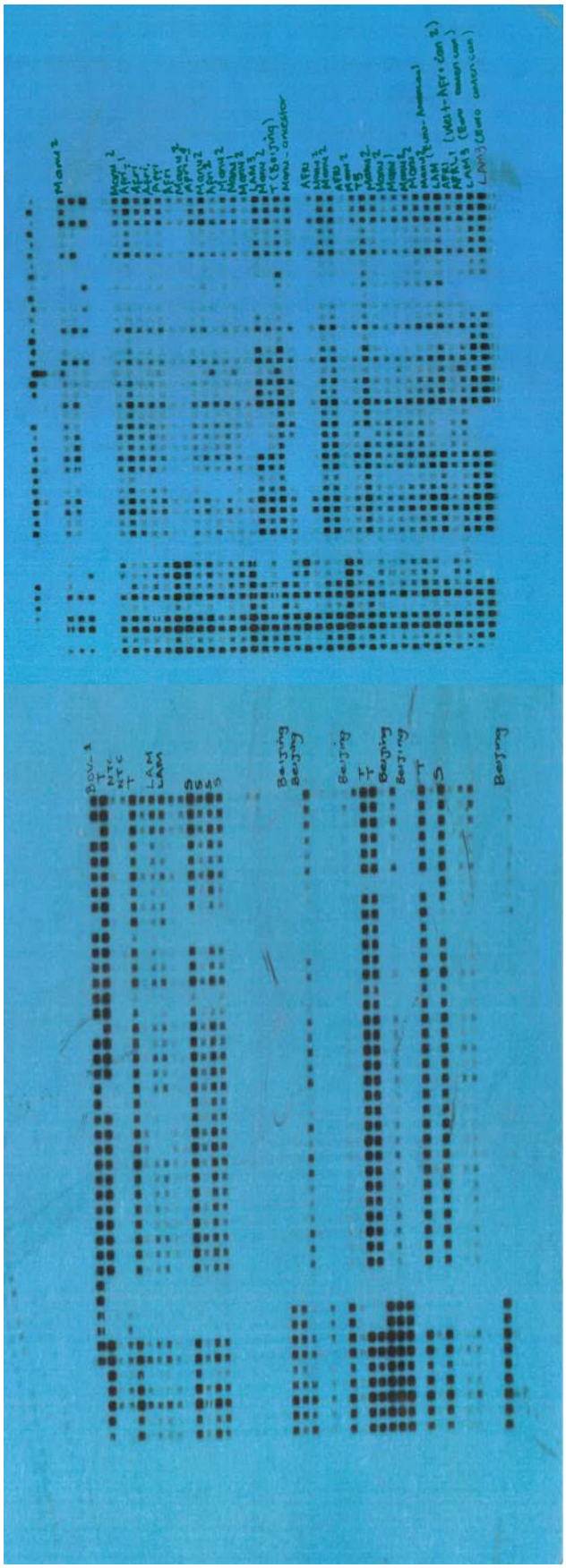

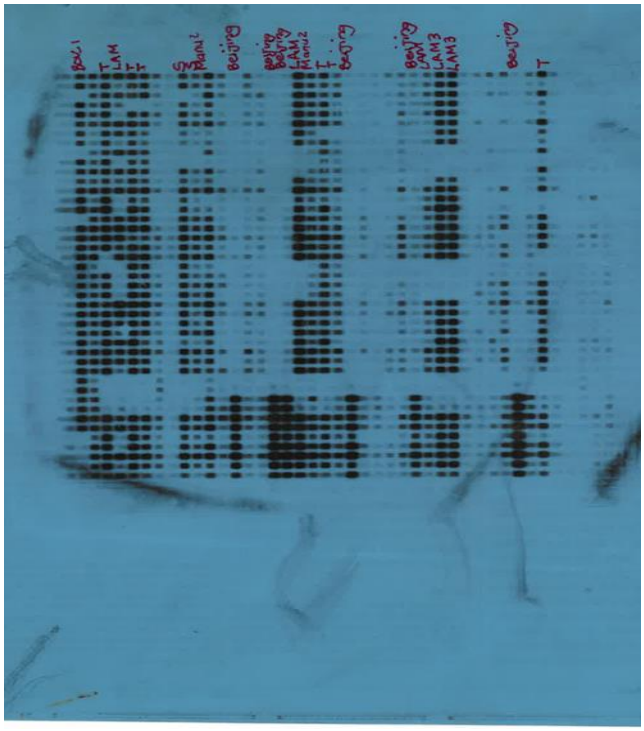

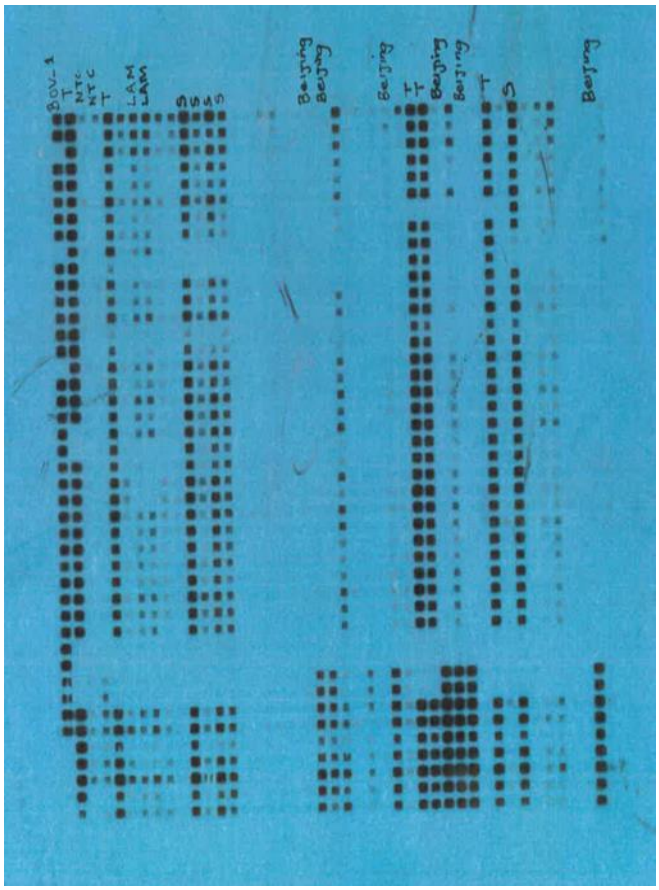

Figure 1: **Straintyping of Mtb sputum samples .** Spoligotypes showing the patterns of different strains obtained from the spoligotyping technique. Spoligotyping is a polymerase chain reaction-based typing system for the differentiation of mycobacterium strains. This technique exploits the genetic diversity in the direct repeat (DR) locus in the *Mtb* genome. A set of 43 unique spacer sequences whose presence or absence is unique per strain is used to classify *Mtb* strains. The dark dots represent the presence of a spacer sequence.

Table 5: DNA extraction. Table showing the concentrations and 260/280 ratio(purity) of the extracted clinical samples.

Sample ID	**ng/µl**	**260/280**
LAM 1	297.85	2.01
LAM 1.1	1427.53	1.98
LAM 1.2	281.63	1.90
LAM 2	496.73	1.97
LAM 2.1	1448.30	1.98
LAM 2.2	103.02	2.05
LAM 3	561.91	1.98
LAM 3.1	206.76	2.01
LAM 3.2	185.64	2.07
LAM 4	1395.52	1.97
LAM 4.1	23.59	1.53
LAM 4.1	50.93	2.02
LAM 5	186.53	2.03
LAM 5.1	319.94	1.96
LAM 5.2	565.33	1.95
Beijing 1	102.30	1.97
Beijing 1.1	1393	1.97
Beijing 1.2	1716.24	2.00
Beijing 2	307.50	1.92

Beijing 2.1	235.35	2.00

Beijing 2.2	228.02	2.06
Beijing 3	225.60	2.04
Beijing 3.1	116.73	2.06
Beijing 3.2	118.42	2.03
Beijing 4	143.28	2.00
Beijing 4.1	92.00	2.01
Beijing 4.2	179.69	2.02
Beijing 5	375.29	2.12
Beijing 5.1	383.66	2.11
Beijing 5.2	645.49	2.13
H37Rv	447.54	1.94
H37RV.1	90.20	2.04
H37Rv.2	342.24	2.06

Table 6: the concentrations and the 260/230 (purity) of the extracted RNA samples

Sample ID	**ng/µl**	**260/230**
LAM 1	1040.58	2.22
LAM 2	1168.53	2.15
LAM 1	473.60	2.23
Beijing 1	324.12	2.04
Beijing 2	568.97	2.06

Beijing 3	1233.12	2.25
H37Rv	849.04	2.06

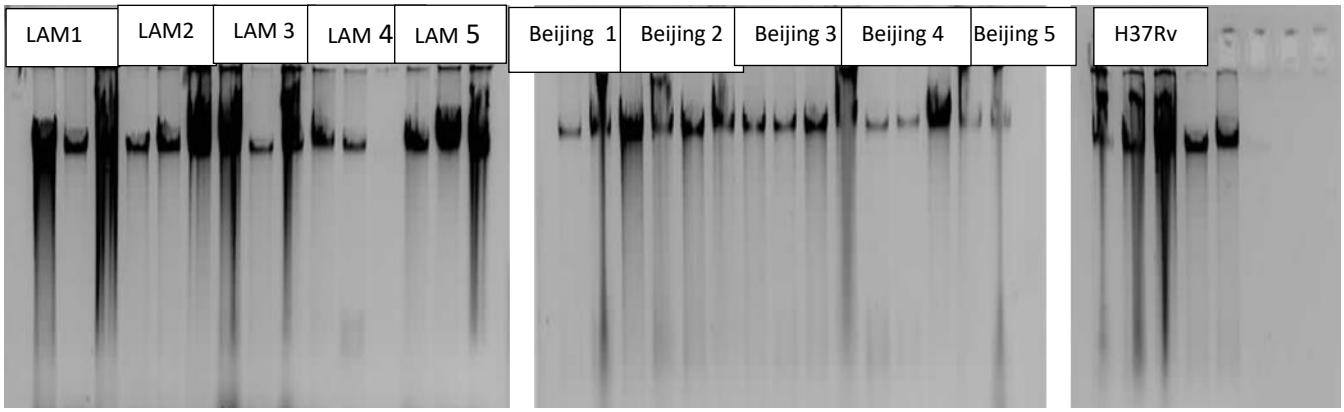

Figure 2: Genomic DNA extraction. Agarose gel electrophoresis of total DNA extraction from *M. tuberculosis* clinical strains (LAM and Beijing).

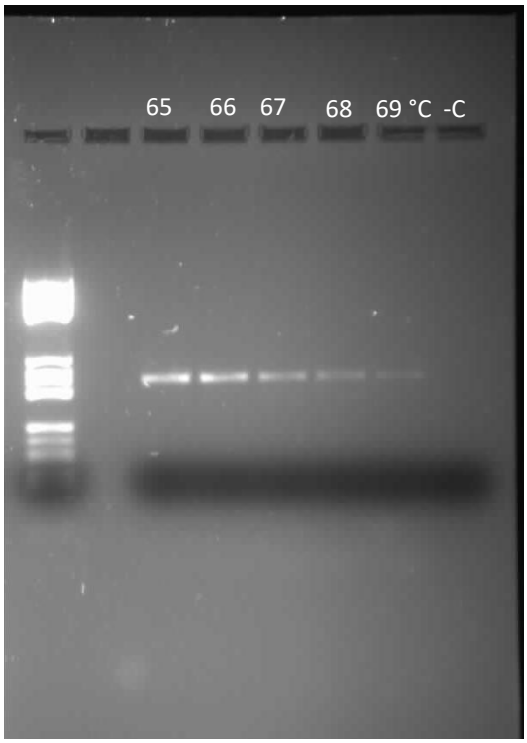

Figure 3: *katG* primer optimisation. Agarose gel electrophoresis of the *katG* primer optimised at different temperatures (65 - 69°C).

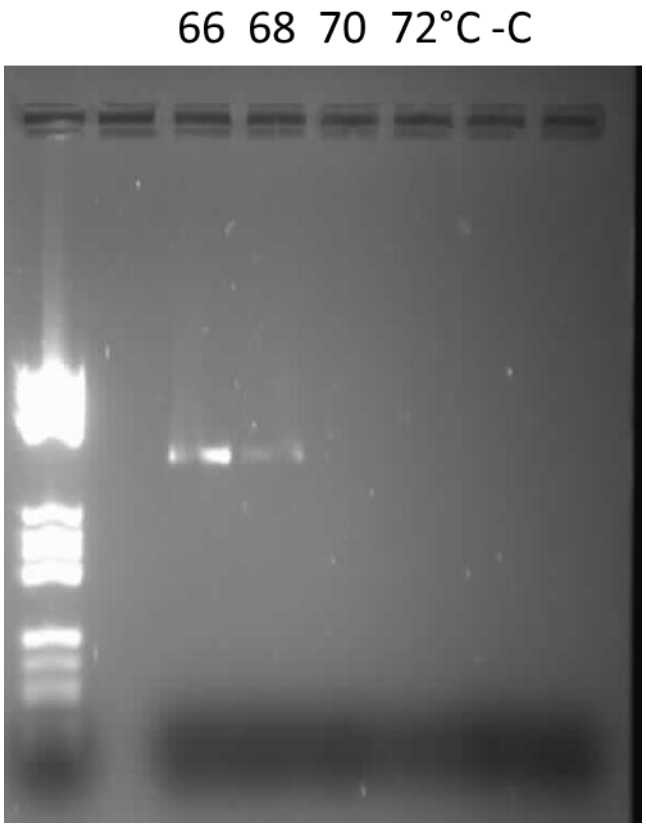

Figure 4: *embB* primer optimisation. Agarose gel electrophoresis of the *katG* primer optimised at different temperatures (65 - 69°C).

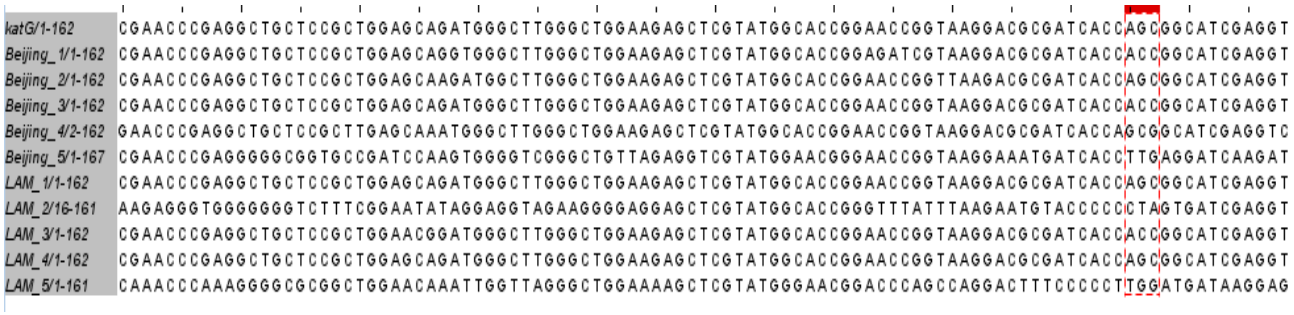

Figure 5: Multiple sequence alignment for the *katG* gene on the clinical strains (Beijing and LAM). The highlighted area shows $katG_{315}$, changes in this area is indicative of isoniazid resistance.

Figure 6: Multiple sequence alignment for the *embB* gene on the clinical strains (Beijing and LAM). The highlighted area shows *embB*$_{306}$, changes in this area is indicative of isoniazid resistance.

Appendix- C- Ethics clearance certificate

UNIVERSITY OF THE WITWATERSRAND, JOHANNESBURG

HUMAN RESEARCH ETHICS COMMITTEE (MEDICAL)

Office of the Deputy Vice-Chancellor (Research & Innovation)

14/03/2022

Ref: W-CBP-220314-02

TO WHOM IT MAY CONCERN

Waiver: This certifies that the following research does not require clearance from the Human Research Ethics Committee (Medical)

Investigator: Ms B Nonkula
Student No. (if appropriate): 1421421
Staff No. (if appropriate):

Supervisor: Professor B Kana

School: Pathology
Department: Molecular Medicine and Haematology
Medical School
University

Project title: *Assessing the propensity of drug-resistant tuberculosis to enter and exit the differentially culturable state*

Reason: In vitro laboratory study
No human participants will be involved in the study

Dr CB Penny
Chairperson: Human Research Ethics Committee (Medical)

Research Office Secretariat:
Third Floor, Phillip Tobias Building, corner of St Andrews and York Roads, Parktown, Johannesburg 2193
Postal address: Private Bag 3, Wits 2050
Tel Nos: +27 (0)11 717 1234/1252/2656/2700
Office E-mail: HREC-Medical.ResearchOffice@wits.ac.za
Website:
https://www.wits.ac.za/research/researcher-support/research-ethics/ethics-committees/

Appendix D- Turn-it in report

turnitin

Digital Receipt

This receipt acknowledges that Turnitin received your paper. Below you will find the receipt information regarding your submission.

The first page of your submissions is displayed below.

Submission author:	Bomikazi Nonkula
Assignment title:	No repository assignment 2
Submission title:	MSc dissertation
File name:	Bomikazi_Nonkula_MSc_dissertation.docx
File size:	8.15M
Page count:	85
Word count:	15,097
Character count:	81,623
Submission date:	30-Mar-2022 05:25PM (UTC+1100)
Submission ID:	1796751137

Copyright 2022 Turnitin. All rights reserved.

MSc dissertation

ORIGINALITY REPORT

13%	10%	8%	3%
SIMILARITY INDEX	INTERNET SOURCES	PUBLICATIONS	STUDENT PAPERS

PRIMARY SOURCES

1	Phyu Win Ei, Wah Wah Aung, Jong Seok Lee, Go-Eun Choi, Chulhun L. Chang. " Molecular Strain Typing of : a Review of Frequently Used Methods ", Journal of Korean Medical Science, 2016 Publication	1%
2	wiredspace.wits.ac.za Internet Source	1%
3	www.ncbi.nlm.nih.gov Internet Source	1%
4	www.frontiersin.org Internet Source	<1%
5	line.travel.sina.com.cn Internet Source	<1%
6	www.atsjournals.org Internet Source	<1%
7	academic.oup.com Internet Source	<1%
8	dfs.by Internet Source	

7. References

Ahmad, S. (2011). Pathogenesis, immunology, and diagnosis of latent *Mycobacterium tuberculosis* infection, *Clinical and Developmental Immunology*, 2011. doi: 10.1155/2011/814943.

Ahmed, A., Rakshit, S. and Vyakarnam, A., (2016). HIV–TB co-infection: mechanisms that drive reactivation of Mycobacterium tuberculosis in HIV infection. *Oral diseases*, *22*, pp.53-60.

Baer, C.E., Rubin, E.J. and Sassetti, C.M., (2015). New insights into TB physiology suggest untapped therapeutic opportunities. *Immunological reviews*, 264(1), pp.327-343.

Bakuła, Z., Napiórkowska, A., Bielecki, J., Augustynowicz-Kopeć, E., Zwolska, Z. and Jagielski, T., (2013). Mutations in the embB gene and their association with ethambutol resistance in multidrug-resistant Mycobacterium tuberculosis clinical isolates from Poland. *BioMed research international*.

Barnes, P.F. and Cave, M.D., (2003). Molecular epidemiology of tuberculosis. *New England Journal of Medicine*, *349*(12), pp.1149-1156.

Belay, M., Ameni, G., Bjune, G., Couvin, D., Rastogi, N. and Abebe, F., (2014*)*. Strain diversity of Mycobacterium tuberculosis isolates from pulmonary tuberculosis patients in Afar pastoral region of Ethiopia. *BioMed research international*, pp.6-13.

Boehme, C.C., Nabeta, P., Hillemann, D., Nicol, M.P., Shenai, S., Krapp, F., Allen, J., Tahirli, R., Blakemore, R., Rustomjee, R. and Milovic, A., (2010). Rapid molecular detection of tuberculosis and rifampin resistance. *New England Journal of Medicine*, 363(11), pp.1005-1015.

Borrell, S. and Gagneux, S., (2011). Strain diversity, epistasis and the evolution of drug resistance in Mycobacterium tuberculosis. *Clinical Microbiology and Infection*, 17(6), pp.815-820.

Bruchfeld, J., Correia-Neves, M. and Källenius, G., (2015). Tuberculosis and HIV coinfection. *Cold Spring Harbor perspectives in medicine*, *5*(7), p.a017871.

Buerger, S., Spoering, A., Gavrish, E., Leslin, C., Ling, L. and Epstein, S.S., (2012*). Microbial scout hypothesis, stochastic exit from dormancy, and the nature of slow growers. Appl. Environ. Microbiol.*, 78(9), pp.3221-3228.

Carranza, C., Pedraza-Sanchez, S., de Oyarzabal-Mendez, E. and Torres, M., (2020). Diagnosis for latent tuberculosis infection: New alternatives. *Frontiers in Immunology*, pp.11.

Chengalroyen, M.D., Beukes, G.M., Gordhan, B.G., Streicher, E.M., Churchyard, G., Hafner, R., Warren, R., Otwombe, K., Martinson, N. and Kana, B.D., (2016). Detection and quantification of differentially culturable tubercle bacteria in sputum from patients with tuberculosis. *American journal of respiratory and critical care medicine*, 194(12), pp.1532-1540.

Chihota, V. N., Niehaus, A., Streicher, E. M., Wang, X., Sampson, S. L., Mason, P., Warren, R. M. (2018). Geospatial distribution of Mycobacterium tuberculosis genotypes in Africa. *PloS one*, *13*(8), e0200632-e0200632. doi:10.1371/journal.pone.0200632

Churchyard, G., Kim, P., Shah, N.S., Rustomjee, R., Gandhi, N., Mathema, B., Dowdy, D., Kasmar, A. and Cardenas, V., (2017). What we know about tuberculosis transmission: an overview. *The Journal of infectious diseases*, 216(suppl_6), pp.S629-S635.

Domenech, P., Zou, J., Averback, A., Syed, N., Curtis, D., Donato, S. and Reed, M.B., (2017). Unique regulation of the DosR regulon in the Beijing lineage of Mycobacterium tuberculosis. *Journal of bacteriology*, *199*(2), pp.e00696-16.

Dookie, N., Rambaran, S., Padayatchi, N., Mahomed, S. and Naidoo, K., (2018). Evolution of drug resistance in Mycobacterium tuberculosis: a review on the molecular determinants of resistance and implications for personalized care. *Journal of Antimicrobial Chemotherapy*, 73(5), pp.1138-1151.

Dowdy, D. W., Basu, S. and Andrews, J. R. (2013) 'Is passive diagnosis enough? The impact of subclinical disease on diagnostic strategies for tuberculosis', *American Journal of Respiratory and Critical Care Medicine*, 187(5), pp. 543–551. doi: 10.1164/rccm.201207-1217OC.

Drain, P.K., Bajema, K.L., Dowdy, D., Dheda, K., Naidoo, K., Schumacher, S.G., Ma, S., Meermeier, E., Lewinsohn, D.M. and Sherman, D.R., (2018). Incipient and subclinical

tuberculosis: a clinical review of early stages and progression of infection. *Clinical microbiology reviews*, *31*(4), pp.e00021-18.

Dulberger, C.L., Rubin, E.J. and Boutte, C.C., (2019). The mycobacterial cell envelope—a moving target. *Nature Reviews Microbiology*, pp.1-13.

Dusthackeer, A., Balasubramanian, M., Govindarajan, S., Priya, S., Nirmal, C.R., Rajadas, S.E., Balasubramanian, A., Mondal, R.K., Thiruvenkadam, K., Hemanth Kumar, A.K. and Ramachandran, G., (2019). Differential culturability of Mycobacterium tuberculosis in culture-negative sputum of patients with pulmonary tuberculosis and in a simulated model of dormancy. *Frontiers in microbiology*, 10, p.2381.

Ei, P.W., Aung, W.W., Lee, J.S., Choi, G.E. and Chang, C.L., (2016). Molecular strain typing of Mycobacterium tuberculosis: a review of frequently used methods. *Journal of Korean medical science*, *31*(11), pp.1673-1683.

Frieden, T. R. *et al.* (2003) 'Tuberculosis', 362, pp. 887–899.

Gandhi, N.R., Brust, J.C., Moodley, P., Weissman, D., Heo, M., Ning, Y., Moll, A.P., Friedland, G.H., Sturm, A.W. and Shah, N.S., (2014). Minimal diversity of drug-resistant Mycobacterium tuberculosis strains, South Africa. *Emerging infectious diseases*, *20*(3), p.426.

Gordhan, B.G., Peters, J. and Kana, B.D., (2019). Application of model systems to study adaptive responses of Mycobacterium tuberculosis during infection and disease. *Advances in applied microbiology*, 108, pp.115-161.

Gordhan, B.G., Peters, J.S., McIvor, A., Machowski, E.E., Ealand, C., Waja, Z., Martinson, N. and Kana, B.D., (2021). Detection of differentially culturable tubercle bacteria in sputum using mycobacterial culture filtrates. *Scientific reports*, *11*(1), pp.1-11.

Gupta, A., Sinha, P., Nema, V., Gupta, P.K., Chakraborty, P., Kulkarni, S., Rastogi, N. and Anupurba, S., (2020). Detection of Beijing strains of MDR M. tuberculosis and their association with drug resistance mutations in katG, rpoB, and embB genes. *BMC infectious diseases*, *20*(1), pp.1-7.

Healy, C., Gouzy, A. and Ehrt, S., (2020). Peptidoglycan Hydrolases RipA and Ami1 Are Critical for Replication and Persistence of Mycobacterium tuberculosis in the Host. *Mbio*, 11(2), pp.1-14.

Isakova, J., Sovkhozova, N., Vinnikov, D., Goncharova, Z., Talaibekova, E., Aldasheva, N. and Aldashev, A., (2018). Mutations of rpoB, katG, inhA and ahp genes in rifampicin and isoniazid-resistant Mycobacterium tuberculosis in Kyrgyz Republic. *BMC microbiology*, *18*(1), pp.1-8.

Jagielski, T., Van Ingen, J., Rastogi, N., Dziadek, J., Mazur, P.K. and Bielecki, J., (2014). Current methods in the molecular typing of Mycobacterium tuberculosis and other mycobacteria. *BioMed research international*, pp. 5-12.

Jilani, T.N., Avula, A., Gondal, A.Z. and Siddiqui, A.H., (2020). Active tuberculosis. *StatPearls [Internet]*.

Kana, B.D. and Mizrahi, V., (2010). Resuscitation-promoting factors as lytic enzymes for bacterial growth and signaling. *FEMS Immunology & Medical Microbiology*, *58*(1), pp.39-50.

Kurz, S.G., Furin, J.J. and Bark, C.M., 2016. Drug-resistant tuberculosis: challenges and progress. *Infectious Disease Clinics*, 30(2), pp.509-522.

Li, L., Mendis, N., Trigui, H., Oliver, J.D. and Faucher, S.P., (2014). The importance of the viable but non-culturable state in human bacterial pathogens. *Frontiers in microbiology*, *5*, p.258.

Maitra, A., Munshi, T., Healy, J., Martin, L.T., Vollmer, W., Keep, N.H. and Bhakta, S., (2019). Cell wall peptidoglycan in Mycobacterium tuberculosis: An Achilles' heel for the TB-causing pathogen. *FEMS microbiology reviews*, 43(5), pp.548-575.

Maningi, N.E., Malinga, L.A., Antiabong, J.F., Lekalakala, R.M. and Mbelle, N.M., (2017). Comparison of line probe assay to BACTEC MGIT 960 system for susceptibility testing of first and second-line anti-tuberculosis drugs in a referral laboratory in South Africa. *BMC infectious diseases*, 17(1), p.795.

Marais, B.J., (2016). The global tuberculosis situation and the inexorable rise of drug-resistant disease. *Advanced drug delivery reviews*, 102, pp.3-9.

Merker, M., Kohl, T.A., Niemann, S. and Supply, P., (2017). The evolution of strain typing in the *Mycobacterium tuberculosis* complex. Strain Variation in the Mycobacterium tuberculosis Complex: Its Role in Biology, *Epidemiology and Control*, pp.43-78.

Moaddab, S.R., Farajnia, S., Kardan, D., Zamanlou, S. and Alikhani, M.Y., 2011. Isoniazid MIC and KatG gene mutations among Mycobacterium tuberculosis Isolates in Northwest of Iran. *Iranian journal of basic medical sciences*, *14*(6), p.540.

Mukamolova, G. V., Turapov, O., Malkin, J., Woltmann, G., & Barer, M. R. (2010). Resuscitation-promoting factors reveal an occult population of tubercle Bacilli in Sputum. *Am J Respir Crit Care Med*, 181(2), 174-180. doi:10.1164/rccm.200905-0661OC

Nurwidya, F., Handayani, D., Burhan, E. and Yunus, F., 2018. Molecular diagnosis of tuberculosis. *Chonnam medical journal*, 54(1), pp.1-9.

O'Garra, A., Redford, P.S., McNab, F.W., Bloom, C.I., Wilkinson, R.J. and Berry, M.P., (2013). The immune response in tuberculosis. *Annual review of immunology*, 31, pp.475-527.

Padarath, K. (2019). The emergence of differentially culturable tubercle bacteria in clinical drug sensitive Mycobacterium tuberculosis strains. Internal CBTBR report. Unpublished.

Pang, Y., Zhou, Y., Zhao, B., Liu, G., Jiang, G., Xia, H., Song, Y., Shang, Y., Wang, S. and Zhao, Y.L., (2012). Spoligotyping and drug resistance analysis of Mycobacterium tuberculosis strains from national survey in China. *PloS one*, *7*(3), p.e32976.

Rad, M.E., Bifani, P., Martin, C., Kremer, K., Samper, S., Rauzier, J., Kreiswirth, B., Blazquez, J., Jouan, M., Van Soolingen, D. and Gicquel, B., (2003). Mutations in putative mutator genes of Mycobacterium tuberculosis strains of the W-Beijing family. *Emerging infectious diseases*, 9(7), p.838.

Rangaka, M. X. *et al.* (2014) 'Isoniazid plus antiretroviral therapy to prevent tuberculosis: a randomised double-blind placebo-controlled trial', *Lancet*, 384(9944), pp. 682–690. doi: 10.1016/S0140-6736(14)60162-8.

Rasoahanitralisoa, R., Rakotosamimanana, N., Stucki, D., Sola, C., Gagneux, S. and Razanamparany, V.R., (2017). Evaluation of spoligotyping, SNPs and customised MIRU-VNTR combination for genotyping Mycobacterium tuberculosis clinical isolates in Madagascar. *PloS one*, 12(10),pp.1-14.

Roetzer, A., Schuback, S., Diel, R., Gasau, F., Ubben, T., di Nauta, A., Richter, E., Rüsch-Gerdes, S. and Niemann, S., (2011). Evaluation of Mycobacterium tuberculosis typing methods in a 4-year study in Schleswig-Holstein, Northern Germany. *Journal of clinical microbiology*, 49(12), pp.4173-4178.

Rosser, A., Pareek, M., Turapov, O., Wiselka, M.J. and Mukamolova, G.V., (2018). Differentially culturable tubercule bacilli are generated during nonpulmonary tuberculosis infection. *American Journal of Respiratory and Critical Care Medicine*, *197*(6), pp.818-821.

Said, H., Ratabane, J., Erasmus, L., Gardee, Y., Omar, S., Dreyer, A., Ismail, F., Bhyat, Z., Lebaka, T., van der Meulen, M. and Gwala, T., (2021). Distribution and Clonality of drug-resistant tuberculosis in South Africa. *BMC microbiology*, *21*(1), pp.1-11.

Saito, K., Warrier, T., Somersan-Karakaya, S., Kaminski, L., Mi, J., Jiang, X., Park, S., Shigyo, K., Gold, B., Roberts, J. and Weber, E., (2017). Rifamycin action on RNA polymerase in antibiotic-tolerant Mycobacterium tuberculosis results in differentially detectable populations. *Proceedings of the National Academy of Sciences*, 114(24), pp.E4832-E4840.

Schluger, N. W. and Rom, W. N. (1998) 'State of the Art The host: Immune response to tuberculosis', *Am J Respir Crit Care Med*, 157(19), pp. 679–691.

Schön, T., Miotto, P., Köser, C.U., Viveiros, M., Böttger, E. and Cambau, E., (2017). Mycobacterium tuberculosis drug-resistance testing: challenges, recent developments and perspectives. *Clinical Microbiology and Infection*, 23(3), pp.154-160.

Sinha, P., Srivastava, G.N., Tripathi, R., Mishra, M.N. and Anupurba, S., (2020). Detection of mutations in the rpoB gene of rifampicin-resistant Mycobacterium tuberculosis strains inhibiting wild type probe hybridization in the MTBDR plus assay by DNA sequencing directly from clinical specimens. *BMC microbiology*, *20*(1), pp.1-8.

Streicher, E.M., Müller, B., Chihota, V., MLAMbo, C., Tait, M., Pillay, M., Trollip, A., Hoek, K.G., Sirgel, F.A., van Pittius, N.C.G. and van Helden, P.D., (2012). Emergence and treatment of multidrug resistant (MDR) and extensively drug-resistant (XDR) tuberculosis in South Africa. *Infection, genetics and evolution,* 12(4), pp.686-694.

Vilchèze, C., (2020). Mycobacterial cell wall: a source of successful targets for old and new drugs. *Applied Sciences*, *10*(7), p.2278.

World Health Organization, (2019). Global tuberculosis report 2019.

World Health Organization, (2020). Global tuberculosis report 2020.

Xu, Y., Jia, H., Huang, H., Sun, Z. and Zhang, Z., (2015). Mutations found in embCAB, embR, and ubiA genes of ethambutol-sensitive and-resistant Mycobacterium tuberculosis clinical isolates from China. *BioMed research international*, pp. 9-21.